Abstract

Integration of Geophysical and Geotechnical Methods for Road Route Characterization: the Addis Ababa-Awash New Detour Road at Lake Beseka: Main Ethiopian Rift, Metehara Area.

Tibebu G/Michael
Addis Ababa University, 2014

Adequate knowledge supported by proper investigation of the sub-surface structure condition is a vital task for effective assessment and control of weakening of road morphology. The present research study was carried out to characterize the general suitability of the proposed route corridor by an integrated geophysical and geotechnical survey.

This research mainly focused on carry out detailed mapping of geological structures, provide information on the subsurface sequence, competence and with a view to extracting geo-engineering information in order to understand the basic impact and interaction of the cracks and its implication on the newly constructed detour road and to evolve the possible remedial measures for the likely engineering geological problems. The survey was aimed at imaging the shallow subsurface with a view to evaluate the inferred geological Structures and competency of the shallow formation as foundation materials.

Geotechnically, in order to assess the general suitability of the construction material for selected segments of the subgrade and embankment, samples were collected and tested for grain size distribution, Atterburg limits, swelling potential, California bearing ratio and in-situ density determination at the site. In general the construction material for the new road is slightly non plastic in nature, gap graded but good CBR. Thus, it is anticipated that this may result in to high deformability, segregation which may lead to instability. Also, the construction materials contain more fine materials than the desired percentage.

Geophysical technique involving Electrical imaging and magnetic methods were applied and the data were processed, analyzed and interpreted. Two to three subsurface layers were delineated within the study area. The first of these is a topsoil of loose sand, peat and/or clay. This layer is in

good correlation with the soil layers in geotechnical test pit logs. The existence of loose sand and silty clay at the top surface is capable of being inimical to road structures. The subsurface layers up to the depth of 2m are mechanically unstable owing to weak, saturated horizons with low resistance value, which may not serve as good foundation materials. In all survey lines, three to four major subsurface geological structures possibly of fissures/fractures are delineated up to the depth of 65m which aids the saline Lake water easily invade the road so that the susceptible to deformation . Hence, Geophysical and geotechnical tests showed good agreement.

From overall assessment, the problem of geologic structures, unsuitable subgrade materials and poor grain size distributions of the subsoil, the engineering structures which may be crossed the section, are not prolong for required designed life owing to high traffic load. Therefore, in addition to tectonic activity of the area, the presence of low penetrative resistance, low resistivity saturated sandy clay and weathered ignimbrites in the study area is identified as the cause of cracking and sinking of road in this area. On the basis of this, shallow subgrade foundation may not be possible in the study area unless adequate soil treatment is done; otherwise shifting to a competent soil and rock section area to depth of pronounced thickness of subgrade materials with less frequency of geological structures is recommended to northern part from the current route line near the periphery of the lake. This would transfer loads of such highway to a stratum of high bearing capacity even if the cost of excavation to the geometric design level is too high.

Keywords: *Main Ethiopian Rift, Lake Beseka, ground cracks, Suitability analysis, In-situ density, and subgrade soil Evaluation.*

Acknowledgement

Many people have contributed in many ways to the success of this work a part of my appreciation to the contribution of these people I would like to express my profound gratitude to each of them;

Firstly, I would like to thank my advisor, Dr. Tigistu Haile for his guidance, supervision to whom I owe a great depth of gratitude for his kind assistance and the long discussions we had on issues regarding the research, as well as other interesting topics during the field work. His help and visit in geophysical data collection and patience through the difficult periods I encountered during this research work. I always remember and cherish your valuable contributions and suggestions during my periodic presentations in the chair of geophysics. The experience of him enabled this research work to be carried out successfully and, in a special way that advise and generously shared his vast knowledge. I am grateful to him that, I had to join a field program he arranged with Oromia Water works enterprise and use of a field campaign of the enterprise to conduct in the unfriendly weather conditions of northern Main Ethiopian Rift at Metehara area is very much appreciated. Finally, I am highly indebted to him and greatly acknowledged for allowing me to use his office as well as his personal computer and arrange my field works by collaborating with the department staff.

From all, I also count myself very lucky to have met Dr. Tigistu who has been like a father in guiding, supervising and provider (both material and inspirational) during this research. Old boy, I really appreciate your contribution to my professional and academic laurels. You have been the beginning and the end and I would always be pleased about everything that you have done in my professional carrier. Like the proverbial teacher, your reward is in heaven; God bless you.

I would like to convey my thanks to Dr. Shimeles Fisseha for providing valuable critical reading of the manuscript, his invaluable comments and technical support for the very important expenses of the thesis work and in due course give to the present shape of this thesis. I will also not forget his great assist and various discussions we had with experts from the Geophysical observatory office.

Dr. Getnet Mewa and Dr. Abera Alemu for providing valuable suggestions related with direct Geophysical data analysis methodology and presentation. .

I also would like to forward my heartfelt thanks to my friend Addisu Haile who helped me in data collection during the field work. I am grateful to my lovely wife Yenenesh Tesfaye and my family; supported me throughout this study, especially during the frustrating periods when my research progressed slowly to my liking. I will always be thankful to you all for your continuous moral and encouragement.

I am also gratified to the Ethiopia Roads Authority (ERA) where I got the direct geotechnical data and lithological logs of the study area. I am also thankful to the Department of Earth Science for their finance and equipments support that was extended for the present research work.

Special thanks go to my friends Tesfaye Regassa for his technical comment, Teshome, Birhanu Keno and Asnake for their valuable help in developing my maps using GIS techniques. I apologize to all of my friends whom I did not mention the names. I equally appreciate and acknowledge all of you. I may have had some problems along the way but these are normal. As the saying goes; only a fool does not learn from his mistakes, I have learnt a lot from the many problems I had and hope to be wise the next time.

GOD BLESSES ALL OF YOU!!!

Table of contents

List of Figures

*****

List of Tables

*****

Lists of Plates

*****

List of Annexes

*****

List of Acronyms

a.m.s.l	above mean Sea Level
CBR	California Bearing Ratio
DEM	Digital Elevation Model
EARS	East African Rift System
EMA	Ethiopian Meteorological Agency
EIGS	Ethiopian Institute of Geological Survey
ERA	Ethiopia Roads Authority
ERT	Electrical Resistivity Tomography
FFS	Fault-Fissure System
GIS	Geographic Information System
GPS	Global Position System
ITCZ	Inter Tropical Convergence Zone
LL	Liquid Limit
MDD	Maximum Dry Density
MER	Main Ethiopian Rift
MSE	Metehara Sugar Estate
NE	Northeast
NW	Northwest
OMC	Optimum Moisture Content
OWWDSE	Oromia Water Works Design and Supervision Enterprise
PL	Plastic Limit
PI	Plastic Index
RSDP	Road Sector Development Prodram
UTM	Universal Transverse Mercator
WFB	Wonji Fault Belt
WWDSE	Water Works Design and Supervision Enterprise
2D	Two Dimensional

*****

CHAPTER 1: INTRODUCTION

1.1 General

The Main Ethiopian Rift (MER), which belongs to the northern most branches of the East African Rift System (EARS), is characterized by active extensional tectonics. It is seismically, tectonically and volcanically active since the early Miocene (Woldegabriel G. et al., 1990). To the south, the MER continues to the Kenya Rift and to the north it is connected with the oceanic rift system of Red Sea and Gulf of Aden at the Afar triple junction. The Rift as it traverses over Ethiopia is characterized by a number of fresh and mineralized lakes. Lakes in the MER are generally located in three basins: the Awash basin, the central Main Ethiopian Rift and the southern basin. Lake Beseka is one of the lakes which is found within the volcanically active rift floor at the northern end of the MER in the Awash basin.

Lake Beseka is located immediately south of Fentale Volcano in the MER. Zones of seismicity generated a deepening basin at the site of the present Lake Beseka (Keir et al., 2005). The Endorheic Lake is situated in a region characterized by normal faults trending N10-20°E, which also form its borders and control numerous hot springs. The lake has a closed catchment with no surface water out flow. Near the lake, there is the Metehara Sugar Estate (MSE) with a developed farmland of about 10,000ha (Tesema Zelalem 1998). In early 1960's, the surface area of Lake Beseka was only 3km^2. In 1976, the lake area was estimated at 27.5km^2 and few years ago it covers around 41km^2 (Tamiru Alemayehu, 2006).

This drastic increase in the lake size has affected several infrastructures amongst which are invasion and inundation of the adjacent farm lands and the main access road and rail lines of the country to the sea.

'Roads' are one of the means of growth of any country and the key factor for the economic growth of any nation. Therefore it is essential that roads must be designed in such a manner so that they meet their performance standards. Despite all efforts, roads may fail to provide safe performance standards. For this many factors are responsible, such as inaccurate estimations of the dynamic axial loads, poor construction material or the inadequate subgrade material. The subgrade, the natural soil surface, which provides the bearing surface to the pavement, may behave variably

owing to the properties of the soils. The property of the subgrade soils, which affect greatly the pavements performance, is its expensiveness.

Road infrastructure in Ethiopia had reached such a level of deterioration by the 1990's that it became a serious hindrance in reviving the country's economy (ERA, 2003). In recent years, the Ethiopian Roads Authority (ERA) has been engaged in a massive Road Sector Development Program (RSDP) to increase the road network in the country (Figure 1.1).

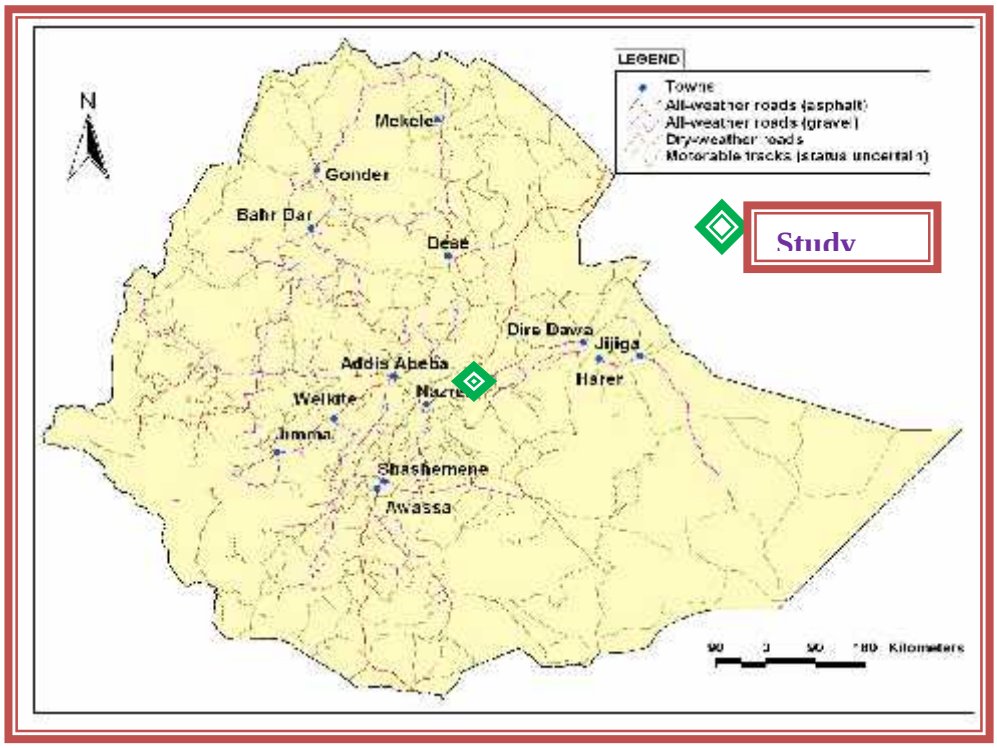

Sources :(from Abinet Gebremedhin, 2006)

Figure 1.1.The study area from simplified Road network in Ethiopia.

One of the road networks being given much emphasis in this drive is the road connecting the country to the sea outlet through Djibouti. This road while passing the study area is affected by several fault systems and covered by volcanic rocks varying from fissural basaltic to viscous acidic lava occurring in an inter-fingering manner.

The geologic structures in the study area are normal faults and fissures trending to N-S to N 20ºE. They belong to the Wonji Fault Belt (WFB) system of faults and exhibit a number of right-stepping en-echelon fault zones obliquely cutting the rift floor (Mohr 1962, 1967, 1987). The capacity of

fractures to channel ground water flow is controlled by interconnectedness of the fractures that are distributed in the host rock. The lithological units of the investigated area consist of basalt, ignimbrite, rhyolite, tuff, scoria and occasionally sediments.

1.2. The Research Problem

Ground cracks and fractures along road cuts are common in some part of the study area. These can cause damage to properties as well as affect human beings.

Ground cracks and fractures in the form of faults and complex disturbances were evident along the Addis Ababa–Awash road, crossing the Main Ethiopian Rift. Examination of historic records and visual manifestations of ground cracks, fractures and fissures in the northern sector of the MER indicated that these features are highly related with rift extension that occur in the form of normal faults, tensional fissures and volcanic activity. The present research study was carried out to characterize the general suitability of the proposed route corridor by an integrated geophysical and geotechnical assessment particularly: the Addis Ababa-Awash New Detour Road at Lake Beseka: Northern Main Ethiopian Rift, Metehara Area. Most importantly the lake growth has affected the highway and railway structures which run along its northern shore. As the Lake size and level increased, construction works to elevate the rail and road line has been continuously undertaken several times in the last three decades. More recently, the rise in the lake level has become so drastic that the earlier remedial measures, albeit incurring a lot of expense, were no more feasible.

To alleviate this problem and provide what is believed to be a lasting solution, a completely new detour road passing over a higher ground has been designed and was under construction on the northern side of the Lake.

Fissures have been described previously at several locations in the MER (Gibson, 1969; Asfaw, Laike Mariam 1992, 1998; Mohr et al., 1983; Mohr, 1987). They generally appear as narrow cracks, which may be several hundred meters long, connecting subsidence pits up to several meters wide. The cracks sometimes appear to close as they become covered by a veneer of vegetation and sediment, and subsequently to reopen.

1.3. Relevance of the Study

The expansion of Lake Beseka is alarming and has had detrimental effect on the surrounding ecological, physical, hydrological and infrastructural environment. Most importantly the lake growth has affected the highway and railway structures which run along its northern shore

(Plate 2.1, and lake has flooded the highway, the only import-export line to the port of Djibouti, several times. It has also affected the farm lands of the Metahara Sugar State farms. As Ethiopia became a landlocked country in 1993, it entirely depends on this route for importing and exporting commodities. In addition to being Ethiopia's sole access to the port, the highway is the main route that links the central, western, and southern part of the country to the eastern part. As the Lake size and level increased, construction works to elevate the rail and road line has been continuously undertaken several times in the last three decades. However, no sooner has the work been completed the lake weathers the road sides and submerges both lines. More recently, the rise in the lake level has become so drastic that the earlier remedial measures, albeit incurring a lot of expense, were no more feasible.

To alleviate this problem and provide what is believed to be a lasting solution, a completely new detour road passing over a higher ground has been designed and was under construction on the northern side of the Lake. This planned road, near completion during the time of this study, is a 2-km long and 2-m high embankment (Tessema Zelalem, 1998). The government had to spend/ allocated US $1.5 Million to raise the submerged part of the railway and highway (WWDSE, 1999).

Therefore, the primary significance of this study is the mapping of the presence and morphology of ground cracks, fractures and fissures and to suggest the possible remedial measures for the present and the possible worst conditions in the future.

1.4 Limitation of the study

Geophysical surveys can offer considerable time and financial savings compared with borehole investigations. At an early stage of site investigation, it may be beneficial to undertake a reconnaissance geophysical survey to identify areas of the site which should be investigated by drilling, i.e., those where anomalous results are obtained.

Once the geophysical data have been obtained, it is possible to produce a model of the geological section which gives a realistic correlation with the data. The best overall model is obtained by using all the available geological information from boreholes and field mapping. Without this input of precise information, which includes knowledge of the fundamental physical properties of the geological materials at the site, the model cannot be constrained or evaluated in practical terms.

The second problem is associated with that of difficulty in conducting the electrical imaging method data acquisition since galvanic contact between the measuring system and the ground. This is because Earth resistivity measurements are made using an array of grounded electrodes with which to inject current into the ground and to measure the potential difference. The use of grounded electrodes can sometimes give problems in areas of high surface resistivity because in such situation, obtaining useful levels of current flow can be difficult. This was specifically the case at the northwest side of the Lake on the scoracious lava flow situated at south of the newly relocated road route.

Lastly, the major constrains in this research were, limitation on time and financial support.

1.5. Objective of the study

General objective:

The general objective of this research is carry out detailed mapping of geological structures, provide information on the subsurface sequence, competence and with a view to integrating geo-engineering information in order to understand the basic mechanisms for the interaction of the cracks and the surrounding surface, and its implication on the newly constructed detour road by deploying of geophysical investigation in conjunction with geotechnical survey. Hence, it helps to understand the dominant factors that affect the route section as the lake level rises.

The specific objectives of this research work are:

- Detailed structural mapping and characterization of the orientation of the structures;
- Characterizing fractures and investigating of the morphology of the fractures; understand the relation between structures and volcanism;
- To provide information on the subsurface sequence, competence, with respect to ground water condition for triggering ground crack if any, with a view to extract and integrating the geo-engineering information of the subsurface that are inimical to the engineering projects
- To characterize the type and appropriateness of the ground and of the soil and rocks for the proposed road corridor,

1.6. Approach and Methodology

This study is conducted using data obtained both from literature review and field work. The geological map for the area is produced from the field work and existing published (e.g. geological map of Nazareth sheet, 1:250,000) and unpublished maps. The morphology of weak zones, the road routes was determined by GPS with vertical and horizontal accuracy of 2-3m.

The methodology followed in the present research process is based on the objectives formulated in the chart. Geophysical and direct geotechnical methods of investigation were employed in which the electrical resistivity imaging, magnetic, and soils and rocks analysis techniques were respectively used. The spatial geophysical mapping and modeling has been assisted using software's such as GEOSOFT, RES2DINV, PROSYS–II software and SURFUR1

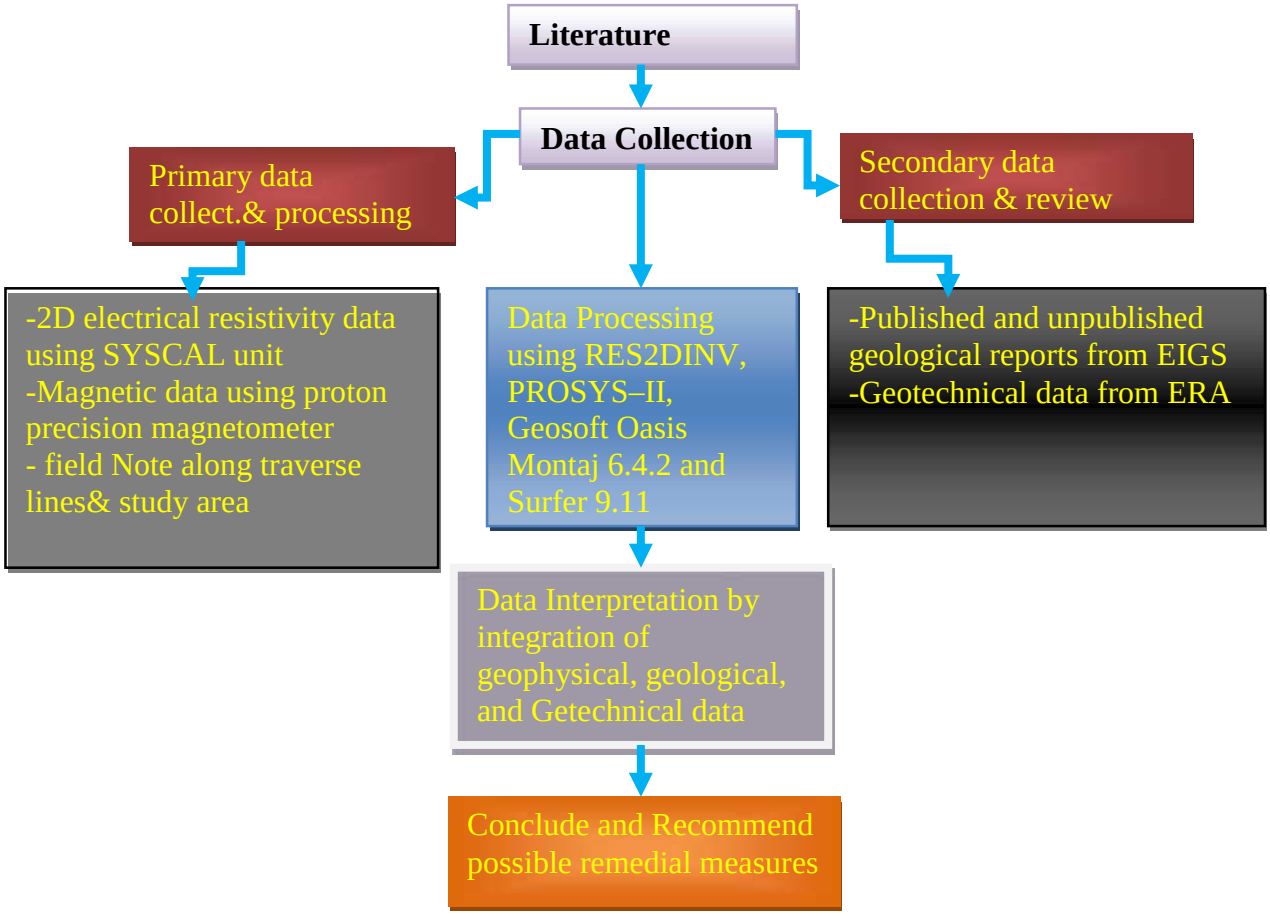

Figure 1.2 Flow chart of the methodologies practical for the study

The major Components of site investigation consisted of three parts. These were

1. Geological field mapping of outcrop fractures and historic tectonic and volcanic activity.
2. Geotechnical and Soils testing data.
3. Geophysical mapping of faults, fractures, and overburden.

The geologic mapping documented the past faults, fractures and addressed hazards related to potential ground cracks and fissures. In general, hazards are greater when the fracture pattern parallels the road-way.

Office work:

- Review, Collection, organization of previous works within and around the study area;
- Understanding the orientation, density and location of fractures with respect to the route alignment and Northern Main Ethiopian Rift from Geological map, aerial photographs and satellite images;
- Collection and Analyzing of Test pit data, Core sample and Geotechnical data concerning soil and rock tests from ERA(Ethiopia Roads Authority)

Field work:

- Description and Collection of data on orientation, morphology, density and location of fractures around the relocated road;
- Inspection and observation of the lithological pattern of the area;
- Observation on how the direction of extension and propagation from fissures or fractures;
- Observation on the types of rocks affected by fractures;
- Conditions of existing road route and railway with respect to fractures
- Geophysical investigation to delineates the density, orientation and nature of fractures and fissures

1.7. Resources Employed

To achieve the objectives of this research work, the following materials were used.

I) Geophysical Equipments:

- Electrical Imaging (The IRIS SYSCAL Resistivity unit) for which general specifications are; weather proof, shock resistant and operating temperature -20 to +70 ^{o} C, internal memory for 2700 readings and power supply; 2 internal rechargeable 12V batteries.

- Magnetic Methods (Proton Precession Magnetometer (Scintrex)) with a general specifications- measurement range 20,000nT to 100,000nT, measurement precision ± 1 nT, resolving power 0.1 nT and working temperature -10 to +50 ^{o}C

II) Digital materials: Software components: Arc GIS 9.1,Arc View 3.3**,** AutoCAD 2007**,**Surfer 9, GEOSOFT,RES2DINV,PROSYS–IIsoftware and Global Mapper

III) Auxiliary materials: Topo maps of scale1:250,000 and 1:50,000and aerial photographs, Geological map of Nazareth (1:250,000) and field equipments: GPS, and digital camera.

1.8. Structure of the thesis

The research project presents systematically the integration of Geophysical and Geotechnical Methods for Road Route Characterization: the Addis Ababa-Awash New Detour Road at Lake Beseka: Main Ethiopian Rift, Metehara Area as a case study and is organized in six chapters.

Chapter 1 INTRODUCTION. This chapter outline the limitation of the study covers problem justifications, the objectives, methodologies, benefits and material used for the research and finally scheme of presentation.

Chapter 2 offers the GENERAL DESCRIPTION OF THE STUDY AREA, in other words, it discusses and describes the location and accessibility of the project site, physiographic features, tectonic and volcanism, previous works, effect of Lake Beseka on the surrounding ecology and environment, infrastructures, regional geology and structures, local geology and structures, soil and climate of the study area.

Chapter 3 presents some basic principles of THEORETICAL BACKGROUND OF GEOPHYSICAL AND GEOTECHNICAL METHODS employed in the work.

Chapter 4 the chapter on DATA ACQUISITION, PROCESSING AND PRESENTATION explains the geophysical approaches for subsurface structures and geotechnical characterization of the sub-grade as a whole and the project road in particular.

Chapter 5 RESULT, DISCUSSION AND INTERPRETATION discuses about the subsurface structures and pavement design considerations that should be taken for the road project in view of the results of the study.

Chapter 6 encompasses the CONCLUSIONS AND RECOMMENDATIONS

CHAPTER 2: GENERAL DESCRIPTION OF THE STUDY AREA

2.1. Location and Accessibility

The study area is located about 195 km east of Addis Ababa, in Oromia Regional State, East Shewa Zone, in Fentale Woreda, Metehara area. It is at the northeastern end of the Main Ethiopian Rift (MER) and falls within the Awash basin. The study area is crossed by one main asphalt road and the Addis Ababa-Djibouti rail way line. There is also a road from Metehara to Addis Ketema and to Metehara Sugar Factory then to Nura Era horticultural farms.

The study area is located in the northern part of Lake Beseka, lying between latitudes 8° 55' 00" and 8° 50' 00" North; 39°50'00" and 39° 55' 00" East and the section of the Asphaltic Addis Ababa-Djibouti road which passes Beseka Lake. From this point the road alignment is being diverted off to the north following few km stretches northerly direction and which joins later the main road.

2.2. Physiographic Features

The Lake Beseka area is an important natural landscape of the country. The topography of the area ranges from flat to undulating plains to from hills, cinder cones, domes to the high Mount Fentale. That is, it has mount Fentale in the north and the low lying plain of the Awash River to the south and east. Most of the watershed is characterized by flat to undulating plains with altitudes ranging from 940 to 1100 m a.m.s.l. Plains with small to high gradient are located in the northwestern and western part of the watershed. Other major topographic features of the Lake Beseka area are the lava flow from Tinish Sabober (Williams's et. al., 2004) scoria cones and spatter and scoria cones. The most fascinating and outstanding Quaternary Fentale volcano is located north of Lake Beseka and rises to 1000m above the surrounding plain and reaches to 2007m at the center of the volcano. Today the volcano is characterized by emanating volcanic gasses and is believed to be an active volcano.

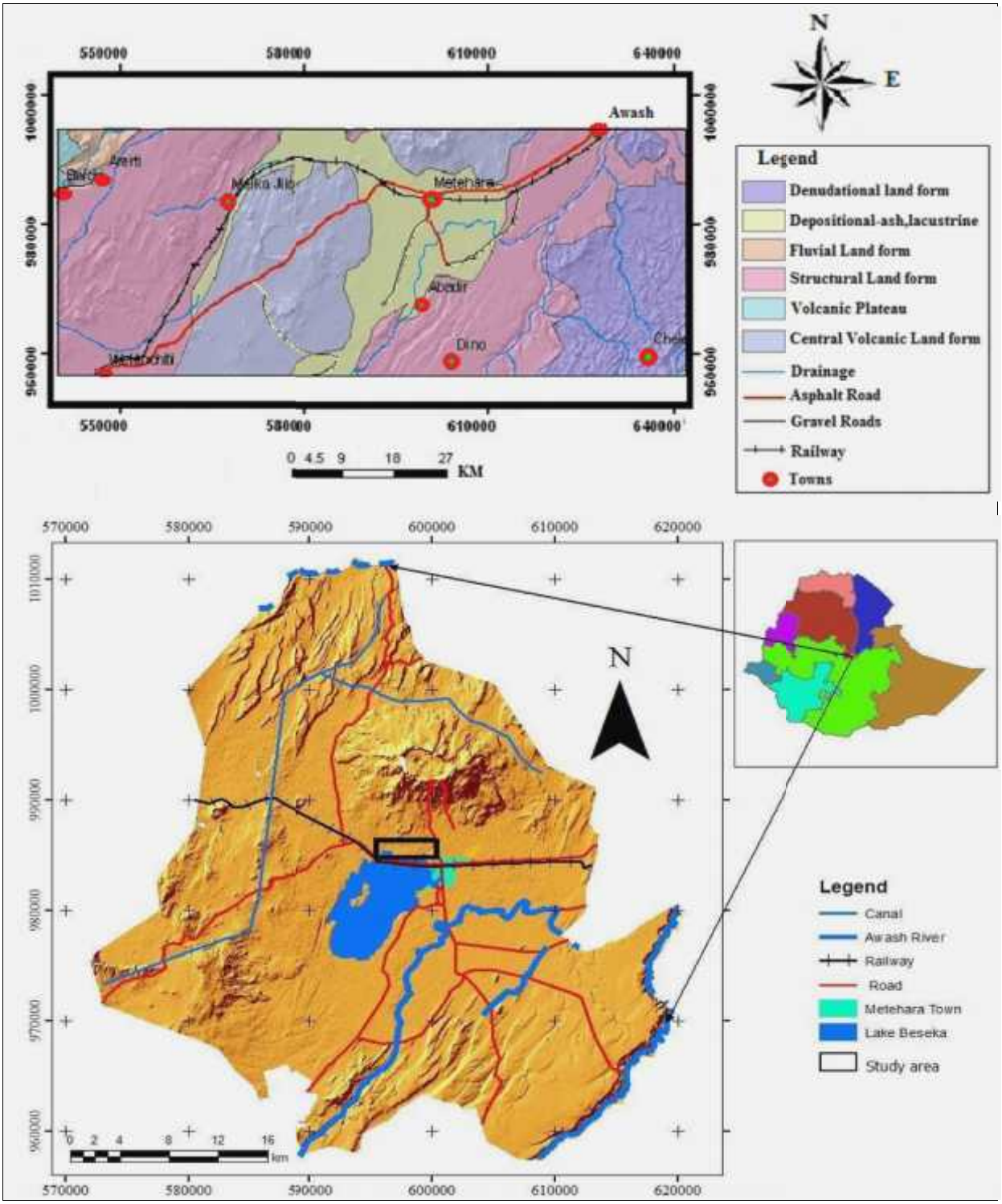

Figure 2.1. Geomorphologic and Location map of Study area and its surroundings.

2.3. Climate

The region is characterized by three main seasons commensurate with the Ethiopian seasons as shown in Table 2.1. The long rainy season in the summer (June – September, known as the 'Kiremt' in Ethiopia) is primarily controlled by the seasonal migration of the Inter Tropical Convergence Zone (ITCZ) which lies to the north of Ethiopia at that time. The 'Kiremt' represent 50 - 70% of the mean annual total (Degefu Wolde., 1987). The dry period extends from October to February (known as 'Bega') when the ITCZ lies to the south of Ethiopia during which time northeasterly trade winds traversing over Arabia dominate the region. The 'Small rain' season (known as "Belg'; contributing 20 to 30% of the annual amount) from March to May coincides with a diminutions of the Arabian high as it moves towards the Indian Ocean causing warm, moist air with a southerly component to flow over most of the country (Griffiths et al., 1975).

Table 2.1 Climate classification in Ethiopia

Altitudes(a.m.s.l) in meter	**Mean Annual temp. (^{o} C)**	**Descriptions**	**Name (local)**
3,300 and above	10 or less	cool	Kur
2,300-3,300	10-15	Cool temperate	Dega
1,500-2,300	15-20	Temperate	Woina Dega
500-1,500	20-25	Warm temperate	Kola
Below 500	25 and above	Hot	Bereha

In the study area the hottest month is June with a mean maximum temperature of 36.77 ºC and a mean minimum of 21.7 ºC. December, the coldest month with an average of 22.49 ºC, the corresponding maximum and minimum values being 30.93 ºC and 13.8 ºC, respectively. As far as precipitation is concerned, the highest average rainfall is recorded in the month of July with values 118.05mm and the minimum is in the month of November with average rainfall of 3.38mm. The mean annual precipitation is 498.80mm. Temperature and rainfall data of the area averaged over a period of 40 years (1966-2007) is summarized in Figure 2.2.

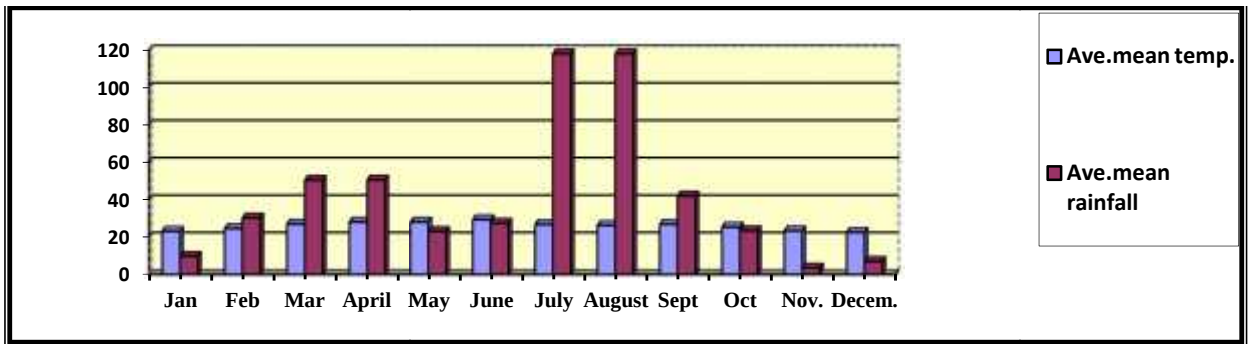

Figure.2.2. Long-term (1966-2007) mean monthly records of meteorological data at Metehara

2.4. Soils

It is known that soil type is closely related to the soil parent material and its degree of weathering. The main parent materials for the soils of the area are basalt, ignimbrite, acidic lava, volcanic ash and pumice, and alluvial and lacustrine sediments. A soil map of the Lake Beseka area exists at the scale of 1:50000 (WWDSE, 1999), and seven major soil units can be identified, of which the most common soil types include: cambisols, lepthosols, and AA Lava flow (MWR, 1999)

The cambisol is a well drained, shallow, and medium to coarse textured, sandy clay loam soil type, which is mainly located in the west and in the northeastern part of the Lake Beseka watershed. It is mainly covered by open grassland and open bushy land. Leptosol is the dominant soil type in the northern part of Lake Beseka. This soil unit is characterized by shallow soil with weakly developed structures, coarse texture, and sandy clay loam to sandy loam and is covered mainly by open bushy woodland. The vegetation of the rift valley is mainly characterized by wooded grassland with Accacia of various species which the local community uses for charcoal production.

2.5. Geology

2.5.1 Regional Geology and Main Ethiopian Rift

The Ethiopian Rift Valley is a large open basin bounded from east and west by long and high mountains of volcanic rocks. Its general outline is in such a way that it is very wide in the north and narrow in the central and southern portions. The complex tectonic and volcanic processes in the Ethiopian Rift have resulted in the formation of volcano-tectonic structural depressions that became sites for many rift valley lakes. The Ethiopian Rift valley contains abundant acidic lavas and

ignimbrites associated with central volcanoes containing wide calderas (Mengesha Tefera et al., 1996).

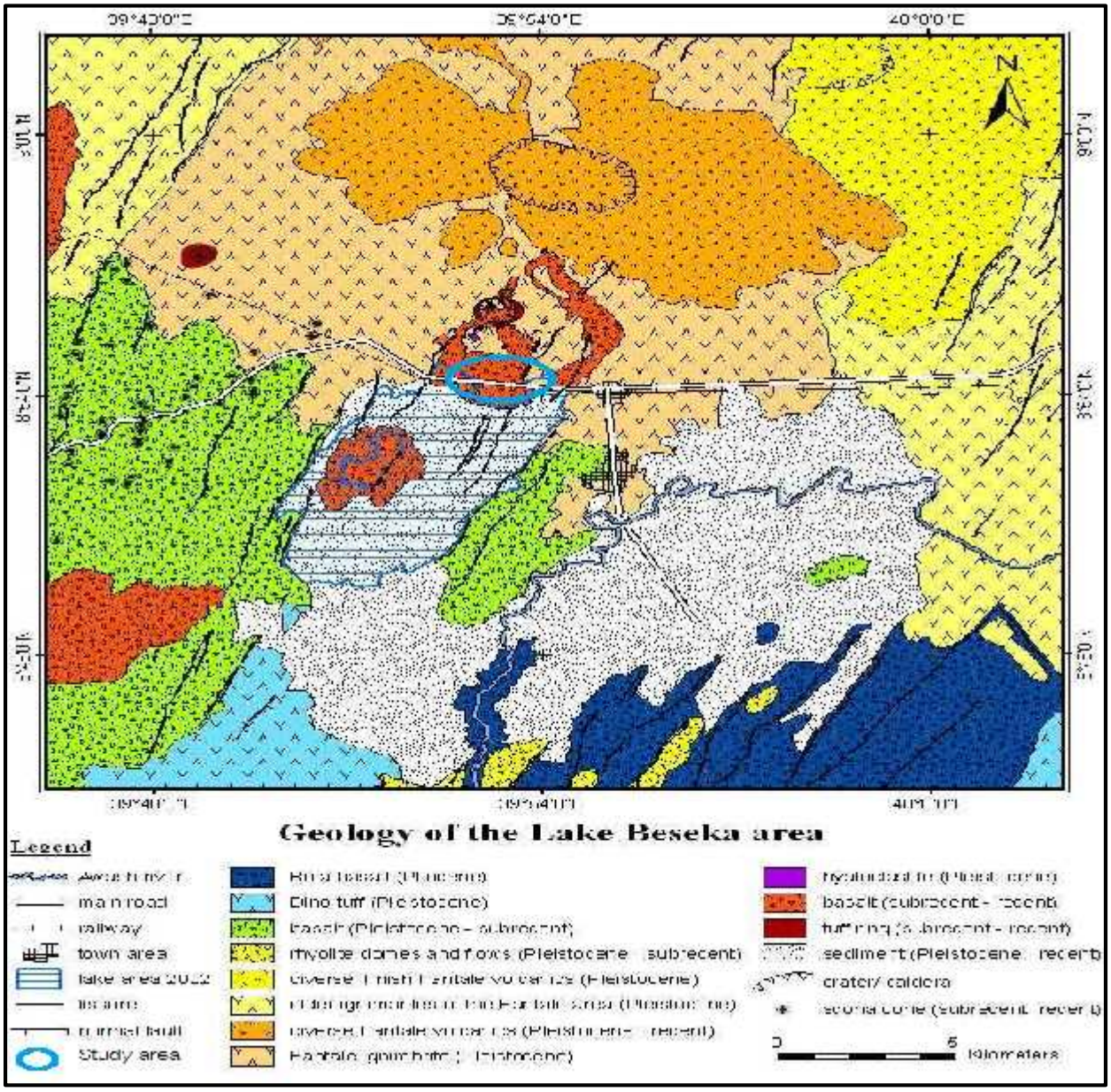

Source:*(from Görner A.& Jolie, E. 2005).*

Figure 2.3.Geological Map of the study area and surrounding.

The Rift valley lies in a unique transitional zone between the continental rifting of East Africa and the sea floor spreading of Northern Afar and the Red Sea (Rooney et al., 2005),and extends from central Ethiopia to Afar in a NNE-SSW direction, cutting the uplifted Ethiopian plateau into the northwestern and southeastern plateau. Throughout the Late Holocene and Quaternary, the MER has been seismically, tectonically and volcanically active, specially confined within a 10-20 km

wide sub axial zone known as the Wonji fault belt (Mohr, 1962,). This belt represents continuous volcano- tectonic activity from the Early Pleistocene to recent times, arranged in en echelon1 fashion and maintaining a NNE-SSW structural orientation along the entire length of the MER. A series of Quaternary volcanoes, mainly trachytes and pantelleritic rhyolites, occur along the Wonji fault belt, often located at offsets (Williams et al., 2004). Some of these volcanoes collapsed into summit caldera, ejecting widespread pyroclastic deposit covering the rift floor along with fissural basalts and lacustrine sediments.

Some authors (Burke K .and Wilson 1976) and others relate the development of the East African Rift to the Afro-Arabian doming in lower Tertiary times. On the other hand, Bahat (1979) maintain that the East African Rift as a whole, initiated as an ancient fracture.

Volcanic and tectonic events in the study area constitute an essential part of the history of the Main Ethiopian Rift. It lies between lat. 8º00`-9 º 00`N and long. 37º30`- 40º00`E. The MER is further divided geographically in to three sectors: northern, central and southern (Woldegabriel G et.al., 1990). The MER divides the 1000km wide uplifted Ethiopian volcanic province asymmetrically into the northwest and southeast plateaus. Older volcanic units (Pre-Pliocene) outcrop on the rift margins and the recent volcanic cover the entire rift (Kazmin et al., 1980).

2.5.2 Regional Structures

The Main Ethiopian Rift (MER) is a 60km wide depression with an overall northeasterly orientation and constitutes an area characterized by active extensional tectonics. Although the average elevation of the plateau on both sides of the rift is 2300m, the mean elevation within the rift floor is 1250m. Three important rift structures, two oceanic (Red Sea and Gulf of Aden) and one continental (East African Rift), come together to form very complex geological features. The Ethiopian rift system is part of the East African Rift System (EARS), a complex tectonic feature with a system of down faulted, non-continuous but related troughs.

Rifting began in the southern and central MER between 18 and 15 Ma, but in the Northern MER it started to develop after 11 Ma (Woldegabriel G. et al., 1990; Wolfenden et al., 2004). Structural and stratigraphic patterns indicate a migration of extensional strain after 2.5 Ma from the border faults to a narrow 20-km-wide sub axial zone of narrow, near N-S trending zones of aligned eruptive centers cut by small offset faults and dykes arranged in a right stepping, en echelon pattern (Boccaletti et al., 1998; Wolfenden et al., 2004). This zone includes rift volcanoes and young fault belts, with a N-NE trend that is oblique to the overall NE trend of the rift (Keranen et

al., 2004). The major active fault zones identified within the rift are predominantly orientated N-S to NNE-SSW and NE-SW (Korme Tesfaye et al., 2004). Volcanic activity and structural deformation of the MER has been concentrated in a NNE trending structure formed by young faults and volcanic centers on the rift floor. This volcano-tectonic belt is commonly known as the Wonji Fault Belt (WFB).

Two main fault systems have been distinguished in the MER: a N30ºE- N40ºE trending fault system which characterizes mainly the rift margins, and a N-S to N20ºE trending fault system, the Wonji Fault Belt (WFB) of Mohr (1962,1967, 1987), which exhibits a number of sigmoidal, overlapping, right-stepping en-echelon fault zones obliquely cutting the rift floor. Similar to other rift systems, the overall architecture of the MER is well expressed by the topography (e.g. Hayward and Ebinger, 1996).

The WFB is the principal active rift axis in the MER and was mainly formed during Quaternary period (Mohr, 1967). The belt is characterized mainly by NNE–SSW trending active extension fractures and normal faults, which are associated, in many places, with fissural or central volcanic activity (Mohr, 1987). The Wonji Fault Belt as such is not a continuous belt but formed from a series of offset segments, each consisting of short and often closely spaced normal faults and fissures (Gibson, 1969, as cited in William et al., 2004). In most cases, normal faults are arranged in a right stepping en echelon configuration (Mohr, 1967, 1968; Boccaletti et al., 1998), and the vertical throws are in the order of several tens of meters in the axial zone to several hundreds of meters in the rift margins (Woldegabriel G. et al., 1990).

The tectonic and volcanic processes of the Ethiopian Rift systems are not uniformly continuous; rather they are characterized by distinct periods of increased and decreased activity

The present MER is made up of northern, central and southern sectors (Woldegabriel G.et.al. 1990). There is a difference of ~15º in the trend of the northern and southern sectors (Figure 2.4); nevertheless, the overall mean direction of the MER remains NE-SW (N40ºE) (Acocella et. al., 2002). The youngest part of the MER is the axial zone, which coincides with the so-called Wonji Fault Belt (WFB), mainly formed during the Quaternary (Mohr 1987; Boccaletti et. al., 1998, 1999). The definition of the WFB has been recently replaced by the concept of magmatic segments, which are described by Ebinger and Casey (2001) a 20-km-wide, right stepping, en echelon-arranged segments of intense magmatism and faulting. This new concept is based on the fact that the MER is magmatically segmented and seismically active (Kurz et al., 2005), and the

extension in the rift is not primarily created by normal faults but by emplacement of magmas and dikes to trigger the normal faults.

Despite the overall NE-SW trend of the MER, the WFB is characterized by active NNE-SSW-trending extension fractures and normal faults. These are often set in a dextral en-echelon arrangement and are associated with volcanic activity. The slightly different trend of the Quaternary WFB with regard to the MER margin suggests a change in the extension direction during Quaternary (Boccaletti et al., 1998).

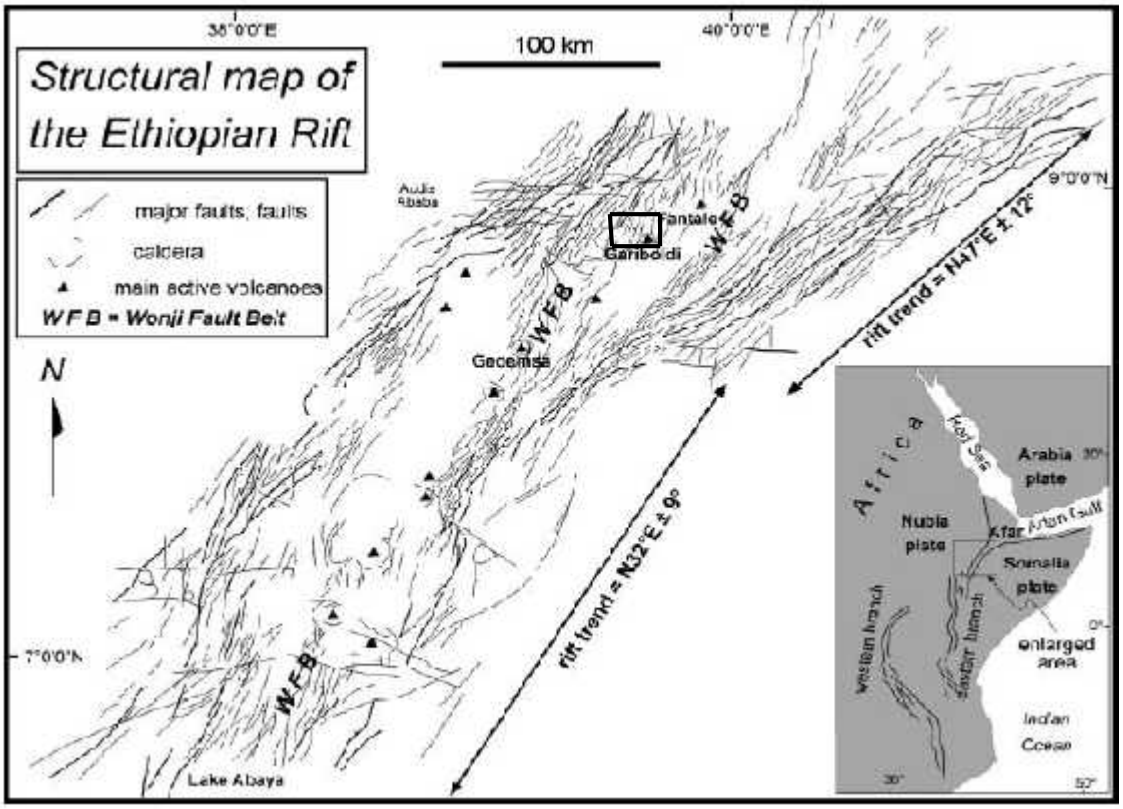

Source: (*After Acocella et al 2002)*

Figure 2.4.Major structures and magmatic segments of the MER. The Fentale area is indicated with small rectangle.

2.5. 3 Tectonic and Volcanism

The Fentale district is one of several magmato-tectonic segments in the Main Ethiopian Rift. Crustal thickness decreases from about 38 km close to Assela area to about 26 km in this magmatic segment. There is a significant drop in altitude from the Assela-Munessa area within the Aluto-Gedemsa magmatic segment to the Fentale segment. The width of the rift valley itself widens from about 70 km near the Assela-Munessa to more than 100 km near the Fentale area. Previous paleomagnetic work in the Assela area showed no rotation that could be seen in paleomagnetism

whereas a previous model (Boccaletti et al., 1999) predicted counterclockwise rotations linked to oblique rifting for the entire Main Ethiopian Rift.The present day widening rate of MER, as estimated using GPS measurements as the central MER over the last 20 years, indicates an extension rate of 4.5 ±1mm/yr (Asfaw Laike Mariam et.al., 1992). More recent high precision GPS measurements show N72^{o} W extension direction, perpendicular to the trend of the WFB (Bilham et al., 1999).

Basalts are usually associated with monogenetic vents and/or fissure eruptions, at the side of the main central volcanoes (Ebinger and Casey, 2001). The MER is, therefore, mostly floored by several basaltic fields, silicic pyroclastic flows and domes and calderas. These are interlayered with and covered by Plio-Quaternary fluvio-lacustrine sediments (Woldegabriel G., 2002).

2.6. Regional Seismicity and the study area

The 'Seismic Risk Map' produced by Laike Mariam Asfaw (1990) for a hundred year return period and 0.99 probability shows that the study area falls within 8 M.M scale. Based on the MM intensity scale, the estimated horizontal earthquake acceleration comes out to be 0.08g, as determined from the MM intensity graph. The maps showing the Seismic Risk zones of Ethiopia and location of the project area are presented in Figures 2.5.

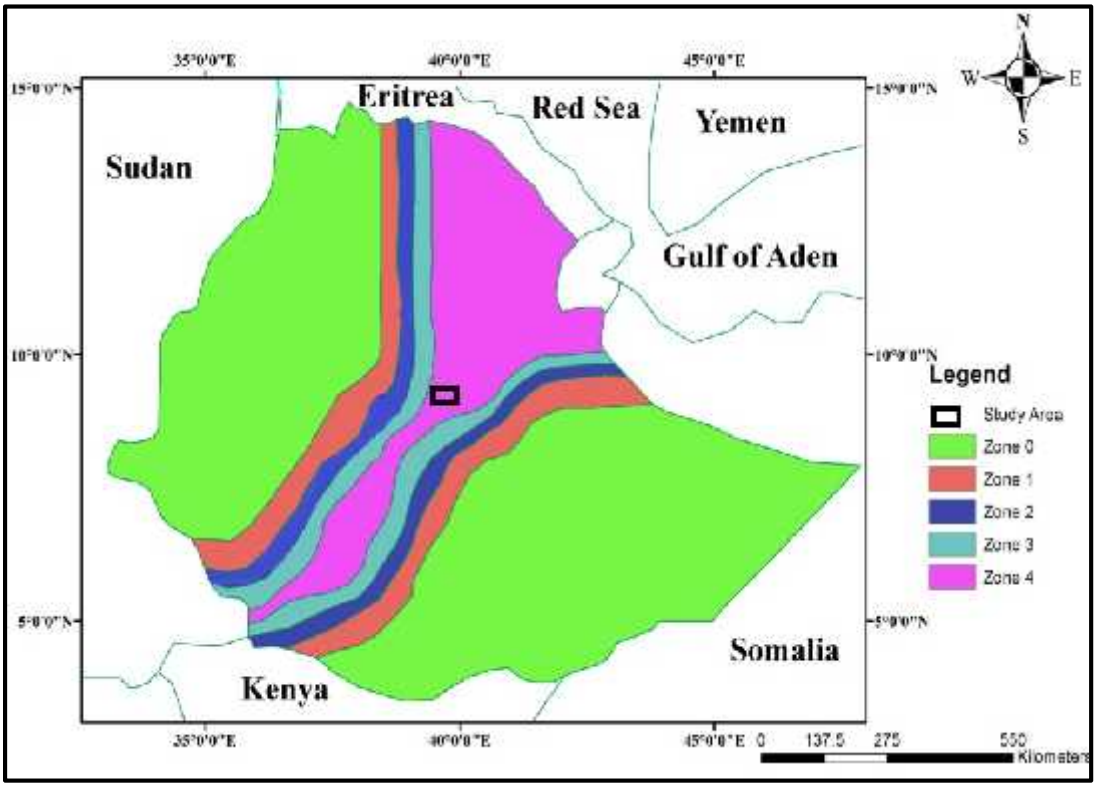

(Source; adopted by the Ethiopian Building Code Standard (EBCS 8))

Figure 2.5. Seismic zoning and seismic risk map of Ethiopia.

In a seismically active region, it may be possible to reduce loss of life and property damage by conducting detailed site specific prediction of seismic ground motion. With the knowledge of earthquake source-mechanisms and path effects, detailed ground motion at any specific site of interest can be determined without waiting for earthquake to occur (Tilahun Mammo, 2005).

Based on the seismicity and the knowledge of the geology and tectonics, the region can be broadly divided into three seismic source zones. These are the Afar Depression, the Escarpment and the Ethiopian Rift System. Each zone is, therefore distinguished by its own specific tectonic, geologic and seismic characteristics (Tilahun Mammo, 2005)

According to the Ethiopia Building Code Standard (1995), the country is divided into five zones of approximately equal seismic risks depending on the known distribution of earthquakes. These zones are no damaging zone (0 zones), less damaging zones (zone 1 and 2) and zones of major damaging (zone 3 and 4). From the seismic hazard map of Ethiopia, the project site falls almost at the center of zone four near to the zone three as shown in Figure 2.5. This map is based on the amplitudes of the ground acceleration to be expected during 100 years return period.

According to the building code, the ground acceleration ratio (α^0) depends on the seismic zones (see Table 2.2 below).

Table 2.2 Bedrock ground acceleration ratio

Zone	**4**	**3**	**2**	**1**
α^0	0.10	0.07	0.05	0.03

The ground acceleration value of the project site is 0.10g for 100 year return period.

2.7. Lake Beseka Graben, and Road Relocation

As outlined above, Lake Beseka is found within the volcanically active rift floor at the northern end of the MER and within the Awash basin. The lake has a closed catchment with no surface water outflow. Near the lake there is the Metehara Sugar Estate with a developed farmland of about 10,000 ha (Tessema Zelalem, 1998).

It is located within 5 to 6 kms wide local graben that is elongated in about NNE-SSW direction. It is developed within highly fractured vesicular and aphyric basalts on its south eastern and western sides and on fissured Fantale ignimbrites on northern eastern and western sides of the lake.
The highway and railroad, Ethiopia's sole access to the harbour, pass just near the northern shore of the lake. The lake water threatens this access more and more each rainy season.

The expansion of Lake Beseka is alarming and has had detrimental effect on the surrounding biological, physical, hydrological and infra-structural environment. The lake growth has affected the highway and railway structures which run along its northern shore , and lake has flooded the highway several times. In addition to being Ethiopia's sole access to the port, the highway is the main route that links the central, western, and southern part of the country to the eastern part. There have been several attempts to alleviate this problem even temporarily. One such attempted resulted in elevating the access through construction of 2-km long and 2-m high embankment (Tessema, Zelalem,1998).The government had to spend US$1.5Million to raise the submerged part of the railway and highway (WWDSE, 1999). Such repeated measures have not resulted in solving the flooding and inundation of the road and rail lines and, as a final and lasting solution, an entirely new detour road has been proposed, is under construction and nearing completion

If the lake continues to expand at current rate and other influencing factors remain the same, the lake will cross the natural water divide and invade the town of Addis Ketema, the newly constructed Asphaltic road and tip off into River Awash. This would be disastrous, as the quality of the river water will deteriorate such that agricultural development downstream (such as in Amibara, Mille, Dubti) would be at risk.

2.8. Ground crack and its effect

Ground cracks, also known as earth fissures in most manuscripts or ground fissures, sinkholes, or collapsing surface elsewhere in literature, are defined as long, linear tensile structures that occur at the land surface with or without vertical offsets (Carpenter, 1993). Along the flanks of the rift, large offset border faults are characterized by rift-ward *en échelon* right-stepping normal faults with a dominant orientation of NNE-SSW and NE-SW directions and distinctive structural styles (Di Paola, 1972; Casey et al., 2006). These right stepping en échelon faults, fissures and chains of Quaternary eruptive centers were collectively referred to as the Wonji Fault Belt (WFB), which Mohr (1962) interpreted as a rift-ward migration of strain from border faults.

Ground cracks were developed in central portion of the Ethiopian Rift Valley when an anomalous heavy rainfall soaked the region in 1996, 1997 and 1998 .The cracks, among other places in the Rift, were observed in Metehara area, around Lake Beseka. With a width of 1-2 m and a depth of unknown and occasionally 6-8m for a length of up to 0.5 km, the cracks were the first major structures observed in the rift floor with no record of seismicity. Deep-rooted ground cracks are formed in and around Abadir farm which adjoins the lake on its southern and south western side. These cracks are visible and increase their size especially during the rainy season and when there is excess water from Lake Beseka. Very wide and long cracks formed many times in the infrastructure area (the roads and rail lines, Metahara and Addis Ketema towns), irrigation area (the Metahara and Abadir farms) with a strike of $N10^{o}E$ that is in the direction of the local faults. At different times these cracks have had great impact on the nearby resources for example, in May 2006, a ground crack that formed in the Abadir farm broke the concrete canals as well as the night storage reservoirs causing the loss of a lot of water.

Over all, these increased incidences in formation of ground fissures and the concurrent and dramatic increase in size of the Lake have presently resulted in permanent damage to property and to the roads as depicted in various plates of [Plate2.1].

2.8.1. Causes and mechanisms of earth fissures

There are a variety of causes and mechanisms through which ground cracks can be formed. Generally, real causes and mechanisms can be related to geological, hydrological and geomorphologic anomalies whereas immediate triggers are usually rainfall and earthquakes. Geological anomalies include strong lithological, structural and weathering heterogeneities, buried faults, fissures, scarps and bedrock highs, soluble rocks and organic soils. Hydrological problems are often related to a decline in groundwater level and the subsequent adjustment in aquifer systems. Topography plays an important role since ground cracks are usually reported to occur in basins, valleys and volcanic depressions.

Plate 2.1 Lake Beseka expansion and its effects on the surrounding biological, physical, hydrological and infra-structural environment

2.8.1. Previous Works *(*The Fantale fissures)

Ground cracks and fractures including tensional fissures are serious problems and are present in almost in all part of the Ethiopian rift and cause economic or social losses on private properties, infrastructures and public properties (Plate 2.1).

Existing literatures indicated that most part of the Ethiopian Rift Valley is affected by NE–SW- or NNE– SSW-trending normal faults (Mohr, 1967; Di Paola, 1972). There are also suggestions for the presence of E–W direction of extensions which can be related to an oblique system of rifting (Boccaletti et al., 1998). Hence, tectonic movements are thought to be active in the region. The presence of faults dissecting recent formations, high seismicity and geothermal activities are common reasons cited by many authors as evidences for this. Therefore, when the ground cracks in Muleti, Lake Shala and Adamitulu area were appearing, there was an understanding that they could be manifestations of this activity or large-scale tectonic processes (Yirgu Gezahegn et al., 1997). However, this idea of linking the cracks to major tectonics has got no substantial evidences so far.

The Fentale region is one of several magmato-tectonic segments in the Main Ethiopian Rift. There is a significant drop in altitude from the Assela-Munessa area within the Aluto-Gedemsa magmatic segment to the Fentale segment. The width of the rift valley itself widens from about 70 km near the Assela Munessa to more than 100 km near the Fentale area. Around the Fentale region, the width of the rift dramatically increases and faults of multiple orientations forming rhomb shaped basins are observed. Based on the geometries of the faults in this particular magmatic segment, Casey et al. (2006)

According to (Williams et al., 2004), to the south of the Fantale caldera the welded tuff is cut by a series of some tensional fissures. They are concentrated within a 4 km wide, 7 km long belt. Beyond this belt they either disappear altogether, grade southwards into normal faults or are covered by the recent basaltic flows. They die out when traced northward up the flank of Fantale and do not cut the caldera wall on either side. At least two less well defined fissures occur northeast of the caldera. If these are included, the total length of the fissure belt is about 15 km.

2.10. Local Geology and Lake Beseka area

Lake Beseka and the new road route are situated in 20 km graben on the axial position of the rift floor in the northern part of the MER. Being part of the MER, the study area has been under intense volcanic and tectonic activities during the Quaternary period. The geology of the Fantale region is shown in Figure 2.6. Preliminary accounts of the Fantale volcano, its volcanic and tectonic setting and its geochemistry, have been given by Gibson (1969). The main volcanic

edifice rises approximately 600 m from the floor of the Rift Valley and its lavas, excluding the welded tuff, cover a roughly oval area of some100 km^2.

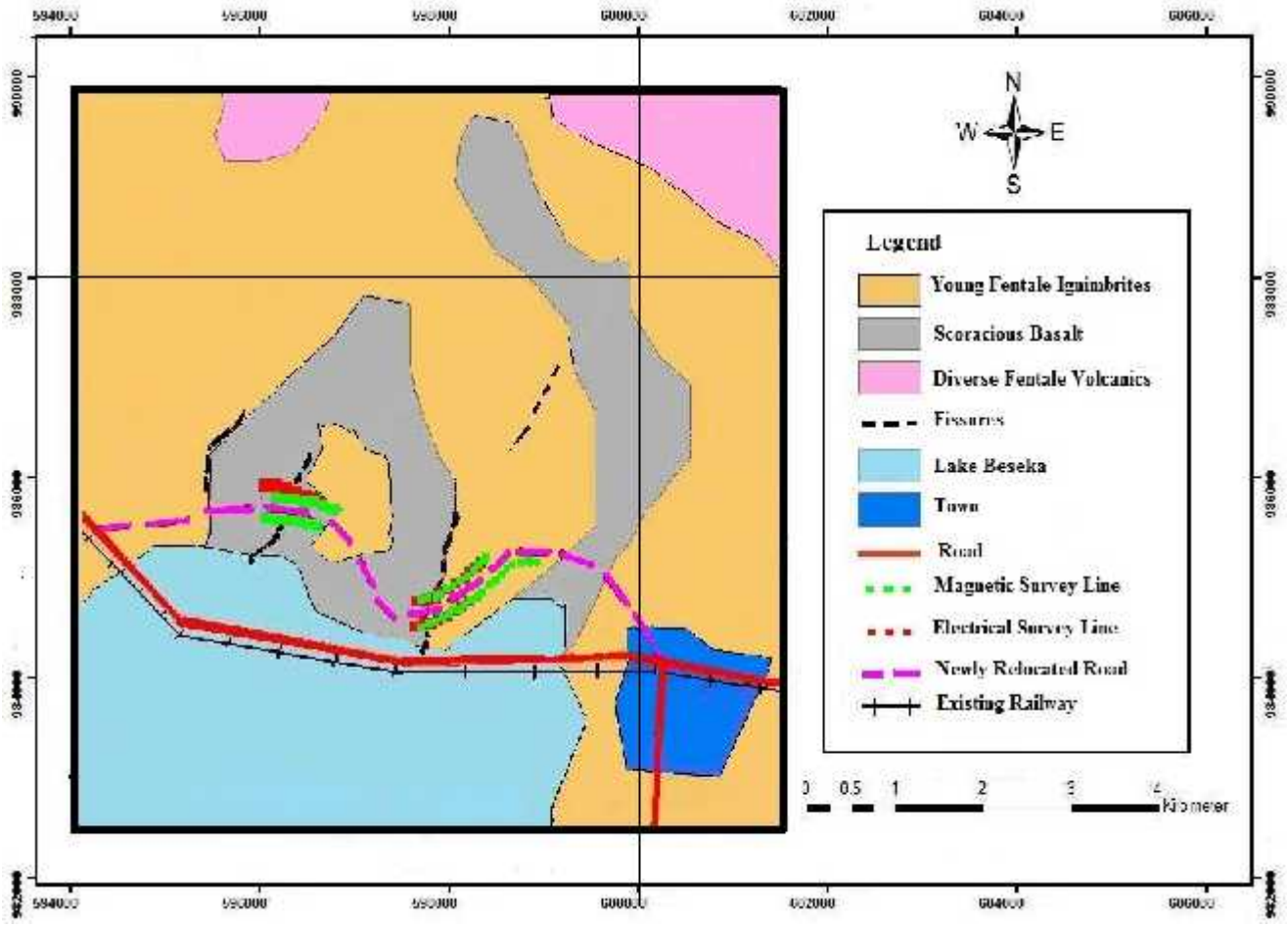

Figure 2.6. Local geological map of study area

The principal rock units in the study area are of two types as shown in the figure above: volcanic rocks mainly basalts and ignimbrites of different ages and different mineralogical composition and some sedimentary rocks of fluvio-lacustrine origin located at the Western and southern part of the study area (Abadir farm) and at the floor of Lake Beseka.

Most of the study area and shores of Lake Beseka are underlain by Pleistocene to sub recent basalt, often coarse grained with phenocrysts (Halcrow et al., 1979). Pleistocene basalts are exposed in most fault scarps and form the southeastern and western edges of Lake Beseka.

The eruption and collapse of the main Fentale caldera resulted in widespread deposition of the Fentale ignimbrite, which is a common rock type in the northern part of the study area. The

volcanic sequence of Fentale includes intermediate silicic flow of Tinish Fentale, rhyolitic lava flow, peralkaline obsidian, and pyroclastic deposit.

Like elsewhere in the Ethiopian Rift Valley, large part of the Awash basin including the study area is partly filled by lacustrine deposits. There is a general assumption that these deposits are the results of a big lake, which occupied once the entire floor of the rift valley, and can be Pliocene to recent in age (Di Paola, 1972). In the study area, lacustrine deposits consist of a heterogeneous sequence of clay, thin lenses of sand and silt, pumice fragments and other volcanic sediments. There is no information about the exact thickness of these deposits as borehole data is not present in the study area for the newly relocated road program. However, elsewhere in the rift, they are reported to be 40–50 m thick on average (Chernet Tadesse, 1985). Dug-holes that are drilled to a depth of up to 42 m in Lake Beseka area assured that the thickness of these sediments can be greater than 70 m. In order to determine the nature of soils in the upper few centimeters to meters of the ground surface, logging was conducted along the test pit. The upper 1.5 m of the ground surface, however, constitutes the top soil which of supports vegetation, aa lava flow and fentale ignimbrite. The predominant and important rock units of the area are briefly discussed below.

2.10.1. Fantale volcanic complex

The geology of the Fantale region is shown in Plate. 2.2 preliminary accounts of Fantale volcano, its volcanic and tectonic setting; and its geochemistry have been given by Gibson (1969). The main volcanic edifice rises approximately 600 m from the floor of the Rift Valley and its lavas, excluding the welded tuff, cover a roughly oval area of some 100 km^2 (Plate 2.2). The majority of lavas were apparently erupted from a centre, or centres, close to the pre-collapse summit of the volcano. They consist largely of trachytes and pantelleritic rhyolites. A trachyte flow about 3 km north of the caldera has been dated at 1.86 ± 0.1 Ma by K/Ar dating (Rex, personal communication 14/6/78). A younger group of trachytes and rhyolites was erupted from a satellite centre about 3.5 km from the centre of the main caldera.

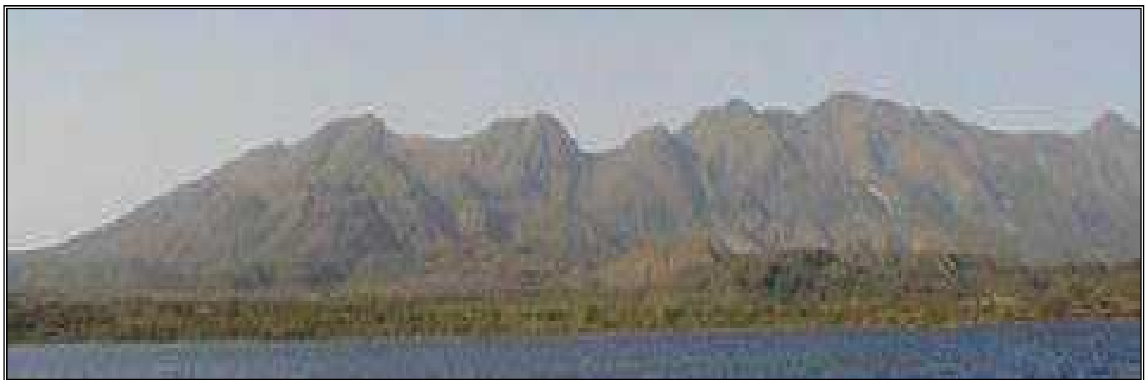

Plate 2.2.The Fantale Volcanic complex with the Lake Beseka on the foreground.

2.10.2. Pleistocene-Sub recent basalts

Compared to the other rocks found in the study area, this rock unit covers a considerably larger area. It is affected by atypical normal faults with varying vertical displacements characterized by hanging wall tilted away from the fault face. Some of the faults are now the boundary of the northwestern edges of Lake Beseka. These basalts are mostly dark grayish, massive, fine-grained, often sub aphyric with large phenocrysts. According to Buctwitz (2006), thin section of this rock shows a groundmass of needle-shaped plagioclase and pyroxene. Recent and sub recent basalts in the study area are intensely affected by factures, and create highly permeable aquifer zones around Lake Beseka. These basalts are fresh and highly jointed; and have a high degree of permeability and productivity (Chernet Tadesse, 1998). In addition to being affected by fractures, the basalts are characterized by primary porosities such as vesicular cavities, cooling joints and scoraceous intercalations. These porosities play an important role in creating favorable conditions for the formation of a weathered permeable zone. Weathering helps to intersect isolated vesicular or scoraceous pore spaces so as to enhance permeability of the formation (Plate 2.3).

Plate 2.3 Fantale sub-recent basalt

2.10.3. Young Ignimbrites of Fantale

In the study area, this unit is found at the northern part as it comes from Fantale Mountain and to Metehara town. This rock is highly affected by fissures (Plate 2.4C& D). North of the lake, there are a number of blisters on the Fantale ignimbrites. According to Tesema (1998), the blisters are formed as particularly a consequence of pyroclastic flows running over water on wet sediments. Thus, we can conclude that blisters would be best demonstrators of paleo-lake environment at that time (Plate 2.4A).

According to Buchwitz (2006), from XRD analyses, the Fantale ignimbrite is characterized by glass, up to 50cm diameter glassy, porphyritic fragments, most likely being lithic fragments of pitchstone than compressed fiamme. According to William et al. (2004), the pitchstone fragments are 168,000 ± 38,000 years of age as dated by fission track dating method.

2.10.4. Lava flows of young Fantale Volcanoes

The Fantale complex comprises two silicic caldera volcanoes: the older Tinish Sabober and the younger Fantale volcano which have a similar history according to William et al., (2004). The caldera eruption led to the deposition of Fantale ignimbrites which dominate the northern Lake Beseka basin. The lava flow, which earlier observers attributed to an eruption in the 1820's and is mostly unvegetated.

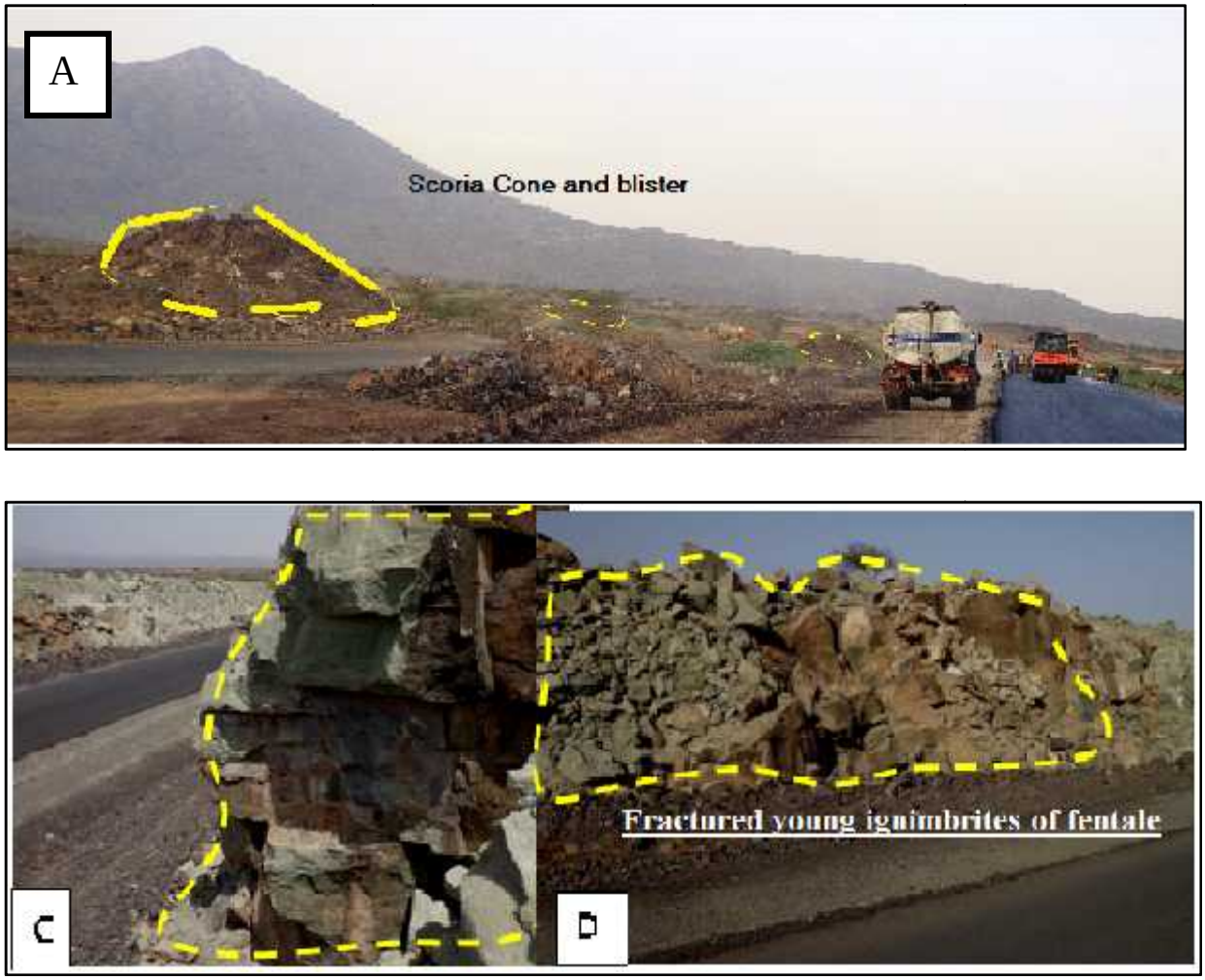

Plate 2.4 (A) Scoria cone and Cluster of Blisters and Fantale Volcano respectively and (C and D, yellow color) are Young ignimbrite of Fentale exactly at newly relocated road, which is used as backfilled materials for very huge fissures.

Recent and subrecent basalts in the study area are intensely affected by factures, and create highly permeable aquifer zones around Lake Beseka. These basalts are fresh and highly jointed; and have a high degree of permeability and productivity. In addition to being affected by fractures, the basalts are characterized by primary porosities such as vesicular cavities, cooling joints and scoraceous intercalations. These porosities play an important role in creating favorable conditions for the formation of a weathered permeable zone. Weathering helps to intersect isolated vesicular or scoraceous pore spaces so as to enhance permeability of the formation.

2.11. Structures in the study area (Local structures)

Fracture is a general term for all types of mechanical discontinuities or breaks in the host rock, including the two main types of fractures: extension fractures and normal faults. The term extension fracture is used when the separation is primarily by movement normal to the failure surface, but shear fracture (fault) when the separation is primarily by movement parallel to the failure surface. Fractured rocks comprise of a network of fractures that cut through a rock matrix. Fractures can be characterized in terms of their dimensions (aperture, length, width), their location (orientation, spacing etc.) and the nature of the fracture walls (e.g., surface roughness)

Visual manifestations of rift extension occur in the form of normal faults, tensional fissures and volcanic activity. This study is concerned with the observation of fractures, fault ground cracks and tensional fissures. Fissures have been described previously at several locations in the MER (Gibson, 1969; Gibson and Tazieiff, 1970; Asfaw Laikemariam, 1992, 1998; Mohr et al., 1967, 1980; Mohr, 1983, 1987a). Asfaw (1998) summarizes many fissures whose appearances were reported between 1956 and 1996. These occur in the thick unconsolidated lacustrine and volcanic sediments which cover the Rift floor. They generally appear as narrow cracks, which may be several hundred meters long, connecting subsidence pits up to several meters wide. In at least one case, they were associated with an earthquake swarm, and in almost all cases they were revealed as a result of sub-surface erosion and consequent slumping following heavy rains. The cracks sometimes appear to close as they become covered by a veneer of vegetation and sediment, and subsequently to reopen.

Existing literatures indicated that most part of the Ethiopian Rift Valley is affected by NE–SW- or NNE–SSW-trending normal faults (Mohr, 1967; Di Paola, 1972). There are also suggestions for the presence of E–W direction of extensions which can be related to an oblique system of rifting (Boccaletti et al., 1998).

Hence, tectonic movements are thought to be active in the region. The presence of faults dissecting recent formations, high seismicity and geothermal activities are common reasons cited by many authors' as evidences for this. In the field, extension fractures appear as open small valleys and are several meters long and reach up to 2-3m wide and approximately unknown depth to occasionally 6m. These valleys are typically open fissure shaped that distinguishes them from stream valleys and their orientations are not necessarily parallel to the local or regional slopes simply disturbed.

As it contact with saline water from the lake, they are mostly filled with blocks falling from their margins as well as sandy silty clay as a result of erosion and deposition there.

The NNE-SSW striking normal faults and fissure systems, which are mostly determining the lake shape, can be observed at the recent eastern and western shoreline and to the north of Lake Beseka. They often alternate with or occur in combination with monocline folds and many of the faults' hanging walls show tilting off the fault face (mostly towards the lake's interior). The observed structures appear to be generated in a process beginning with slight monocline folding and fissure formation which is followed by faulting when the displacement is growing. The greatest amounts of displacement (at a single fault) can be observed in the southeast and southwest of Lake Beseka where basalt rocks form the lake margins.

Interaction among the major faults systems have induced formation of complex fault patterns on the most active systems (Wonji Fault Belt) and facilitated the formation of secondary fault-related open structures. These secondary structures have served as the eruption sites for some of monogenetic volcanoes (e.g., scoria cones) in the rift valley (Korme Tesfaye et al. 2004), with chains of scoria cones having developed along the fracture of traces.

Close interaction between faulting and recent magmatism can be defined by the presence of alignment of cones along the orientation of faulting direction. In addition to the linear alignment of the scoria cones along those fissures, which helps to understand the interaction of faulting and magmatism, cone shape is also affected by the orientation of the structure, and is elongated along the fault direction. East and north of the study area, very small scoria cones and blister caves aligned along and cutting the fault/fissure, are good example of the relationship between faulting and volcanism.

Most of the fissures are open fractures with little or no vertical displacement and commonly with exact matching of opposite sides. Each main fissure is actually formed of a closely spaced group of gashes. They reach depths up to at least 6 m and individual gashes range in width from a few centimeters to 3 m (Plate 2.6 and plate 2.8). Fissures 1 and 2 are transitional northwards into normal faults. The orientation of the fissure belt is NNE-SSW, paralleling the dominant fault trend of the Wonji Fault Belt and sub-parallel to the NW-SE trending rift margins.

A general structural map of the Lake Beseka and Fentale areas is shown in Figure 2.7.

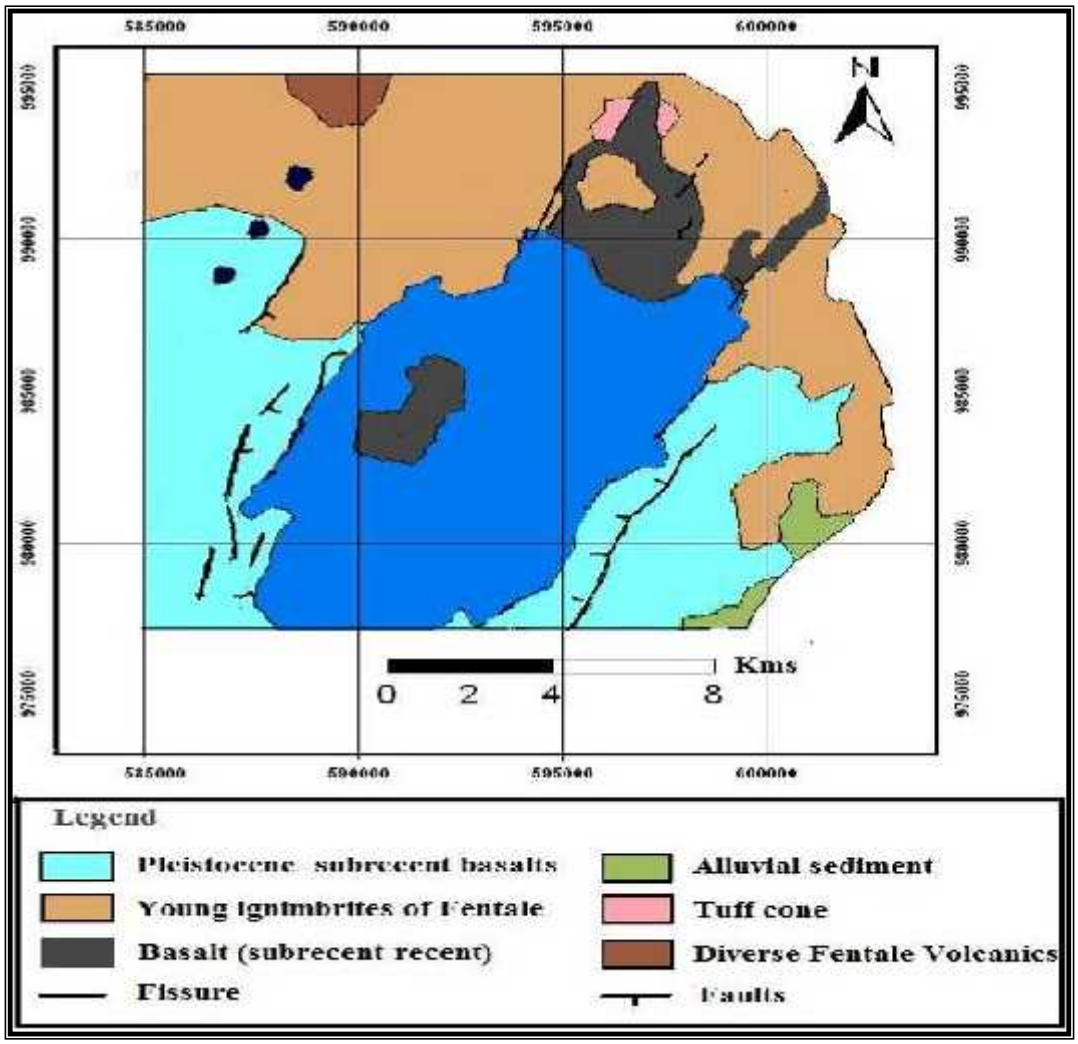

Source: (Modified from Geological map of Nazareth sheet 1:250000, and unpublished map)

Figure 2.7. Structural Map of the study area and the surrounding

2.12. Assessment of the Morphology and characteristics of Cracks and Fissures

A detailed survey and mapping of the fissures was carried out using aerial photographs as a base. Four lines magnetic and three Electrical imaging lines were then surveyed, crossing the fissures at right angles (running East–West), and the width (opening) and spacing's of each component of the two major fissures was measured by meter tape along each line. A detailed plan of the fissures and survey lines is shown in Plate 2.6 where the widths shown are the total width of each fissure as shown in the Table 2.3.

Recent faults seem to be affected by dyking. The faults within the area of investigation have very atypical morphologies. Profile across the fissure from field observation (Plate.2.5 and figure 2.8) indicates that the faults show the morphology of typical faults. The footwall remains flat and the concave hanging wall curves up and dips away the fault plane (Kurz et al., 2007) as shown in figure below.

Plate2.5.Fissures and fractured zones running in a N–S direction crossed by the new road.

Table 2.3 Measured widths (m) of fissures in the NW and NE of Lake Beseka.

Survey Lines direction (E-W)	**Fissures orientation (N-S)**		**Average extension and length the fissures in the direction of North-South**
	One	**Two**	
Line 1	2.5	Not crossed	2-2.5 and 350m for fissure one
Line 3	3		
Line 2	Not crossed	Trace (≈ 0.2)	>2 and more than 700m long
Line 4		2	

For the total length of the fissure located northwest as shown in figure 2.8 and parts of a fissure located northeast as shown (Figure.2.9), GPS measurements were taken along the direction of the fissure at both sides of the fissure and across the fissure at intervals about 20-30m (see Annex)

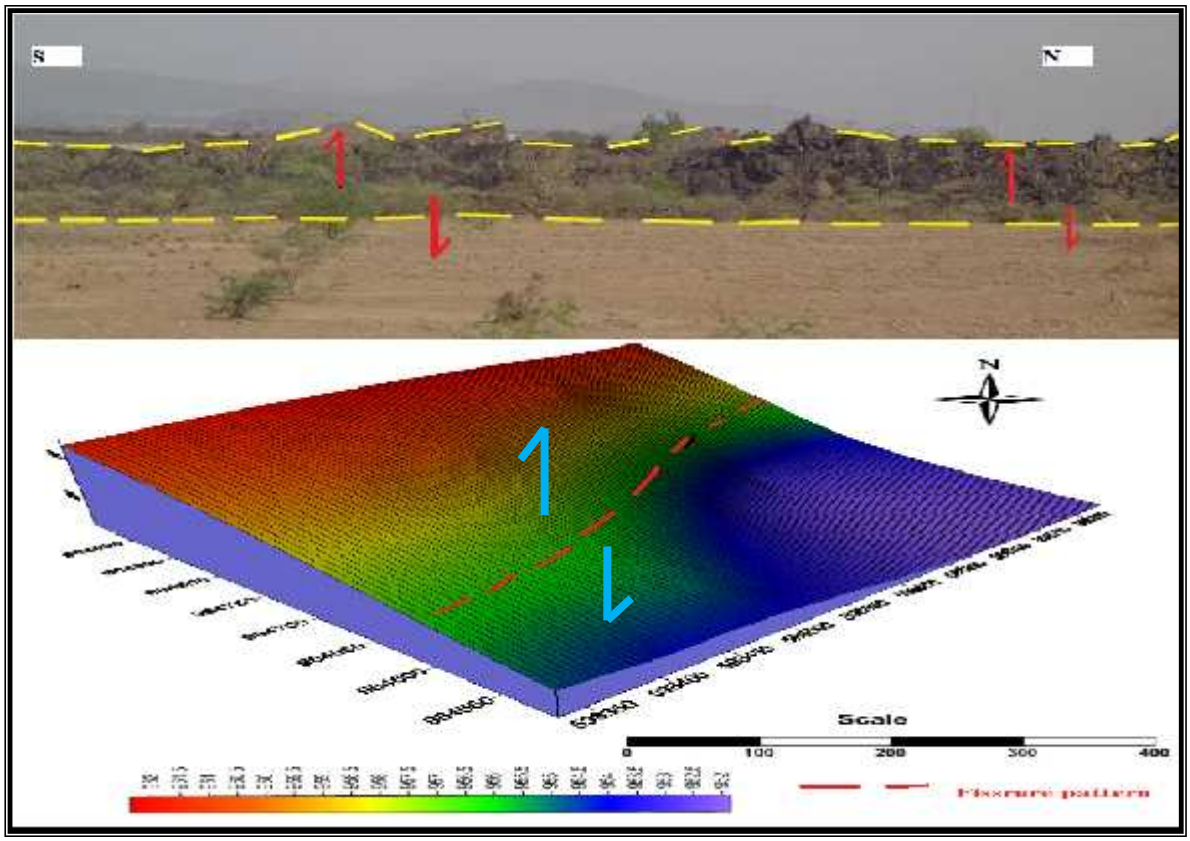

Figure 2.8 3D model of the physiographic features and fissure/crack alignment (line 2 and 4)

The NNE-SSW striking normal faults and fissures system, which are mostly determining the lake shape, can be observed at the present northeastern and northwestern shoreline of the north and south of Lake Beseka. The open fissures reach up to 3-5m width and about unknown depth. The wider fissure were found northwest of Lake Beseka (Plate. 2.6)

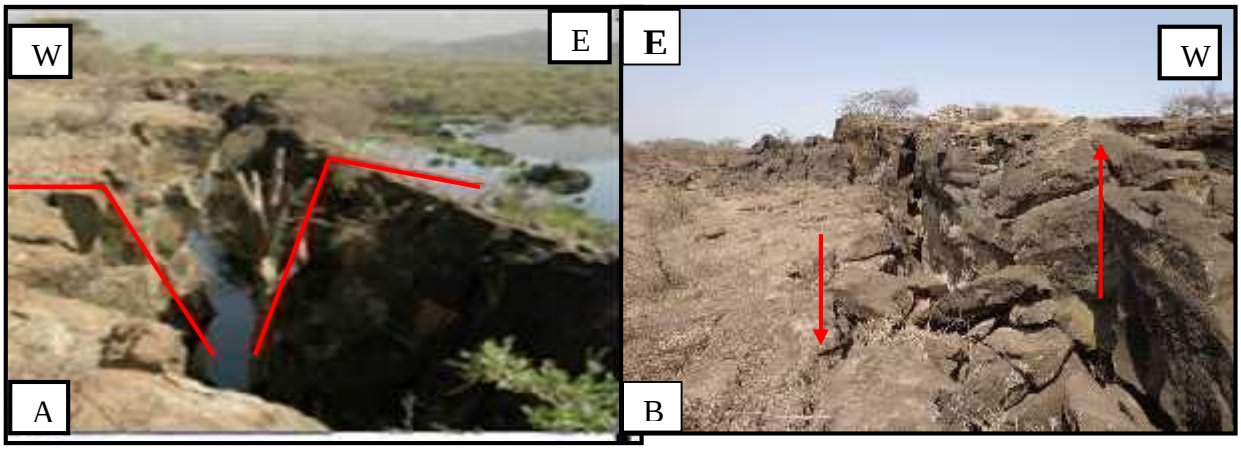

Plate.2.6 Fracture outcrops at NW **A)** Fissure form northeast of Beseka, hanging wall dipping to East which is very close to the lake and gradually opened as it contact with the water from the lake. **B)** Fissure and fractures form northwest of Beseka, hanging wall dipping to east (15°-20°) and has vertical offset of 1.5-2m.

Extension fractures of the atypical faults in the field have vertical small offset shown by faults (Plate 2.6). But towards the end of the total length these fractures, at north, they are characterized by vertical extension fracture die out which is the termination of the normal faulting.

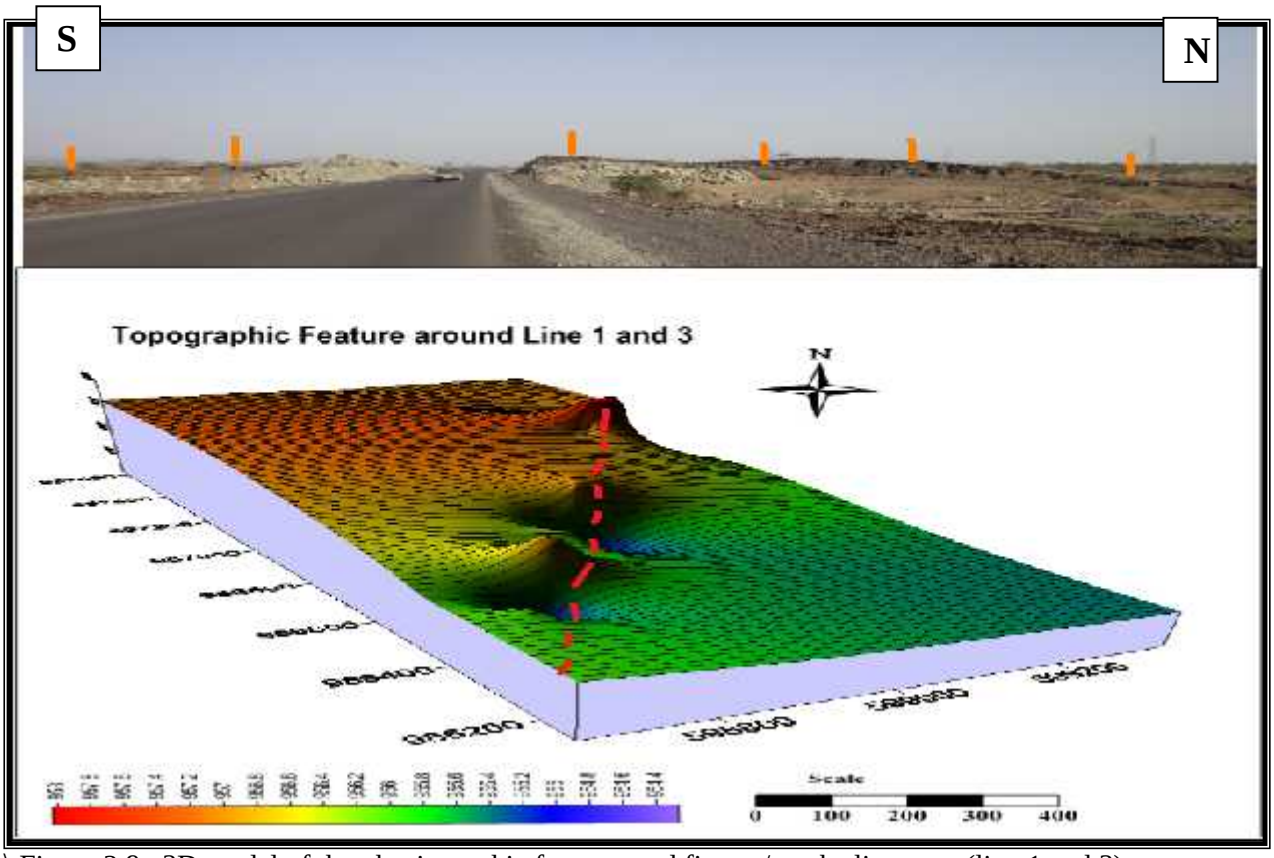

\ Figure 2.9 3D model of the physiographic features and fissure/crack alignment (line 1 and 3)

Plate.2.7.Topographic feature and extended fissure and fractured zone

It is situated at the NW of Lake Beseka, in south part of the new route near the lake shore which used these fissures for Lake Beseka advancement through the cracks at NW.

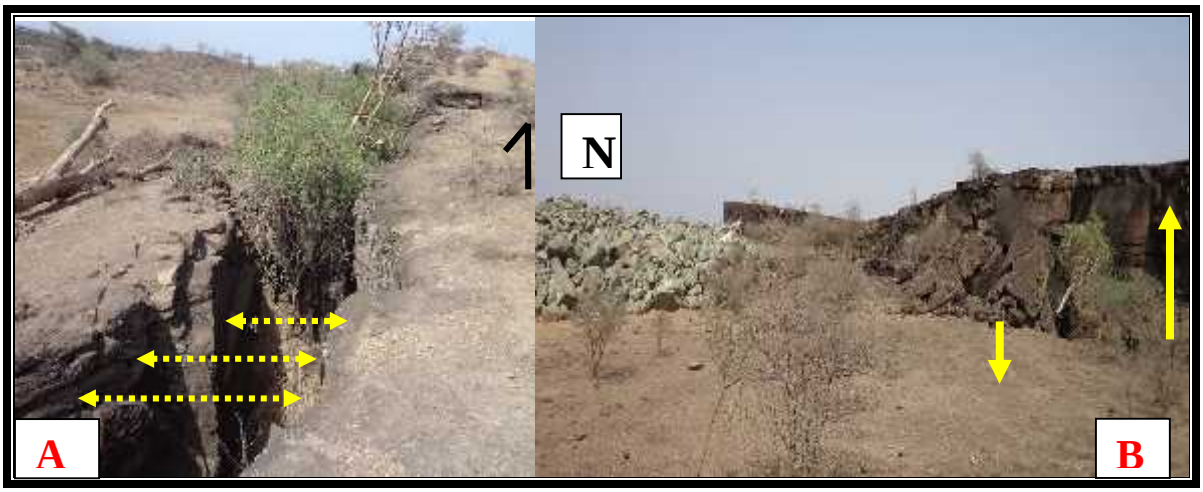

Plate.2.8 Extension Direction

(A) (E – W), propagation at northeast and (B) Vertical extension fracture (N – S) crossed by new asphaltic road under construction and northwest of Lake Beseka respectively.

The proposed extension direction is either mainly E-W (roughly perpendicular to the EARS trend (Ebinger, 1989; Morley et al., 1992; Foster and Jackson, 1998 Boccaletti et al., 1998, 1999; Chu and Gordon, 1999) or NW-SE, i.e. oblique to the EARS trend (Strecker et al., 1990; Chorowicz et al, 1992).

From site observation, dyke induced fault was recognized at northern section of Lake Beseka. Right step and vertical stress above an upward-propagating dyke is enlarged and leads to fracturing. Then the fissure propagates to the surface almost parallel to the region structural orientations. After reaching the surface on the upper side of the monocline as a nearly vertical fracture, vertical and horizontal spacing grows resulting in a normal fault with atypical profile and in the meanwhile the dyke may propagate further to the surface.

Besides field notes, analysis from aerial photographs also help us to understand the alignment of local faults and fissures with respect to Wonji Fault Belt (WFB), which is constituted by a number of right-stepping en-echelon fault/fissure arrangements as shown in (Figure.2.10A) and also the presence of left-steeping segments (Figure.2.10B). From the structural map of the study area there are also right-steeping fault arrangements within the faults found at the North western and north eastern edges of Lake Beseka.

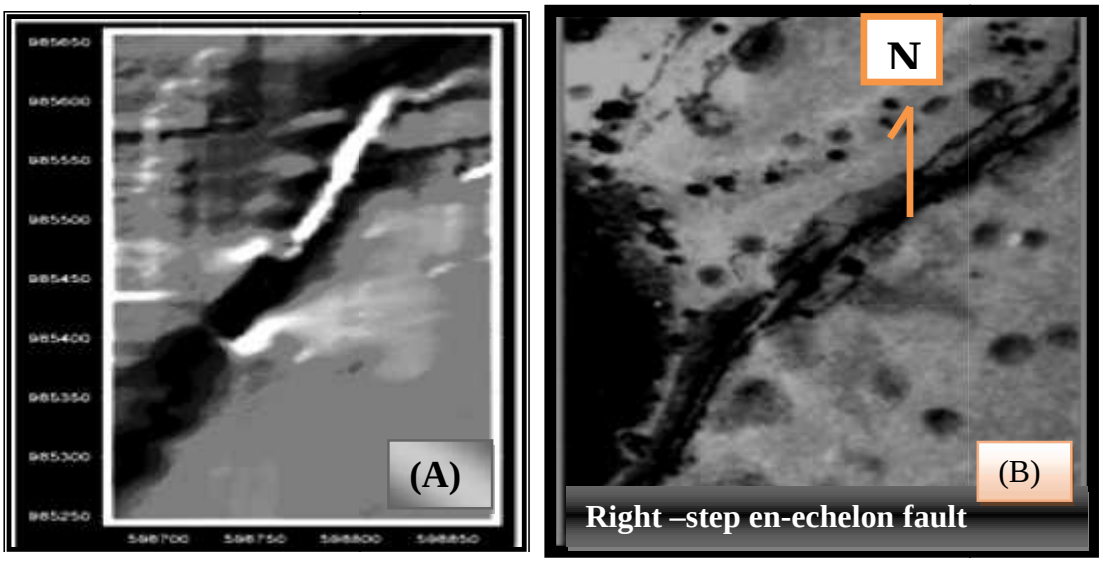

Figure.2.10 Aerial photograph (1975) showing fault/ fissure morphology in the NE of Lake Beseka (A) Show along and across the fissure features in the NW of Lake Beseka, (B) Right-stepping segments in fault/ fissure system.

Early works (McKenzie et al., 1970; Le Pichon and Francheteau, 1978), based on plate kinematics observation at Afar triple junction, proposed a NW-SE extension direction for the MER since the Late Miocene, which is the inferred age of the onset of rifting (Weldegabrieal G. et al., 1990). These results have been supported in part by subsequent field surveys and remote sensing studies on Quaternary structures (Chorowicz et al., 1992; Korme Tesfaye et al., 1997), (Mohr et al., 1968; Bilham et al., 1999).

Nevertheless, an increasing number of studies, especially in the last decade, have suggested an overall E-W extension direction for the MER. These studies are based on plate kinematics calculations Miocene-Quaternary extension, (Chu and Gordon, 1999), focal mechanism studies present day extension; (Foster and Jackson, 1998), and Test pit excavation breakout data present day extension. On the basis of both the general fault pattern and structural analysis, the recent evolution of the Ethiopian Rift has been related to a nearly E-W oriented extension direction, which trends about 50^{o} to the rift axis (Boccaletti et al., 1992,; Abebe Bekele, 1992). Such stretching direction is consistent with the occurrence of both the diffuse horizontal left lateral shear component along some WFB faults (Boccaletti et al., 1992, Abebe Bekele, 1992).Some other works, based on structural considerations on Quaternary faults (Mohr, 1968; Gibson, 1969) and focal mechanism interpretation, suggest a Quaternary left-lateral component of shear along the MER. This component is kinematically consistent with an E-W extension direction.

In the area under investigation, especially near the New road relocation at north of Lake Beseka, it is observed development of fractures interaction at different phase. Primarily, the fracture fragments are propagating towards each other and characterized by common configuration. Again these fracture segments are bending toward each to other to form an overlap zone. (Plate 2.9) the last stage is constituted by further propagation of one of the fractures and linkage with the other. This leads to the abandonment of the less propagating segment and to the development of a single continuous structure.

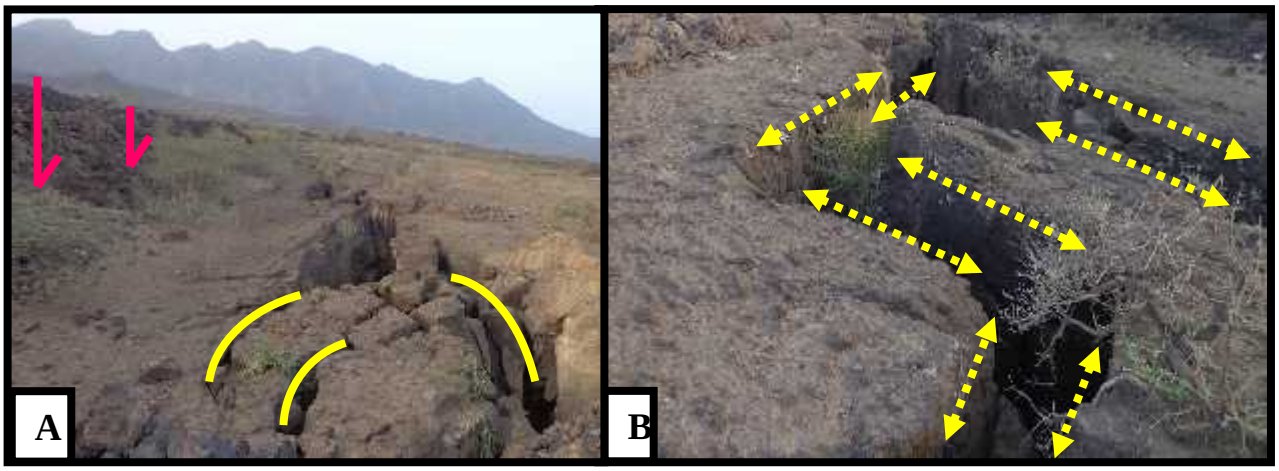

Platee.2.9 Fissure pattern and Geometry at NE of the Lake Beseka

A) Vertical movement, fracture interaction and Right – stepping fault and fractures interaction at different phase B) Fractures segments and linkage with the other and finally Saline water from Lake Beseka expand to northing using cracks/fissures as a conduit and opening direction also propagating as contact with water.

CHAPTER 3: THEOREYOF GEOPHYSICAL ANDGEOTECHNICAL METHODS

3. 1. Geophysical Methods

3.1.1 Introduction

Geophysical methods help to resolve geotechnical problems and are capable of mapping engineering properties of soils and rocks. Geophysical tools are designed to measure specific parameters, and are generally used to measure spatial variation in these specific parameters within the area of interest. The specific parameters measured by geophysical tools are functions of the physical properties of the Earth's subsurface. Among the common applications of geophysics in highway engineering investigations, the following can be mentioned:

Subsurface characterization: bedrock depth, rock type, layer boundaries, water table, locating fractures, weak zones, etc. The routinely studied Engineering properties of Earth materials include; stiffness, density, electrical resistivity, porosity, among others.

Highway subsidence, detecting fault and fractures beneath roadways, locating buried manmade objects, buried utilities; underground storage tanks are the other targets of geophysical investigations in engineering geophysics.

3.2. Electrical Imaging methods

At present, field techniques and equipment to carry out 2-D resistivity surveys are well developed. One technique used to extend horizontally length covered of the survey, particularly for a system with a limited number of electrodes, is the roll along method. After completing the main sequence of measurements, one of cable is moved to the end of the line.

A more accurate model of the subsurface is a two-dimensional (2-D) model where the resistivity changes in the vertical direction, as well as in the horizontal direction along the survey line. In this case, it is assumed that resistivity does not change in the direction that is perpendicular to the survey line. However, at the present time, 2-D surveys are the most practical economic compromise between obtaining very accurate results and keeping the survey costs down.

3.2.1 Forward Modeling

Forward modeling in electrical prospecting is a technique to model a subsurface by estimating the actual resistivity of the different geological structures. The estimation is made by calculating the resistivity of the respective ground structure using the fundamental theoretical equations.

The resistivity response for a 2-D model is calculated and displayed as a 2D inverse model for comparison with the original field data. This approach is used to generate realistic subsurface geometries in definable model structures (Reynolds, 1997).Forward modeling operates through a process which divides the subsurface is into a large number of small rectangular cells (McDowell et al., 2002).

3.2.2 Basic Inverse Theory

Geophysical data inversion is a method designed to find a model that gives rise to a parameter similar to the actual measured parameters or data. The model is an idealized mathematical representation of a section of a subsurface earth, having a set of model parameters that are the physical quantities that are estimated from the observed data. The instrument measures the apparent resistivity of the subsurface materials. This is not the true resistivity of the sub surface materials. The relationship between the apparent resistivity and the true resistivity is a complex relationship. The complex mathematical formulation required to determine the true subsurface resistivity from the apparent resistivity values is inversion problem. A program developed to solve this problem is referred to as an inversion program.

The optimization method basically tries to reduce the difference between the calculated and measured apparent resistivity values by adjusting the resistivity of the model blocks. A measure of this difference is given by the root-mean squared (RMS) error. However, the model with the lowest possible RMS error can sometimes show large and unrealistic variations in the model resistivity values and might not always be the "best" model from a geological perspective. In general the most prudent approach is to choose the model at the iteration after which the RMS error does not change significantly. This usually occurs between the 3rd and 5th iterations. In all optimization methods, an initial model is modified in an iterative manner so that the difference between the model response and the observed data values is reduced. The set of observed data can be written as a column vector **y** given by

$$y = col(y_1, y_2, ...y_m)$$

Where **m:** is the number of measurements.

The model response **f** can be written in a similar form $f = col(f_1, f_2, ... f_m)$

The difference between the observed data and the model response is given by discrepancy vector **g** that is defined by: $g = y - f$

In the least square optimization method, the initial model is modified such that the sum of squares error **e** of the difference between the model response and the observed data values is minimized and is given as (Loke, 1999). $e = \sum_{i=1}^{n} g^2 = g^T g$

The above equation can be rewritten as $e = \sum_{i=1}^{n} \sqrt{(m_i - r_i)^2}$

Where, r_i is the i^{th} calculated resistivity value, m_i is the i^{th} observed apparent resistivity and n is number of measured data. To get minimum **e** (root mean square error, RMS) the smoothness constrained least square method is used. It is given as

$$d\left(J^T J + U.F\right) = J^T g - UFr$$

where, $F = f_x f_x^T + f_z f_z^T$, f_x is vertical flatness filter, J is matrix of partial derivatives, U is damping factor, d is model perturbation factor, r is a vector containing the logarithm of the model resistivity value and g is discrepancy vector.

3.2.3. Field Survey and Instrument Configurations

The 2D imaging data were collected using IRIS SYSCAL Pro R1 plus Switch 72 instrument. The instrument consist 72 electrodes which are connected via a multi-core cable with a takeout at every 5m spacing for electrode connection. The 2D Electrical Imaging data are acquired along traverses which were selected to collect a representative and detailed information about the area around the dam foundation.

Table 3.1 Setting of SYSCAL unit and Electrode configuration

Electrode configuration type: Combination of Wenner Schlumberger			
Equipments type : SYSCAL R1 Plus Switch 72			
Parameter/ Setting	EISurveyL-2	EI Survey L-3	EI Survey L-4
Electrode spacing (m)	5	5	5
Length of Outline (m)	450	360	540
Depth of investigation (m)	65	65	65
Number of electrodes	90	72	108
Number of data points	945	648	1215
Sequence type	Main	Main and 1-Roll Along	Main and1-Roll Along

Measured resistivities in Earth materials are primarily controlled by the movement of charged ions in pore fluids. Although water itself is not a good conductor of electricity, ground water generally contains dissolved compounds that greatly enhance its ability to conduct electricity. Hence, porosity and fluid saturation tend to dominate electrical resistivity measurements. In addition to pores, fractures within crystalline rock can lead to low resistivities if they are filled with fluids.

3.3. Magnetic method

3.3.1. Introduction

The aim of a magnetic survey is to investigate subsurface geology on the basis of anomalies in the Earth's magnetic field resulting from the magnetic properties of the underlying rocks. Although most rock-forming minerals are effectively non-magnetic, certain rock types contain sufficient magnetic minerals to produce significant magnetic anomalies.

One of the applications of magnetic method in engineering site investigation is to locate contact between different lithologic units and geological structures that exhibit magnetic contrasts such as faults or dykes. To interpret the magnetic data in terms of such subsurface indications, the magnetic data are presented in different forms.

3.3.2. Basic Concepts

The applicability of magnetic methods is so wide that it is generally a sound policy to include a magnetic survey in every comprehensive Geophysical campaign i.e. it is used for reconnaissance survey. The principal operation of magnetic survey is quite simple. When a ferrous material is placed within the Earth's magnetic field, it develops an induced magnetic field.

The earth's magnetic field is generated by electrical currents circulating in its outer core. Values of total intensity of the earth's magnetic field vary from about 74 000 gammas (1 gamma = 1/100 000 oersted) at the poles to 30 000 gammas at the equator. The major variations in field strength and polarity direction relate to major continental scale and deep seated geological factors. Minor and local variations depend upon the nature of near-surface geological materials. Irons bearing geological bodies are magnetic and the materials of which they are composed have high "magnetic susceptibility". The intensity of the earth's magnetic field tends to be higher over bodies of minerals of high magnetic susceptibility. Magnetic susceptibilities of common minerals and rocks are given in the section of chapter 5.

Around a bar magnet, a magnetic flux exists, as indicated by the flux lines in figure 3.1, and converges near the ends of the magnet, which are known as the magnetic poles. If such a bar magnet is suspended in free air, the magnet will align itself with the earth's magnetic field with one pole (the positive north seeking) pointing towards the earth's North Pole and the other (the negative south-seeking) towards the south magnetic pole. Magnetic poles always exist in pairs of opposite sense to form a dipole. When one pole is sufficiently far removed from the other so that it no longer affects the other, the single pole is referred to as a monopole.

If two magnetic poles of strength P_1 and P_2 are separated by a distance r, a force F exists between them. If the poles are of the same sort, the force will push the poles apart, and if they are of opposite polarity, the force is attractive and will draw the poles towards each other. Note the similarity of the form of the expression below with that for the force of gravitational attraction;

both gravity and magnetism are potential fields and can be described by comparable potential field theory.

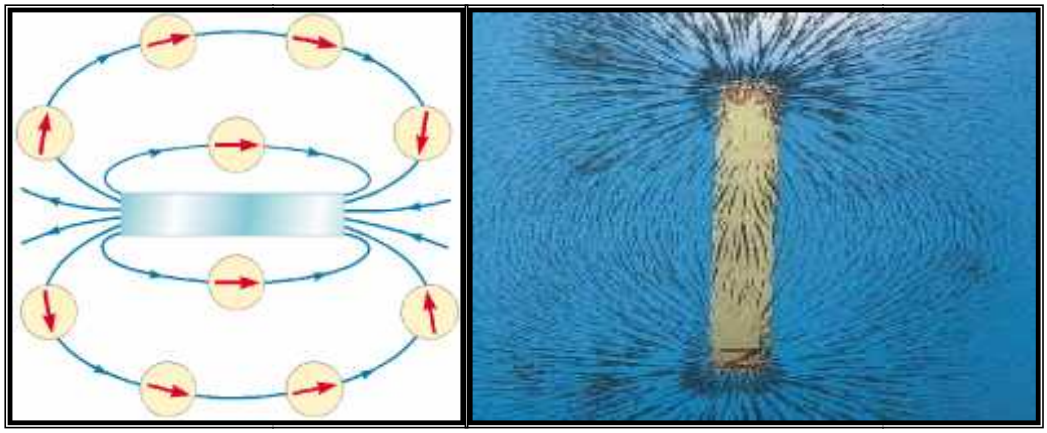

Figure 3.1 Compass needles trace the magnetic field lines and magnetic field pattern

$$F = \frac{p_1 p_2}{\mu r^2}$$

Where:μ is a constant of proportionality known as the magnetic permeability,

$P_1$and P_2 are the strengths of the two magnetic monopoles, and

r is the distance between the two poles.

The constant, μ depends upon the magnetic properties of the medium in which the poles are situated. This force is attractive, if the poles are different in sign, and repulsive in they are of like in sign.

Magnetic susceptibility is a physical property that changes significantly from one rock type to another. Another such property is natural magnetization. Knowledge of the distribution of any of these properties within the ground would convey information about the subsurface Geology.

$\boldsymbol{J = KH}$, H = Applied field (in the lab).

Where: H= Magnetic field intensity (Earth's field). J = Induced magnetization &

K= Magnetic susceptibility.

Each of the properties mentioned above is the source of a potential field which is intrinsic to the body possessing that property and which acts at a distance from it.

A more practical quantity than the force is the strength of the magnetic field existing at a point in space, as a result of a pole strength p1 located at a distance r from it. The magnetic field strength H is defined as the force per unit pole:

$$H = \frac{F}{p_2} = \frac{p_1}{\mu r^2}$$

The poles of a magnet exist in pairs and they referred as dipoles. The magnetic moment M of a dipole with strength p and a distance L apart given by: **M = PL**

In magnetic prospecting, the susceptibility is the fundamental material property whose spatial distribution we are attempting to determine. In this sense, magnetic susceptibility is analogous to density in gravity surveying. The ratio of the flux density B (also called magnetic induction) to the magnetizing field strength H is a constant called the absolute magnetic permeability (μ). Practically, the magnetic permeability of water and air can be taken to be equal to the magnetic permeability of free space (vacuum), denoted by $\mu_0$which has the value of $4\mu x10^{-7}$ Wb/Am. For any medium other than a vacuum, the ratio of the permeability's of a medium to that of free space is equal to the relative permeability μ_r such that $\mu_r = \mu/\mu_0$and, as it is a ratio, it has no unit.

$B = \mu H$ since $\mu = \mu_r\mu_0$, the above equations becomes, $B = \mu_r\mu_0 H$. In magnetic prospecting, we measure **B** about $\mathbf{10^{-4}}$of the earth's main field**.**

Dykes, folded or faulted sills, lava flows, basic intrusions, metamorphic basement rocks and ore bodies that contain magnetite all generate large-amplitude magnetic anomalies. Other targets suitable for study using magnetic are disturbed soils at shallow depth, open pits and fractures, all of which are of interest in engineering studies.

3.3.3 The Earth's magnetic field

The geomagnetic field at or near the surface of the Earth originates largely from within and around the Earth's core. Ninety percent of the Earth's magnetic field looks like a magnetic field that would be generated from a dipolar magnetic source located at the center of the Earth and aligned with the Earth's rotational axis. The remaining 10% of the magnetic field cannot be explained in terms of simple dipolar sources.

The main field is the largest component of the magnetic field and is believed to be caused by electrical currents in the Earth's fluid outer core. For exploration work, this field acts as the induced magnetic field. The external magnetic field is a relatively small portion of the observed magnetic field that is generated from magnetic sources external to the earth. This field is believed to be produced by interactions of the Earth's ionosphere with the solar wind. Hence, temporal variations associated with the external magnetic field are correlated to solar activity. The crustal

field is the portion of the magnetic field associated with the magnetism of crustal rocks. This portion of the field contains both magnetism caused by induction from the Earth's main magnetic field and remnant magnetization (Thomas, 2003).

3.3.4 Time Varying Earth's magnetic field

It was recognized that the Earth's magnetic field changes its direction and intensity with time. These variations resolved in to secular variation, diurnal variation and variations due to magnetic storms. It is clear that the geomagnetic and magnetic poles positions drift with time, known as secular variation in the magnetic field. In addition, the intensity of the main magnetic field is decreasing at about 5% per century. The rate of change, although very significant on a geological time scale, does not affect the data acquisition on a typical exploration survey unless it covers large geographical areas and takes many months to complete. Diurnal variation is the variation in the magnetic field that occurs over the course of a day and related to variations in the Earth's external magnetic field. These are caused by changes in the strength and direction of the currents in the ionosphere. This variation can be on the order of 20 to 30 nT per day and should be accounted when conducting exploration magnetic surveys.

In addition to the predictable short-term variations in the earth's field, there are transient disturbances, which by analogy with their metrological counterparts are called magnetic storms. Such storms cause considerable disruption in magnetic prospecting operations. The oscillations that take place while they are going on are so rapid and unpredictable that it usually is not feasible to correct for them as with diurnal variations. Magnetic surveys must generally be discontinued during storms of any severity. From the equator to latitude of 600, the oscillations during such storms may have amplitude as great as 1000 gammas.

3.3.5. The earth's magnetic elements

A vector is used to represent the earth's magnetic field at an observation site. This vector is described by a combination of seven quantities we call the magnetic elements. Magnetic declination, d, is the angle between geographical north and the direction of north that is indicated by a compass. Inclination, i, is the angle between the field direction and a horizontal plane. The total field intensity F can be separated into a vertical component Z and a horizontal component H in the magnetic north direction. That horizontal component can be separated into an intensity

component X in the geographical north direction and an intensity component Y in the geographical east direction. These seven magnetic elements are related in the following ways:

$F^2 = H^2 + H^2 = X^2+Y^2+Z^2$, $F=H/\cos i = z/\sin i$ $\cos d=X/H$, $\sin d = Y/H$

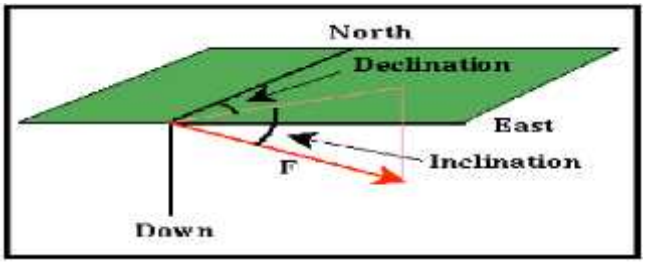

Figure 3.2: The elements of magnetic field.

As far as exploration geophysics is concerned we can separate the earth's magnetic field in to the following three parts: 1. the main magnetic field, which is produced in the core of the earth and accounts for the very large regional variations in the field intensity and direction. 2. The external magnetic field, which is produced by electric currents in the earth's ionosphere consisting of particles ionized by solar radiation and put into motion by the solar tidal force. 3. The anomalous magnetic field, which is produced by ferromagnetic minerals in the earth's crust.

Mathematically we can write the above as follow

$$B_T = B_{ext} + B_{inter} = B_{ext} + B_D + B_{rm}$$

Where: B_T: the total magnetic field,

B_{ext}: External magnetic field; B_{rm}: The field of rock magnetism

B_D: Dipole field, which is generated by the fluid outer core.

3.3.6. Noise and Corrections for Magnetic Variations

All magnetic data sets contain elements of noise and will require some form of correction to the raw data to remove all contributions to the observed magnetic field other than those caused by subsurface magnetic sources. In ground magnetometer surveys, it is always advisable to keep any magnetic objects (keys, penknives, wristwatches, etc), which may cause magnetic noise, away from the sensor. It is also essential to keep the sensor away from obviously magnetic objects such as cars, metal sheds, power lines, metal pipes, electrified railway lines, walls made of mafic rocks, etc. There are several ways of correcting magnetic data according to the various magnetic

variations. For the secular variation of magnetic data a model is known as International Geomagnetic Reference Field (IGRF) has been prepared from comparison of individual magnetic responses in different areas of magnetic observatories. So, it has become standard processing practice for magnetic survey that the applicable IGRF (updated to the time of the survey) is subtracted from the observed values of the total magnetic intensity. The most significant correction is for the diurnal variation in the Earth's magnetic field. The necessary corrections are mostly attempted by the reoccupation of the base station which is located in or near the survey area. Variations in magnetic field due to magnetic storms can be so rapid, unpredictable, and of such large amplitude, that normally no corrections can be made. Magnetic surveying is therefore generally discontinued under these conditions.

3.3.7. Magnetics Instruments

In the vast majority of the cases where the magnetic targets have a substantial strike length, survey profiles should, whenever possible, be conducted across strike. In ground based surveys, it is important to establish a local base station in an area away from suspected magnetic targets or magnetic noise and where the local field gradient is relatively flat. A base station was carefully selected and established in an area away from the magnetic noise like buildings, iron sheet, railway, etc. A base station should be quick and easy to relocate and reoccupy. As the survey progresses, the base station must be re-occupied every half of an hour in order to compile a diurnal variation curve for later correction (Reynolds, 1997).

3.3.8. Magnetic Data Reduction

All magnetic data sets contain various components and elements of noise and as such require some form of correction on the raw data to remove all contributions to the observed magnetic fields other than those caused by the sub surface magnetic sources. The most significant correction is for the diurnal variation (ΔB) in the earth's magnetic field. Base station readings taken over the period of a survey facilitates the compilation of the diurnal variation. Measurements of the total field made at other stations can easily be adjusted by the variation in the diurnal curve. The dipole field was determined from international geomagnetic reference field (IGRF) map is subtracted from the measurements at each station to generate magnetic anomalies as:

$$\Delta B = B_{obs} \pm \delta B - B_d$$

3.4 .Geotechnical Methods (Direct Methods)

3.4. 1. Introduction

Field investigation involves exploring the ground conditions at and below the surface. It is the Prerequisite for the successful and economic design of engineering structures and earthworks. Insufficient or inadequate information of subsurface with respect to the character of the ground can lead to the production of an unsatisfactory design, which may subsequently result in serious damage, or even failure of the structure. Any attempt to save on cost by having a low budget for an investigation may cause additional expenditure later if unfavorable ground conditions are found during and after construction. (Raghuvanshi, T.K. (2010).

The purpose of this section is to provide information on various direct subsurface explorations, laboratory and in situ testing methods, and classification of soils formation. This information helps to establish engineering geological properties of soils and rocks that are important for design of relocated road embankment conditions. The execution of a conventional subsurface exploration and testing program usually includes pits, laboratory and in situ testing.

3.4.2Field Investigation for Sub grade Soils

3.4.2.1. Sub grade soil survey

The purposes of the sub grade investigation include; evaluation of depth and nature of the sub-grade soil along the route corridor, assessment of suitability of the soil, and identifying the location, depth and nature of problematic sub grade soil sections along the project stretch. This would enable to suggest possible treatment or remedial measures that would suit the pavement design. The sub grade soil investigation carried out comprises field survey and laboratory test result analysis and has been discussed in the following subsections.

3.4.3. Visual identification

Surface assessment, geological and physiographical observations and explanations can give indicators of types of soils. The morphological description includes a multitude of many characters such as role of ground water table situation, color of the soil, soil consistence, soil texture, soil structure, etc. Most of the relevant physical properties to give indicators of bearing capacity potential are obtained by performing geotechnical index tests such as Atterberg limits, unit weights

and grain size distribution. Other tests include direct tests to determine the swell potential including volume change tests. (Nigatu Fekadu, 2006)

The soil extension survey was carried out in such a way that different soil types along the alignment have been recorded and classified according to color, texture and composition. In many cases, there is no clear distinction between the individual soil types and could not be made due to their similarity in origin and soil properties and highly affected by geological processes.

To examine the vertical extent of different types of the sub-grade soils, test pits were excavated at required intervals and the position of each test pit was marked by hand held GPS. Field identification of sub-grade soils has been based on color, texture as well as on the assessment of their plasticity, fine content and coarse fractions.

Upon completion of the sampling processes the vertical profile of each test pit has been logged. Graphic log and descriptions of the materials for each test pit is shown in Annex, on test Pit Graphic log.

3.4.4. Laboratory Tests for Subgrade soil

The laboratory investigations work encompasses the testing on representative samples of the subgrade soils. The purpose of the testing is to evaluate the strength and the suitability of the road subgrade soil. This is done by assessment of the test results against the recommended specification requirement.

3.4.4.1. In-Situ Density (compaction) Determination Test

The in-situ density of the sub-grade under existing road has been determined at 1-2km interval where samples for laboratory CBR test were collected. The tests were conducted immediately on the newly relocate route layer on the roadbed using sand replacement method in accordance to AASHTO T-191-93. At each location the surface of the sub-grade to be tested was trimmed and smoothed to form a suitable seat for the measuring apparatus. Then a hole was excavated through the guide of the base plate. The material from the hole to a depth of 150 mm was carefully collected in a polythene bag, weighed, tightly sealed, and labeled for subsequent natural moisture content determination. Dry, free-flowing sand of known density was then poured into the hole from the standard sand cone apparatus. From the weight of the sand the volume of the hole was determined. The test does provide a rough index of the relative strength and compressibility of the soil in the vicinity of the test. In the present project area there are three in-situ density determinations conducted at Km: 1+ 500, 2+800 and 5+800.

3.4.4.2 Atterberg limits and derived index

Soils containing clay exhibit a property called plasticity. Plasticity is the ability of a material to be moulded (irreversibly deformed) without fracturing. This behavior is unique to clays and arises due to the electrochemical behavior of clay minerals. (Indian Standard (IS – 1498, 1970).

The stiffness or consistency of fine grained soils depends on their moisture content, and varies with variations in the amount of moisture present. Depending on its moisture content, a soil can exist in viscous liquid, plastic solid, semi solid and solid states. Atterberg limits define the moisture contents at which the soil changes from one state to another. These include the liquid limit (LL), the plastic limit (PL), shrinkage limit (SL). They are determined by tests carried out on the fine soil fraction passing the 425μm (No. 40) sieve. Plasticity index (PI=LL-PL) is the numerical difference between the liquid and plastic limits. Thus, it indicates the range of moisture content over which the soil remains deformable (in plastic state). Shrinkage limits (AASHTO T92) is the lowest water content at which a clayey soil can occur in a saturated state. It is the moisture content at which no further volume change occurs with further reduction in moisture content. The plasticity index is the size of the range of water contents where the soil exhibits plastic properties. The PI is the difference between the liquid limit and the plastic limit (PI = LL-PL). Soils with a high PI tend to be clay, those with a lower PI tend to be silt, and those with a PI of 0 (non-plastic-NP) tend to have little or no silt or clay (Holtz et.al, 1981).

The Plasticity Index of the subgrade soil is a critical factor in the present research, which usually decides the life and stability of the pavement structure. The distribution of PI values with respect to existing chainage is presented in next section.

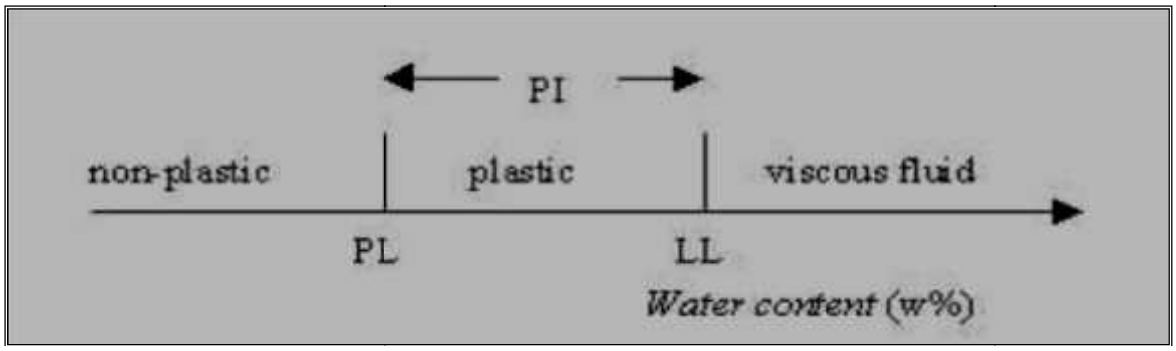

Figure 3.3. Change in soil states as a function of soil volume and water content

3.4.4.3. California Bearing Ratio (CBR) Test

The CBR test is now widely used for evaluating the stability or strength of subgrade soil and other flexible pavement materials for pavement design throughout the world. The CBR values obtained from either laboratory tests or in-situ (field tests) have been correlated with flexible pavement thickness requirements for this road project.

In this test, a plunger is made to penetrate the soil, which was compacted to the prevalent dry density and moisture content anticipated in the field (or to MDD and OMC as specified) in a standard mould (CBR mould) at a specified rate of penetration. Depending upon the prevailing climatic conditions of the site, the compacted specimens are immersed in water for four days before the penetration test. The soaking process is to simulate the worst moisture condition of the soil that may occur in the field. During this period, the sample is loaded with a surcharge load that simulates the estimated weight of pavement layers over the material tested. Any swell due to soaking was also measured. The load was applied by cylindrical metal plunger of 50 mm diameter, the standard penetration rate used is 1.27mm/minute and readings of the applied load were taken at appropriate intervals of penetration (0.5mm, 1.27mm (0.5")) up to a total penetration of usually not more than 7.5 mm-12.7mm.The CBR is then determined by reading off from the curve the load that causes a penetration of 2.54 mm and dividing this value by the standard load (13.34kN) required to produce the same penetration in the standard specimen as

$$CBR = \frac{Unit\ load\ \ for\ 2.54\ mm\ \ penetration\ in\ test\ specimen}{Unit\ load\ \ for\ 2.54\ mm\ \ penetration\ in\ sandard\ crushed\ rock} \times 100$$

Similarly, the CBR at 5.08 mm penetration was obtained by dividing the load causing a penetration of 5.08 mm with the standard load of 20kN required to produce the same penetration in standard crushed stone. The CBR corresponding to 2.54mm penetration is normally greater than that at 5.08mm pen, and is accepted as the CBR of the soil (provided that it is greater than that obtained at 5.08mm penetration). AASHTO T193 test procedure stipulates that, if the CBR at 5.08 mm pen. is greater than that at 2.54mm pen, the entire test should be repeated on a fresh sample. If the 5.08 mm penetration CBR in the repeat test is still greater, and then it is accepted as the CBR of the soil exhibited.

The design CBR of the subgrade soil, therefore, should be evaluated at the moisture content and density representative to the subgrade condition during the service time of the pavement structure.

A road section for which a pavement design is undertaken should be where the subgrade CBR can be reasonably expected to be uniform. Identification of sections deemed to have homogenous subgrade conditions is carried out on the basis of geology, drainage conditions and topography, and considering soil categories which have fairly consistent geotechnical characteristics (e.g. grading, plasticity, CBR). (Tanzania Manual, 1999,)

3.4.4.4. Grain size Distribution Analysis (Gradation test)

Grain size is the size of individual particles in a given soil material. Soils with different grain size have different engineering geological properties. Because of this one should carry out analysis for the proportion of particle size of soils in a given soil sample.

Soils are primarily identified as coarse grained, fine grained, and organic soils. On a textural basis, coarse-grained soils are those that have 50 percent or more by weight of the overall soil sample retained on the No. 200 sieve; fine-grained soils are those that have more than 50 percent by weight passing the No. 200 sieve. Highly-organic soils are, in general, readily identified by visual examination. Each soil type gravel, sand, silt and clay is identified by grain size. Based on the diameter or size range adopted from ASTM, soils can be classified as gravel (>4.75 mm); sand (4.75 – 0.075) mm; silt (0.075 – 0.002 mm) and clay (< 0.002 mm).

The natural swelling potential of soil is directly related to the total amount of clay-mineral particles (particles that are <2 μ m in diameter) in it. The swelling potential increases with the increase of clay minerals. Moreover, particle size distribution of soil minerals are critical for getting hold of many soil properties such as water holding capacity, rate of movement of water through the soil, kind of structure of soil, bulk density and consistency of soil. The distribution of particle sizes larger than 0.002 mm is determined by dry sieve, while a sedimentation process using a hydrometer determines the distribution of particle sizes smaller than 0.002 mm.

The gradation tests (AASHTO T 27) are conducted by using sieve analysis and for materials finer than 0.075mm, hydrometer analysis is used. The range of values of gradation test results for natural gravel, borrow materials and selected materials for embankment construction at 1+715km, 3+900, and 4+285km and are presented in Annex 3.

3.4.4.5. Classification of soils

Soils in nature rarely exist separately as gravel, sand, silt, clay or organic matter, but are usually found as mixtures with varying proportions of those components. Grouping of soils on the basis of certain definite principles would help the engineer to rate the performance of a given soil either as a sub-base material for roads and foundations of structures, etc. The Classification or grouping of soils is mainly based on one or two index properties of soil which are described in detail in the sections below. The methods that are used for classifying soils are based on grain size distribution and limits of soil. The systems that are quite popular in engineering sector are the AASHTO Soil The Unified Soil Classification System (USCS) and International Association of Engineering Geology (IAEG) are the important methods to classification soils for geotechnical investigation of foundations while AASHTO soil classification system is used to classify soils in the case of highway (Murthy, 2002). The AASHTO Classification System is based on the Public Roads.

In this system of classification, soils are categorized into seven groups, A-1 through A-7, with several subgroups, as shown in table below. The classification of a given soil is based on its particle size distribution, LL, and PI. Soils are evaluated within each group by using an empirical formula to determine the *group index (GI)* of the soils, given as;

$$\mathbf{GI = (F - 35)[0.2 + 0.005(LL - 40)] + 0.01(F - 15)(PI - 10)}$$

Where, **GI** = group index.

F = % of soil particles passing 0.075 mm (No. 200) sieve in whole number based on material passing 75 mm (3 in.) sieve,

LL = liquid limit expressed in whole number, and **PI** = plasticity index expressed in whole number.

General Classification	Granular Materials (35% or less passing No. 200, 75 mm)							Silt-Clay Materials (more than 35% passing No. 200, 75 μm)			
	A-1			A-2							A-7
Group Classification	A-1-a	A-1-b	A-3	A-2-4	A-2-5	A-2-6	A-2-7	A-4	A-5	A-6	A-7-5, A-7-6
Sieve analysis, % passing:											
No. 10 (2.00 mm)	50 max	.....	.....	.....	.....	.....	.....	.....	.....	.....	
No. 40 (425 μm)	30 max	50 max	51 min	.....	.....	.....	.....	.....	.....	.....	
No. 200 (75 μm)	15 max	25 max	10 max	35 max	35 max	35 max	35 max	36 min	36 min	36 min	36 min
Characteristics of fraction passing No. 40 (425 μm):											
Liquid limit	.....		.....	40 max	41 min	40 max	41 min	40 max	41 min	40 max	41 min
Plasticity index	6 max		N.P.	10 max	10 max	11 min	11 min	10 max	10 max	11 min	11 min†
Usual types of significant constituent materials	Stone fragments, gravel and sand		Fine sand	Silty or clayey gravel and sand				Silty soils		Clayey soils	
General rating as subgrade	Excellent to good							Fair to poor			

*Reprinted by permission of the American Association of State Highway and Transportation Officials.
†Plasticity index of A-7-5 subgroup is equal to or less than LL minus 30. Plasticity index of A-7-6 subgroup is greater than LL minus 30.

Figure 3.4 Table of AASHTO soil classification systems.

The GI is determined to the nearest whole number. A value of zero should be recorded when a negative value is obtained for the GI. Also, in determining the GI for A-2-6 and A-2-7 subgroups, the LL part is not used, that is, only the second term of the equation is used. Classifying soils under the AASHTO system is finding the correct group for the particle size distribution and Atterberg limits of the soil from the classification fig above. The group is then designated using the GI value. Granular soils fall into classes A-1 to A-3.

A-1 soils consist of well-graded granular materials, A-2 soils contain significant amounts of silts and clays, and A-3 soils are clean but poorly graded sands. A-4 soils cover non-plastic or moderately plastic soils, and A-5 contains similar material to Group A-4 but exhibits high LL. A-6 soils are typical plastic clays exhibiting high volume change between wet and dry states. Group A-7 covers plastic clays, having high values of LL and PI and show high volume change.

USCS has been modified several times to obtain the current version. The fundamental premise used in the USCS system is that, the engineering properties of any coarse-grained soil depend on its particle size distribution, whereas those for a fine-grained soil depend on its plasticity. Thus, the system classifies coarse-grained soils on the basis of grain size characteristics and fine-grained soils according to plasticity characteristics.

In this system of classification, material that is retained in the 75 mm (3 in.) sieve is recorded, but only that which passes is used for the classification of the sample. Soils are designated by letter symbols with each letter having a particular meaning as defined as follows:

A gravel or sandy soil is described as well graded or poorly graded, depending on the values of two shape parameters known as the coefficient of uniformity, Cu, and the coefficient of curvature, Cc given as

$$C_u = \frac{D_{60}}{D_{10}} \text{ and } C_c = \frac{(D_{30})^2}{D_{10} \times D_{60}}$$

Where, D_{60} = grain diameter at 60% passing

D_{30} = grain diameter at 30% passing

D_{10} = grain diameter at 10% passing

Accordingly, gravels are described as well graded if Cu is above 4, and Cc is between 1 and 3. Sands are also described as well graded if Cu is above 6, and Cc is between 1 and 3. (ASTM, Manual).

CHAPTER 4: DATA ACQUISITION, PROCESSING AND PRESENTATION

4.1 Concept and depth of investigation in 2D Electrical Resistivity

The concept consists in using multi core cables, which contain arrangement of cables and electrodes with take out at every 5meters for up 72 electrodes. The measuring unit includes relays, which automatically carry out the sequence of readings introduced in its internal memory. The system takes readings for many combinations of transmission and reception pairs so as to achieve some kind of mixed profiling and sounding pairs (ABEM, 2004). The total length of the cable is the product of the electrode spacing by the number of electrodes and that determines the depth of investigations.

The final depths of 2D electrical imagining survey depends primarily on; geometry of cables (type of array, number of electrodes, spacing between electrodes and the number of segments). Secondly, the measurability of the signal by the equipment, namely the amplitudes of the signal and of the existing noise, the power specifications of the equipment and its ability of filtering the noise through the stacking process (Loke, 1999).

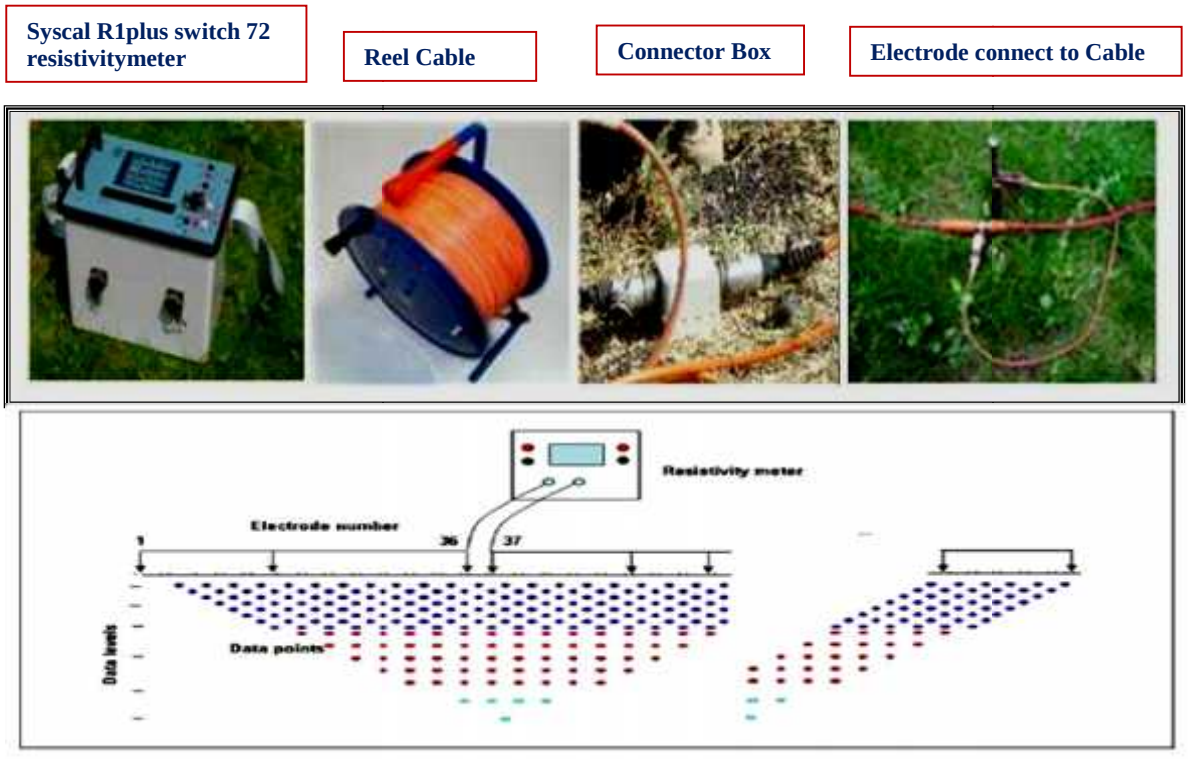

Figure 4.1 Generalized survey procedures and models with the main sequence in the left, roll along in the right and data points of 2-D resistivity imaging (Tigistu Haile, 2010).

4.2 2D Electrical Resistivity Data Acquisition

Multi-electrode (usually 72-electrode or 48-electrode), micro-processor based 2-D Resistivity Imaging System offers good opportunity to obtain the resistivity images to reasonable depths around 50-100 m (much depends on local geological conditions) below the surface level. For a good lateral and vertical resolution the hybrid Wenner-Schlumberger profiling is preferred.

The multi-electrode Resistivity Imaging System, IRIS made SYSCAL Pro $R1^+$ Switch 72, was used in the study region. A *GARMIN* GPS was used for the location of the position of the electrodes and this data was used for the topographic correction for all the profiles in the RES2DINVprogram.

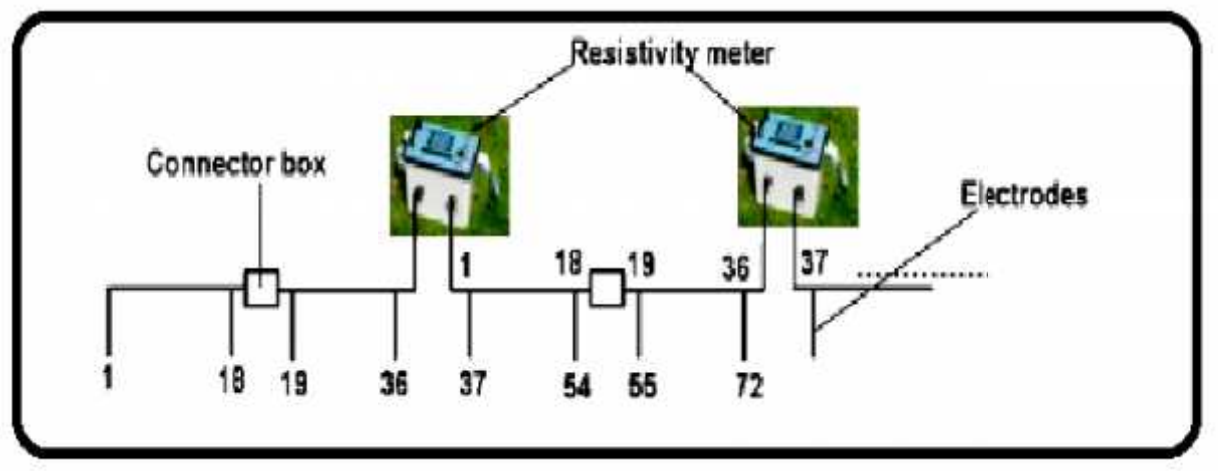

Figure 4.2 Field layouts of 2D electrical imaging with the main and the roll-along

The 2D Electrical Imaging data are acquired thoroughly along selected traverse lines which were used to collect a representative and detailed information about the area around the newly relocated road corridor.

Totally three profile lines were selected for the survey, in which all of the profiles are nearly parallel to the route line with running E-W orientation while one profile is perpendicular to the rift axis with NE-SW orientation.

The first traverse line lies on the *AA lava flo*ws which are situated at the Northwest of lake Beseka and it is impossible to acquire necessary data owing to the difficulty in electrode penetrate in to the ground. But the paired two parallel profiles (L_1& L_3) and (L_2& L_4) on the northwest and northeast is about 250m apart respectively. The Second profile (L_2) is directly at the southern part of newly

relocated road where the fissures were crossed and it is surveyed by one main and one roll along sequences which covers a horizontal distance of 450m. The other profiles$L_{4,}$ which are parallel to $L_{2,}$ are positioned at northern area of new road and surveyed by one main and two roll along sequences which cover a horizontal distance of 540m. While the forth profile (L_3) is oriented nearly parallel to the first profiles ,oriented on the northwest of Lake Beseka and north of new road and surveyed by one main, covers distance of 360m with no roll along due to massive sub-recent lava and cluster of blister cave scatter on the line . These three profiles L_2, L_3 and L_4 are surveyed by one main and different roll along sequences and running east to west directions almost parallel to the new road and nearly perpendicular to Ethiopian rift axis. The main sequence contains 648 data points covering 360m horizontal distance while each of the roll along sequences contain 297 data points covering a horizontal distance of 90m. The set of connections of the instrument at the field is indicated in Figure below.

The survey of this project consists of three 2D electrical imaging profiles with multi-electrode system using Wenner array. The spacing between line 2 and 4 is 200 m. In addition, as our area has limited space particularly with small electrode separations, the Wenner-β is more suitable for investigation targeting cavities The RES2DINV inversion software's were used to interpret the measured data. This software uses the rapid least squares inversion method to model the final resistivity section.

Table 4.1 Traverse line (Survey line) orientation, Electrode number and the coordinate

Generally, lines are positioned on the Northwest and northeast of Lake Beseka, running east -west ward across the visible fissures and Parallel to the road and nearly perpendicular to Ethiopian Main Rift.									
Line No.	**Survey line w.r.t road and Lake Beseka**	**Co-ordinate**	**Electrode No. and arrangement (One main and roll along)**						
			1	**18/19**	**36/37**	**54/55**	**72**	**90**	**108**
2	***North east*** of Lake Beseka and ***South of New road***	Easting (x)	598404	598479	598558	598640	598707	598791	
		Northing (y)	984512	984561	984607	984664	984708	984733	
		Elevation (z)	954	955	954	953	953	954	
3	**North west** of Lake Beseka and **North of New road**	Easting (x)	596817	596903	596983	597049	597111		
		Northing (y)	985902	985894	985845	985786	985726		
		Elevation (z)	963	961	962	963	962		
4	**North east of Lake Beseka and North of New road**	Easting(x)	598332	598426	598512	598592	598668	598749	598831
		Northing(y)	984812	984772	984781	984823	984862	984904	984947
		Elevation(z)	960	960	960	960	961	961	962

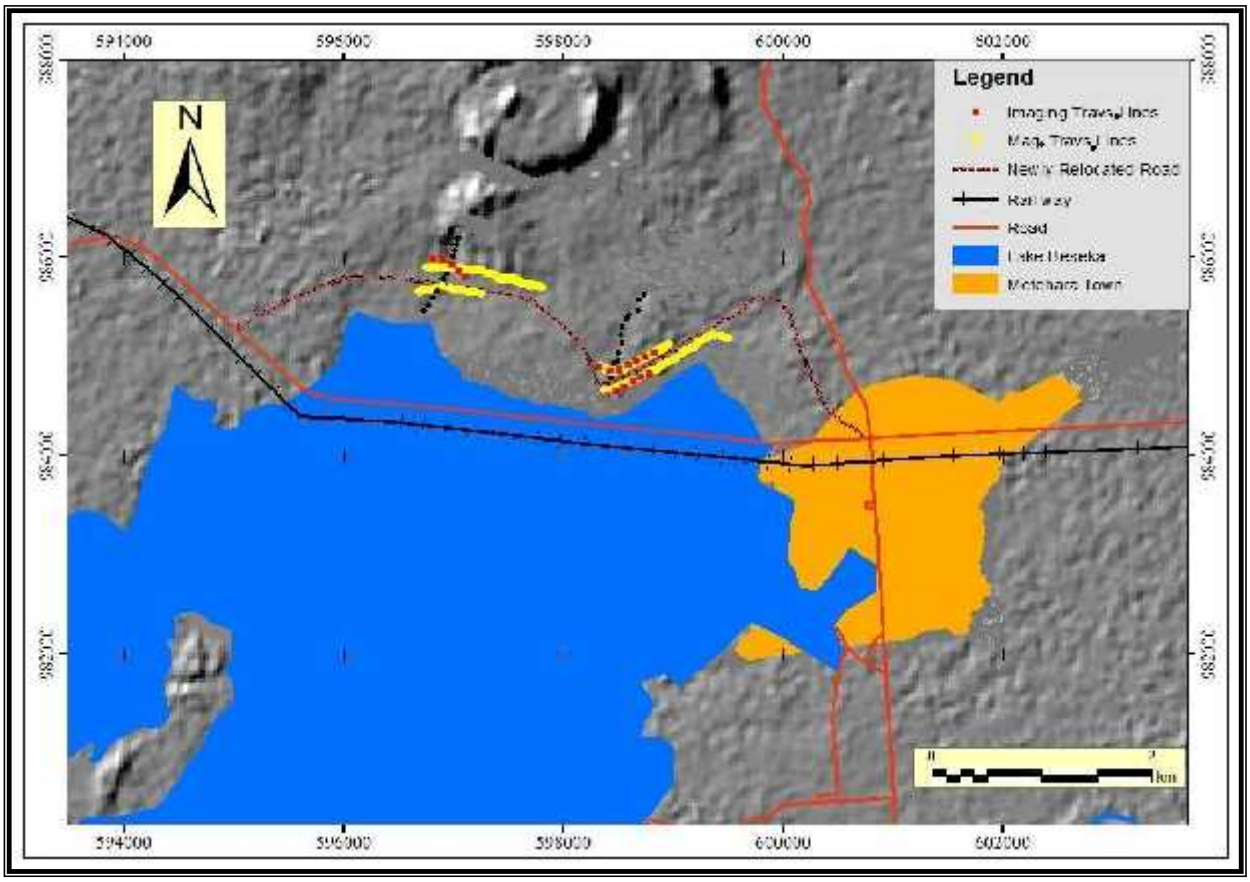

Figure.4.3 survey line with the newly relocated road and Lake Beseka on DEM.

4.3. 2D Electrical Resistivity Data Processing and Presentation

The data generated at each of the profiles (one main and many roll along sequences) are downloaded to a computer using the Prosys-II software. Then the data from each roll along sequence is added to the main sequence before the processing stage with the help of this software. After the summation, the final raw data is filtered, by automatic filtering, and the noisy data is rejected. Finally the filtered data is saved in the Prosys-II software in ".dat" form and exported to RES2DINV software for processing.

The filtered data, which is exported toRES2DINV software, is inverted by least square inversion and with 5-7% iteration processes and representative a minimum misfit model which would give similar subsurface apparent resistivity is produced for the purpose of analysis.

An automatic iteration process that fits the modeled data with the calculated one proceeds to analyze the data. A root mean square error (RMS) of the process was 5-14.7% and it was taken to be acceptable. The final output of RES2DINV software, the inverted 2D model resistivity

section, is the processing product of 2D survey. Finally such figures are used for interpretation purpose and to correlate the results of 2D imaging analysis with results of other methods.

4.4 Magnetic Methods Data Acquisition

Magnetic data were collected using Proton Precision Magnetometer instrument. Measurement of total magnetic intensity was made along traverse lines running perpendicular to the inferred to the geological structures observed in the study site. The magnetic data were also collected along the selected traverse line over the area in order to prepare the magnetic contour map which reveals the magnetic trends of geologic interest. Based on the approximate geometry, depth and trend of the anticipated geological structure/barrier, the station spacing was chosen to be 18 - 20m.

The surveying was stated by establishment of a base station within the study area at a place which is easily accessible and as far as possible from magnetic noise. A base station, far from artificial disturbances such as power lines, high traffic road, railways, metallic fencing and footings, etc, is chosen for monitoring and correcting diurnal variations. For each day, readings were taken at the base station almost every 30 minutes, apart from at the beginning and end of the survey.

In addition to the magnetic readings the geographic coordinates of the point at which the readings are taken and the time of reading is recorded using Global Positioning System (GPS). Similar to that of the electrical resistivity data, magnetic data are collected along the predefined profile lines, which were used to conduct electrical resistivity surveys. Magnetic data were collected from 124 data points with average spacing of 18-20m along the selected profile lines.

At the field survey three magnetic readings were taken for a specific point and then average of this readings were used for the processing and interpretation purpose.

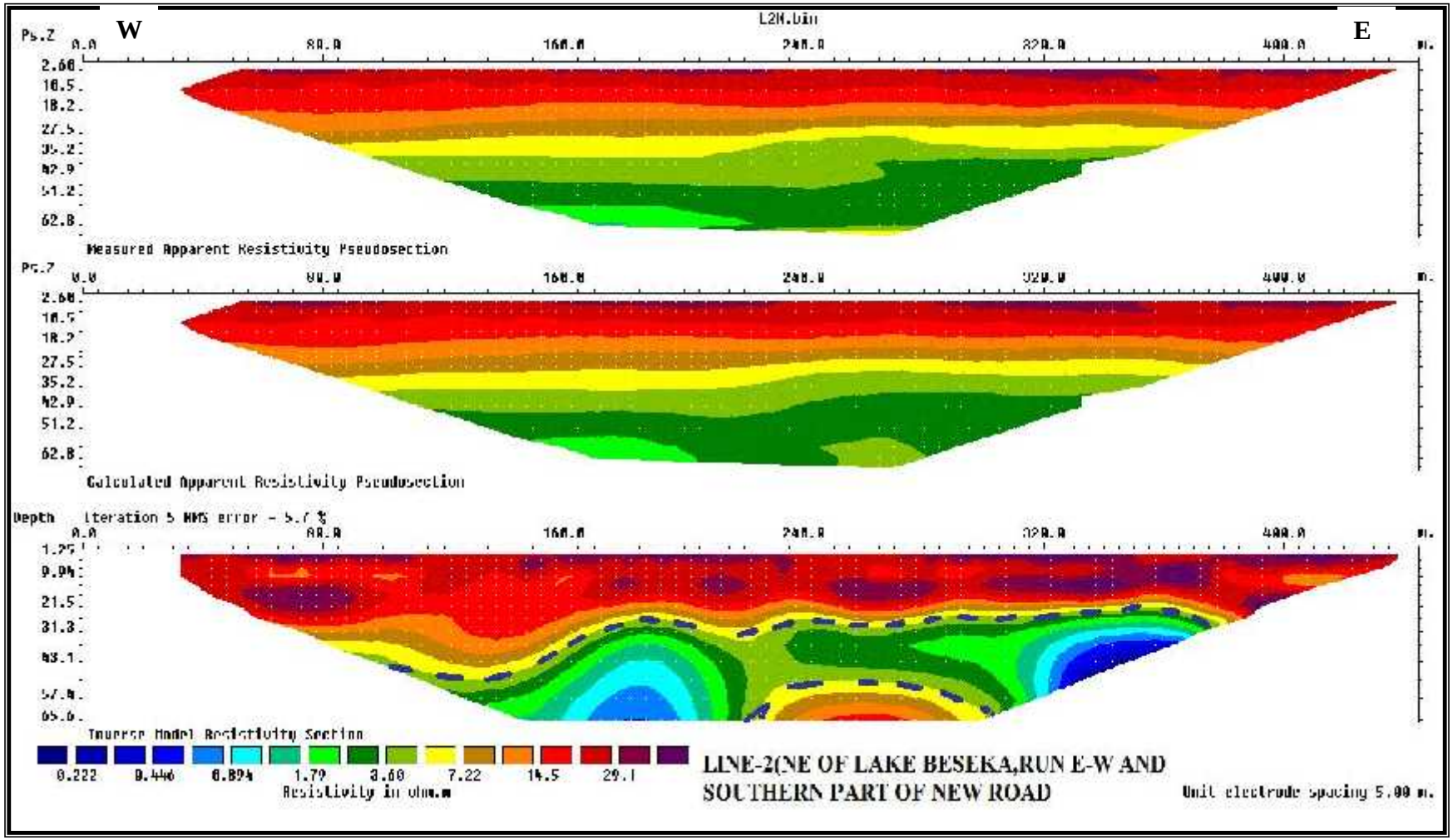

Figure 4.4 Measured calculated and inverted 2D model resistivity section.

The distribution of magnetic data in the study area is shown in Annex 4, and it is clear from the figure that the magnetic data are well distributed over the investigated area. Based on this distribution, the study area embrace different anomalies which exemplify by very higher magnetic anomaly and it covers the northwestern, and the western measurement of the northeastern, part of the study area.

4.5. Data Processing and Presentation

The observed magnetic data were corrected for diurnal variation using the base station readings taken during the survey. The main magnetic field at the base station is obtained from the International Geomagnetic Reference Field (IGRF). The IGRF value at the base station is subtracted from the diurnal corrected total magnetic field of each station. The resulting magnetic data have been smoothed and remove erratic features probably originating from cultural noise. The corrected and smoothed total field magnetic values were presented in the form of profile and also contoured to produce magnetic map.

This helps to counter check and integrating the results from the two methods for detail interpretations. The total study area with the magnetic survey is of about 500 km by 2.5 km dimension and is found within the low latitude magnetic equator. Because the survey covers very small area, the variation of magnetic field with latitude and longitude is insignificant and hence normal corrections were not done. In addition to this, in magnetic equatorial regions where inclination is less than 15degrees, reduction to the pole is generally unstable and cannot be derived (Getech, 2007).

In addition to the magnetic anomaly map, data enhancement techniques were applied to produce other maps, which may help to recognize more features. These are done by using the geosoft software package program called MAGMAP. Analytic signal was done by using this Geosoft software package program.

By wave filtering method a long wave length and short wave length parts of the spectra were separated which may enable to see the nature of the data at different depth levels. Rather than reduction to the pole and normal corrections, other data enhancement technique was applied to produce magnetic map, which may helps to highlight particular characteristics or features to aid qualitative interpretation.

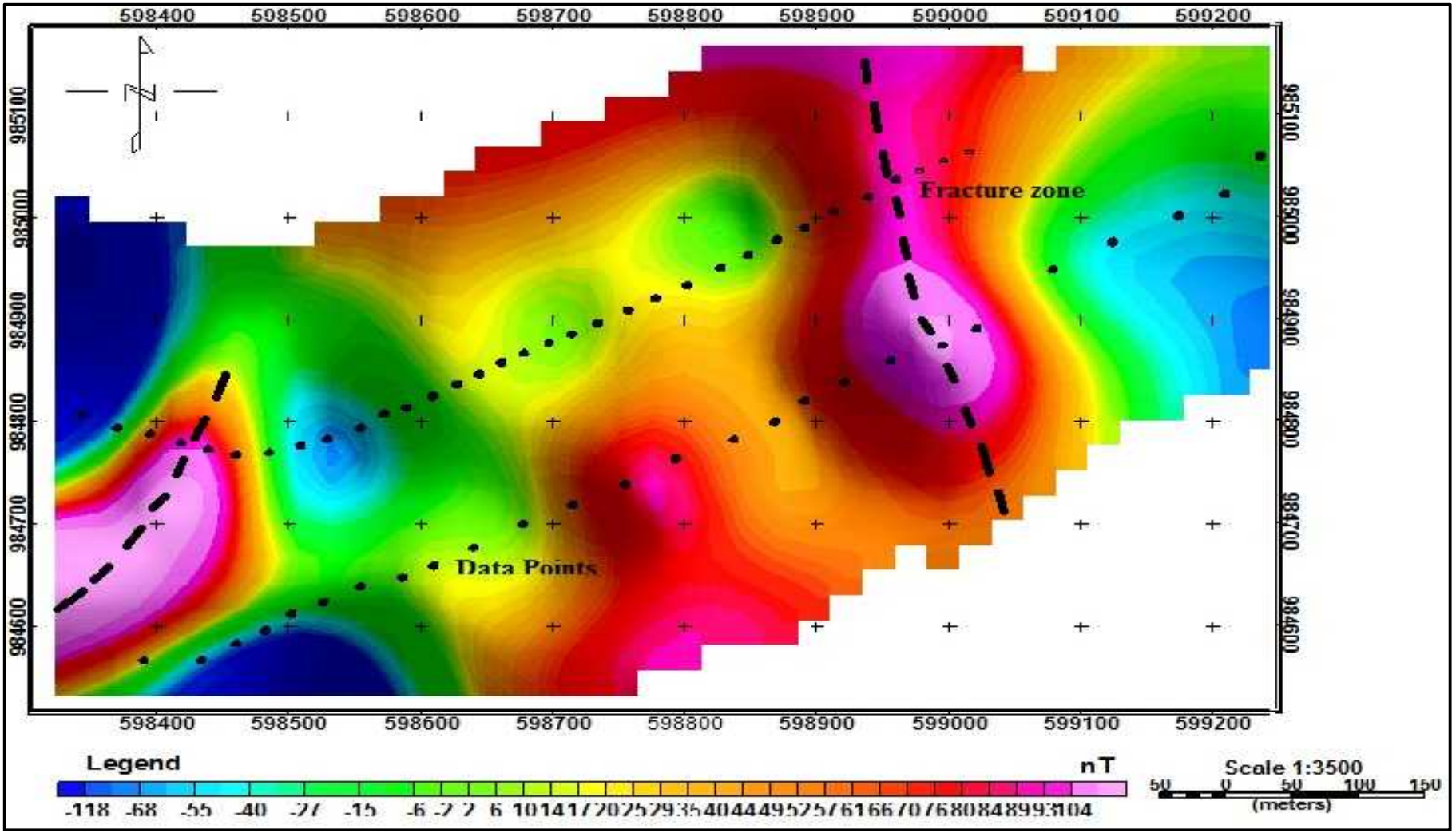

Figure 4.5 Total magnetic anomaly map of Line 2 and 4 situated on the NE of Lake Beseka.

CHAPTER 5: RESULT, DISCUSSION AND INTERPRETATION

5.1 2D-Electrical imaging and magnetic Profiles in association with Geotechnical Assessment

Knowledge of subsurface conditions and soil profiles are essential to the engineering design of projects like the present research, roadways engineering structures. One major risk for such projects is that the subsurface geology will differ from the assumptions made in the initial design and cost estimation stages of the project.

To overcome the cost of such miscalculation due to differing site and subsurface conditions, geotechnical investigations including geophysical work must be conducted to map the density, extension of fractures, fault or fissures and related geological structures around the project area. This is because in addition to aiding engineering design, the geophysical interpretation leads to a better understanding of hazards that may exist.

The 2D electrical resistivity imaging and magnetic methods are the most effective methods that can provide a detailed picture of the underground conditions without digging (direct exploration). In many cases, resistivity image surveys can be planned, executed, and the data interpreted in a matter of hours while causing minimum or no impact to the environment. Proper use of resistivity image surveys can provide significant cost saving over other exploratory methods.

Interpretation is compiled and completed based on integration of results from the field investigation note, 2D electrical imaging and magnetic method survey. Additionally, a correlation between the inverse model resistivity segment and the magnetic anomaly outline plot, which is surveyed along the same survey line with the 2D electrical imaging, is done.

This chapter also includes interpretation of resistivity imaging model, magnetic anomaly map, analytical signal map, tilt derivative map, 3D Elevation and topo map and geotechnical approaches which are developed using different geophysical plotting software. The detailed interpretation of the study goes as follows:-

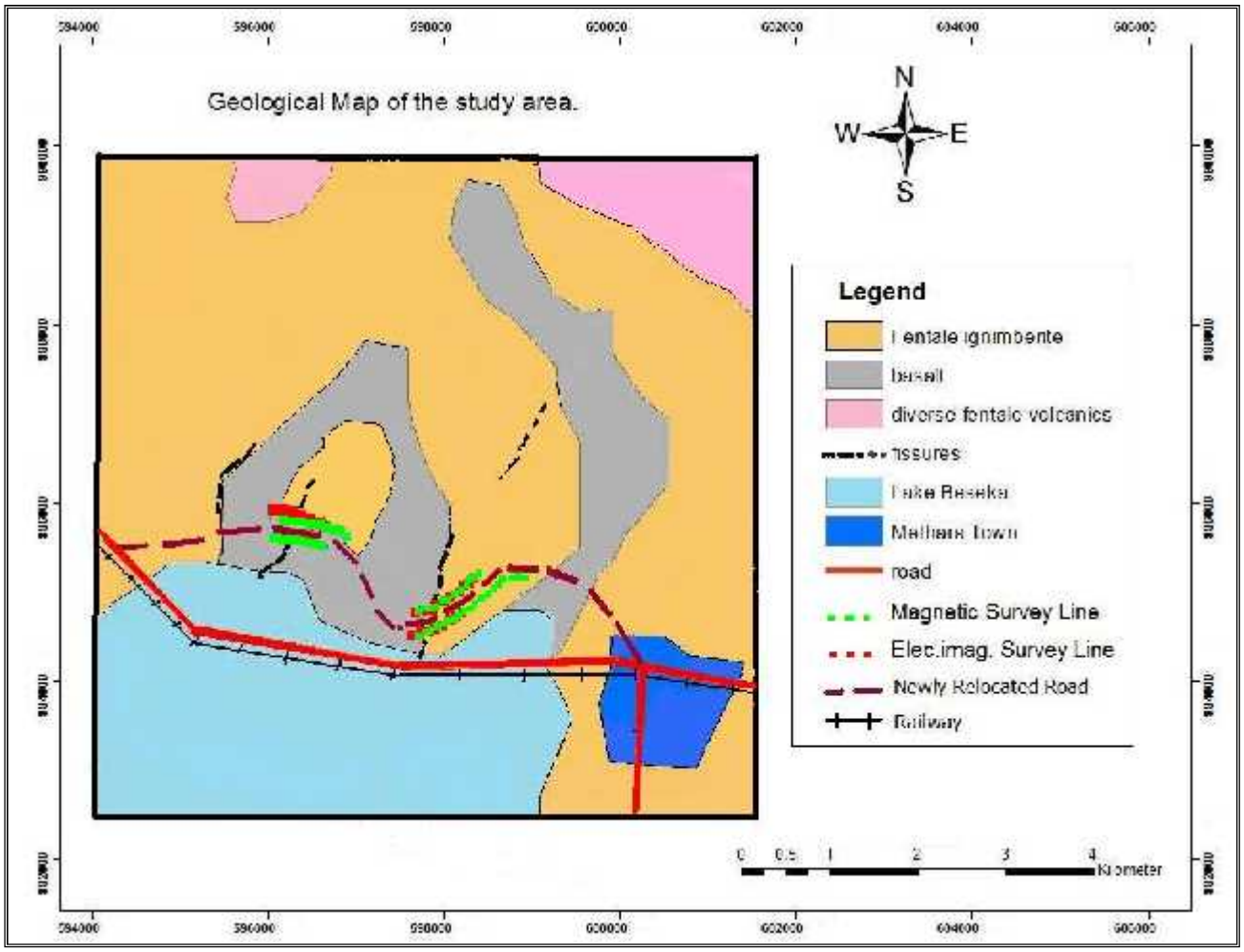

Figure.5.1 Geological map of the study area and Geophysical survey lines

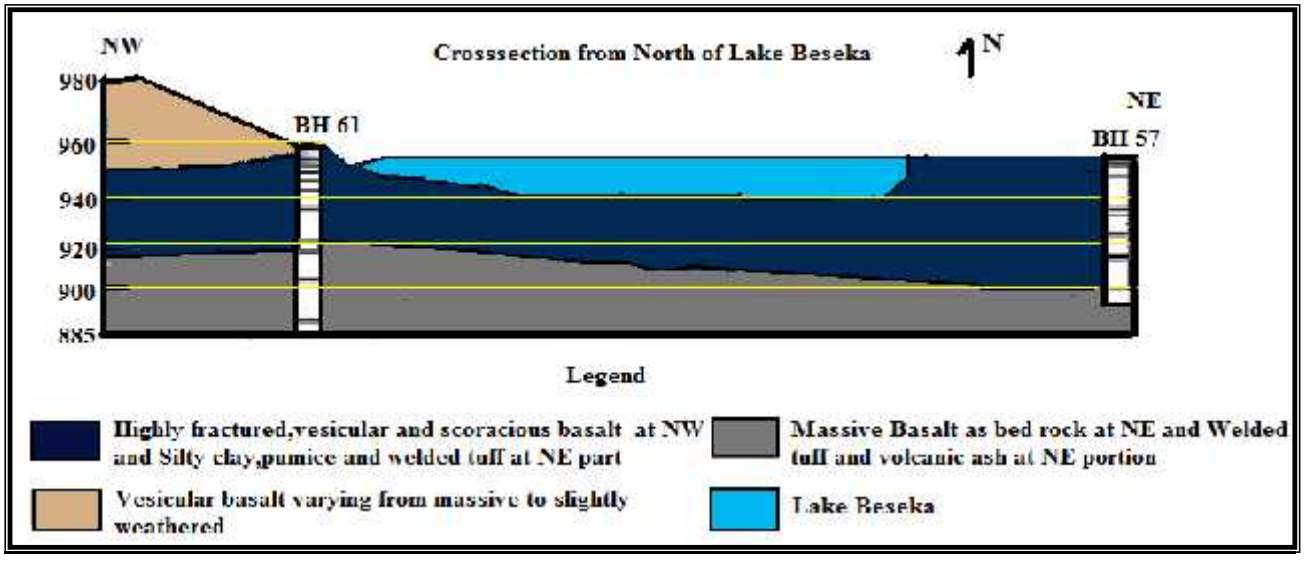

Figure.5.2 Regional geological cross section of North of Lake Beseka periphery area (*BH from WWDSE*)

Table 5.1 Resistivity and magnetic susceptibility of some common soils and rocks

Mineral or rock types	Susceptibility (k) (rationalized SI units)	Mineral or rock types	Resistivity (ohm- m)
Dolomite (pure)	-12.5 to 44	Igneous and Metamorphic Rocks	
Dolomite (impure)	20,000	Granite	$5x10^3$-10^6
Limestone	10 to 25,000	Basalt	10^3-10^6
Sandstone	0 to 21,000	Slate	$6x10^2$-$4x10^7$
Shale	60 to 18,600	Marble	10^2-$2.5x10^8$
Schist	315 to 3000	Quartzite	10^2-$2x10^8$
Slate	0 to 38,000	Sedimentary Rocks	
Gneiss	125 to 25,000	Sandstone	8-$4x10^3$
Serpentenite	3,100 to 75,000	Shale	20-$2x10^3$
Granite	20 to 50,000	Limestone	50-$4x10^2$
Rhyolites	250 to 37,7000	Soils and waters	
Pegmatite	3,000 to 75,000	Clay	1-1000
Gabbro	800 to 76,000	Alluvium	10-800
Basalts	5000 to 182,000	Groundwater (fresh)	10-100
Oceanic Basalts	300 to 3,6000	Sea water	0.2

5.1.2. Discussion of the Result

The table shown above is the resistivity and susceptibility of some common rocks. The 2D inversion model and the magnetic anomaly map obtained from the inversion of the magnetic data set for all lines displayed as horizontal profile plot were described below.

Profile -1 (only Magnetic method employed)

In this survey only magnetic method is appropriate as it was difficult to deploy the electrical resistivity imaging profile due to ground contact problems owing to recent and subrecent basalts covering the study area. This basalt is characterized by factures, and easily permeable around northwest of Lake Beseka comprising the newly relocated route corridor.

The amplitude variation of magnetic anomaly of profile-1 was plotted on Figure 5.3.This profile shows considerable varying amplitude of magnetic anomaly signatures. The minimum negative peak value is -322.950 nT at a distance of 280m and maximum positive peak value is 491.519 nT at a distance of about 260m. The magnetic profile shows an irregular morphology in response to the weak and fractured zones. These lower peaks, which indicate the presence of weak zone, appear at a distance of about 40 – 80m and 280m from thewest to the east direction of the survey line.

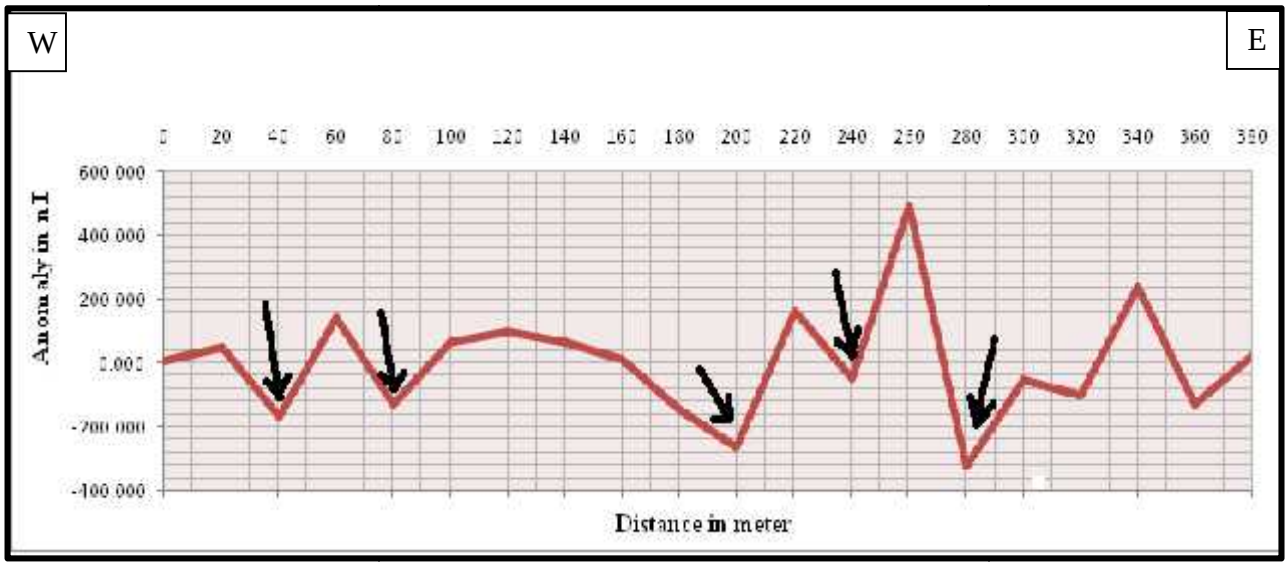

Figure.5.3.Ground magnetic Anomaly profile Map of Profile -1

The maximum magnetic anomaly of 491.519 nT is possibly the response of slightly to highly weathered scoracious basalt. The thickness of this layer varies on both sides of the section.

From the geotechnicalpoints of view, the basalts set up are fractured and highly jointed; and have a high degree of permeability and course grained texture. In addition to being affected by fractures, the basalts are characterized by primary porosities such as vesicular cavities, cooling joints and scoraceous intercalations. These porosities play an important role in creating favorable conditions for the formation of a weathered permeable zone and for simple invade of the water from the lake.

Profile- 2

Profile two is surveyed in a E-W directon. The first layer signal is possibly a very low resistivity ranging from 0.222-0.894 Ω m at depth of 22.5m, which is similar to the responses from profiles- 4 of the first layer .It, is interpreted possibly as, the overburden soils exhibit with pronounced thickness along the profile. At the east end of this line, the depth reaches about 20m from the surface. Thinning out progressively along the survey line, the soil ultimately vanishes at the NE end where the underlying weathered rock crops out at the ground surface. The high resistivity areas near the surface are due to the outcropped Fentale ignimbrites layers. Approximately at depth of 23 m, the very low resistivity values (1.79 – 3.60Ωm) are probably of a conductive, moderately saturated silty sand soil horizon, which is believed to be filled in cracks/fissure structure. The moisture is probably the effects of saline water from the lake intrude in the fissure structure below top sandy silt soil and along some scattered cluster of blister caves. Thus, the image at 21.5 to 57.4m depths show the geological structure filled with lake water and some materials collapse into the deep open cracks. Due to the collapse structure, the void structure filled with highly saturated silty sand materials which result in low resistivity values of 0.222-0.894 ohms and gradually collapse, deformed and deteriorate the rigid asphaltic Road.

The magnetic profile, correspond with 2D electrical imaging of Profile-2 was plotted as shown in the Fig 5.4a. The profile shows considerable amplitude variation in the magnetic anomaly signatures. The minimum negative peak value is -74.654 nT at a distance of about 270 m and the maximum positive peak value is 66.116 nT at a distance of about 198 m from the middle part of the line. There is indeed a positive correlation between the magnetic anomaly plot and the 2D electrical profile in detecting the weak zones. This anomaly plot shows the presence of fractured zone at the middle part and is coincide with 2D electrical imaging plot. The anomalies on the middle section is high as compare to NW tip and NE tip side of the survey line, possibly this indicating a depth increase to the bottom of the bedrock in the NW part.

The part on the NW side appears to have relatively moved downward compared to the blocks in the northeastern side. From electrical imaging and magnetic profile signatures, the fractures could be possibly interpreted as local normal faults dipping to east. Therefore, owing to subsurface saturated horizons and fractures zone gradual deformation and reopen of the fissures cause deterioration and sinking of ridged asphalt concrete.

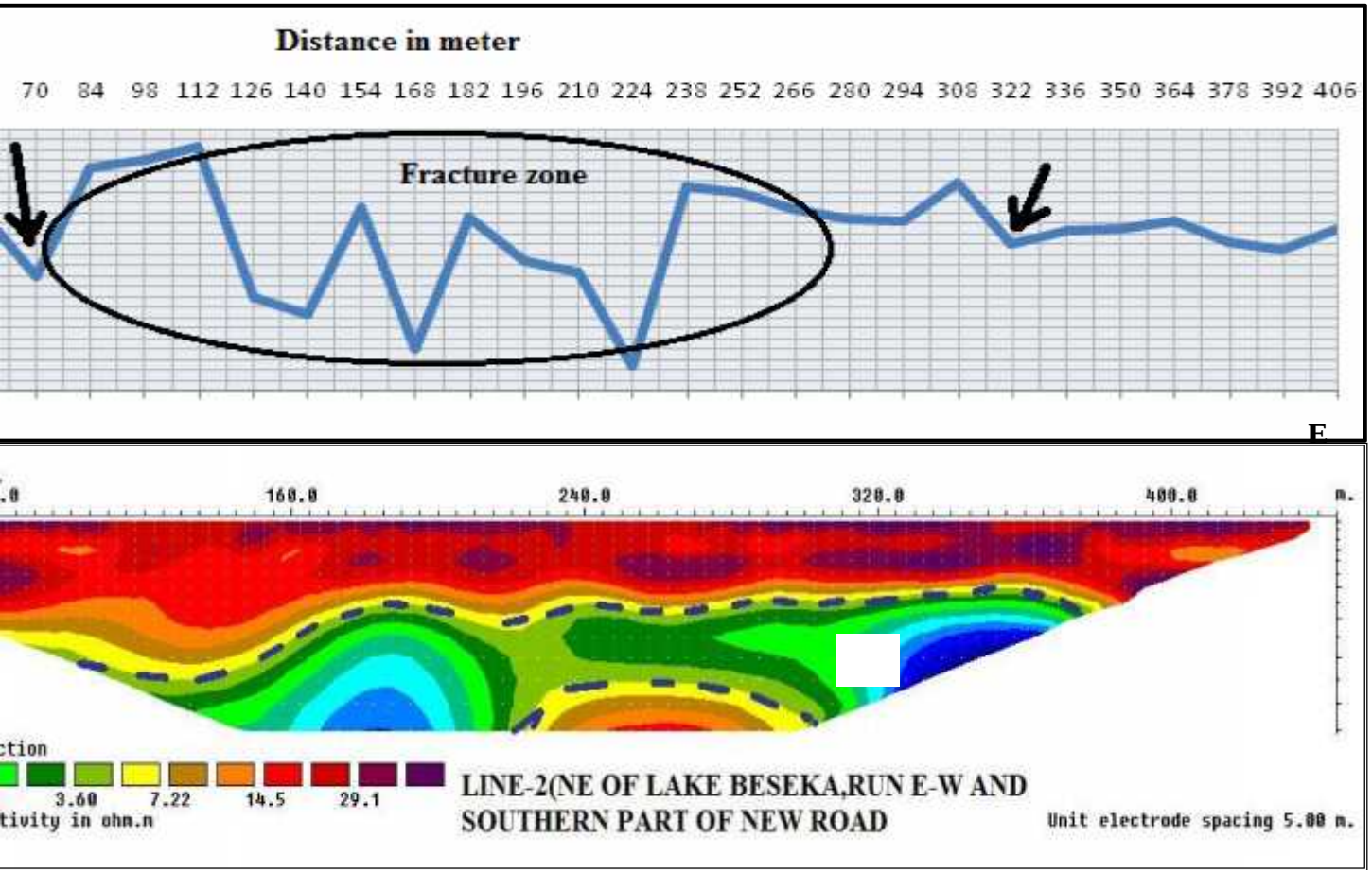

del and magnetic profile map L -2 located in NW of Lake Beseka

Profile- 3

The length of this profile is again 360m the extension of the main sequence only. The 2D electrical resistivity section obtained on this line is characterized by a high degree of fracturing. Along the profile, the electrical resistivity of the top part lacks uniformity. It has very low resistivity varies from 7.65 to 20.7 Ω m with minimum thickness of 0.8- 1.25m, possibly attributed to the moderately saturated sandy silt situated at the middle part the line, from 160m to 320m .Even if the survey line crosses the part of the AA lava flow, the sandy silt materials filled the fractured zones and saturated with fluid to a certain degree. As compared to the top portion, the bottom section relatively thicker (from 21m – 43m), probably of fractured and dry weathered volcanic tuff having a resistivity range of 120 - 400Ωm. It was observed that a patch of water has been accumulated between fractured sections from80 – 300m sides in the lower fragment. This is indicated on the 2D electrical resistivity section as a localized low resistivity patch right beneath the 160m mark. Moreover, the very low resistivity at the greater depth is possibly due to high degree of weathering and water percolation from the surface along the fractures.

The magnetic profile follows more or less the same survey line to the resistivity survey line on which the 2D electrical imaging of Profile-3 was plotted in Figure 5.5a. The minimum negative peak value is 90 nT at a distance of about 500m and the maximum positive peak value is 100 nT at a distance of about 480m from the initial station position on the Northeastern side of the line. The magnetic field profile roughly coincides with the 2D electrical resistivity profile plot. The magnetic profile clearly shows erratic pattern which is indicative for the presence of lateral variations mostly associated with fractured zones. This is more visible from a distance of 100m – 500m. Some of the cracks could also be interpreted as localized faulting and/or major fracture zones with vertical to near vertical orientations mapped on the 2D electrical resistivity section. This is owing to its location visa-vis the western margin of the rift and contributed for the formation of cluster of separated boulders rather than a continuous rock bed.

This model may also suggest that such features could result due to various tectonic activities that might have occurred over the area. This saturated fractures possibly deformed and collapse and result in the sinking of the road.

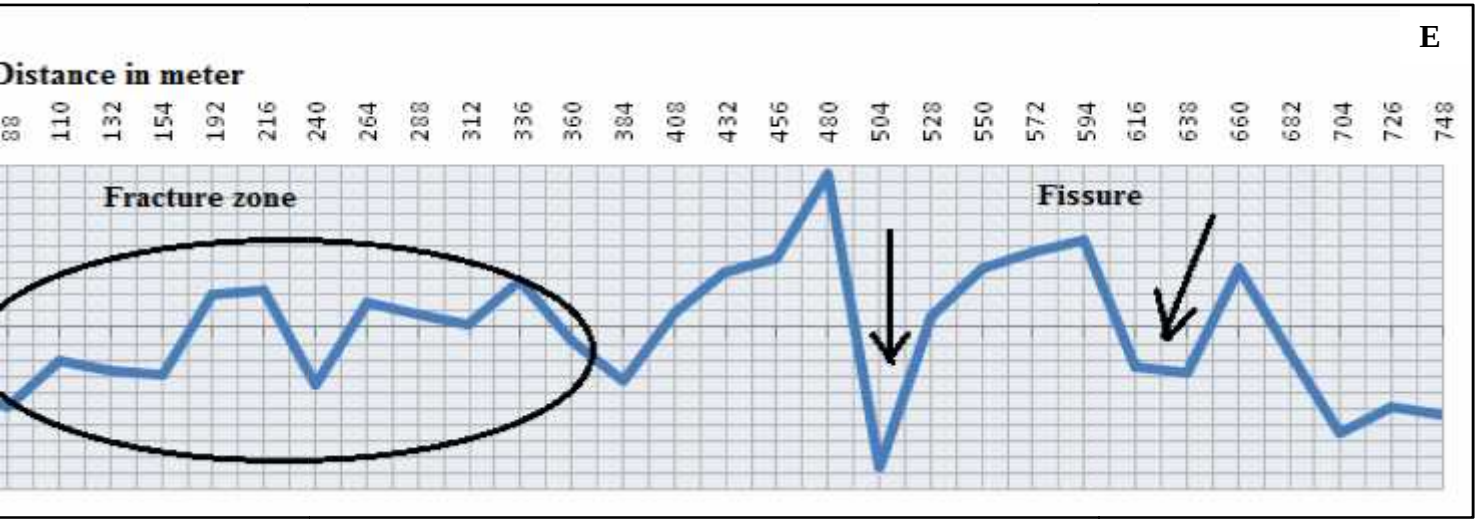

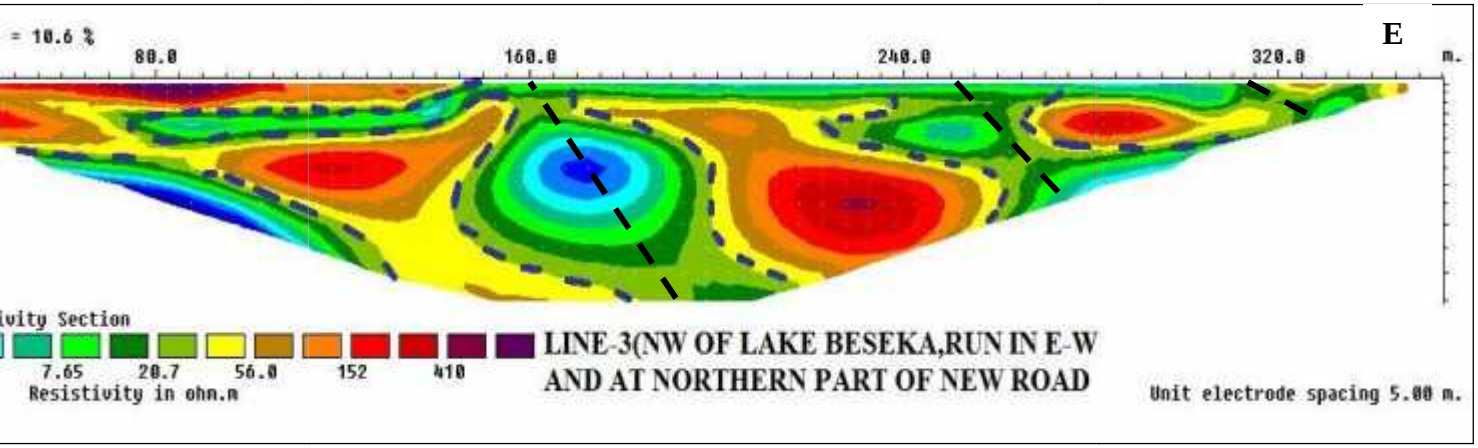

odel and magnetic profile map L-3 located in NW of Lake Beseka

Profile-4

Similar to Profile -2, this survey traverse runs almost perpendicular to the general rift trend and North of Survey Line -2.It is oriented roughly from the east to west. The line runs parallel to the newly relocated route corridor and passes the scattered cluster of Blister caves. It is intended to map possible structures that may be oriented almost perpendicular to the profile-2 as discussed above and propagated to the north, crossing profile-4. Subsequent cautious was taken for unnecessary data exclusion and filtering process of the 2D electrical resistivity raw data. A total of 1242 data points were used for the inversion modeling on this profile.

Similar to that of profile-2, the imaging layers consists of the top most part which is characterized by relatively high resistivity ranging from 36 – 107Ωm and with an average minimum thickness of 22m. The portion of this layer of high resistivity values, from a distance of 130m – 450m, might be attributed to dry to slightly saturate silty sand. The formation for electrical resistivity value 100 Ohm-m and above, occupying the distance of 0 -130m could be attributed to AAlava flow situated at the northwest section. The rock mass has been mapped to be shallow at the NW end and dips towards east, to a depth of about 10m from the level of measurement. This may be owing to lava flows from Fentale volcanic or intrusions of basalts through cracks and fissures at depth.

Referring to the bottom middle section of the 2D inverse resistivity model, the distinct horizons are mapped as a conductive region may represent moderately water saturated materials, between depth ranges of 22 - 57m. These structurally week zones serve as conduits for seepage of mineralized water from the lake. The very low resistivity responses may be the combined effect of lake water along with high temporal weathering condition. The layer underlying the saturated horizons possibly interpreted as slightly weathered volcanic tuff (welded tuff). Therefore, like profile 2 it has its own impact to the ridged asphalt concrete road.

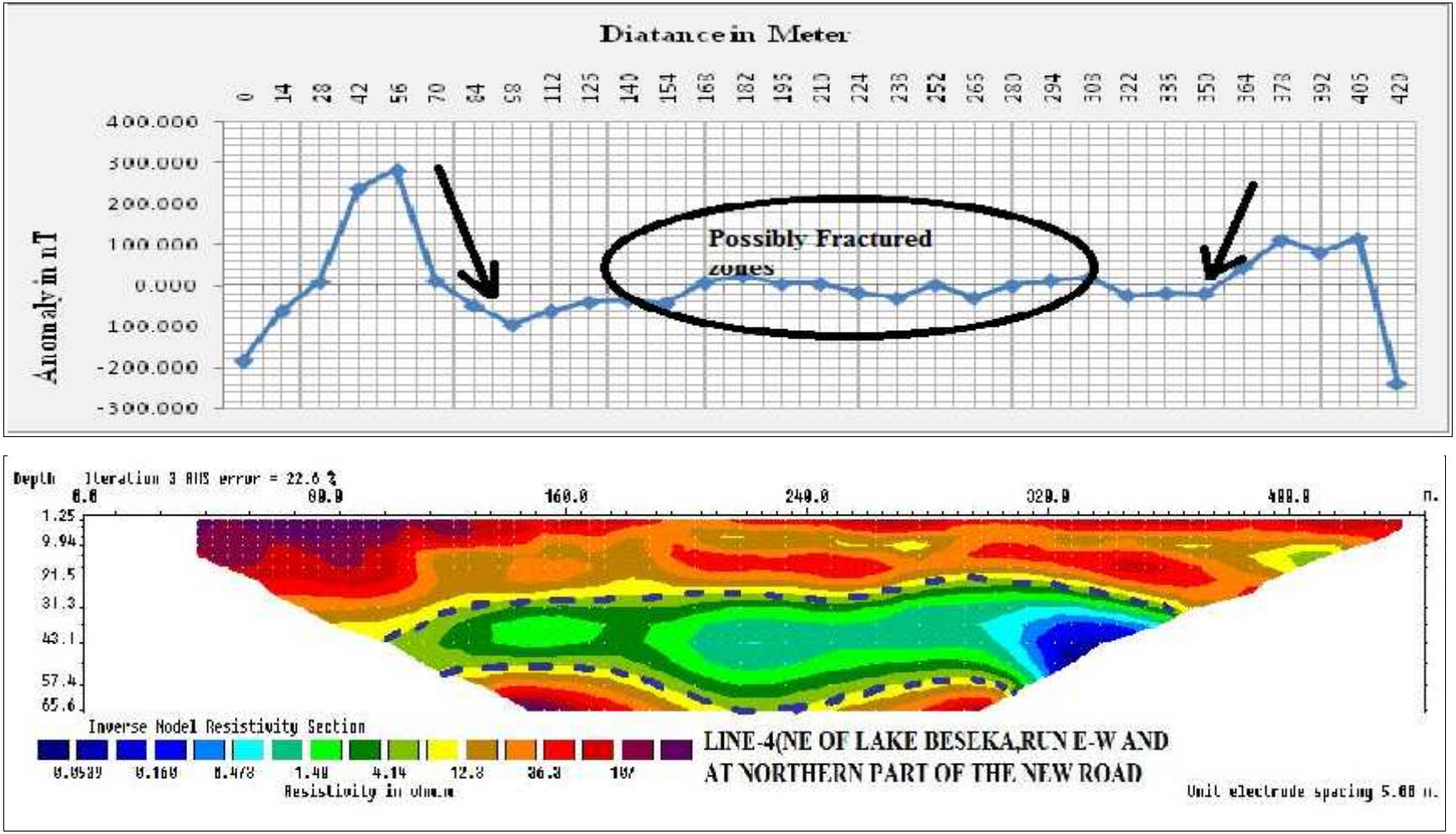

Figure.5.6 2D inversion model and magnetic profile map of Profile -4 is located in Northeast of Lake Beseka

5.2 Combination of the 2D Inversion Models and total magnetic anomaly

5.2.1. 2D inversion models of Profile -2and 4 and total magnetic anomaly map of line 2&4

From the Figure below , the top layer with high resistivity value is relatively thick in the western part of the study area on both the profiles, with a decreasing exposure to eastern side. The thickness of the second layer is significant in the western part at depth of 22m – 57.4m in all the profiles. However, the thickness of this layer also considerably decreases on the eastern side as compared to the western side of the fissure axis crossing the route under construction.

In the map of magnetic anomaly the zones represented with high responses are on the western tip and central part relative to the other regions. The high magnetic anomaly response is probably due to the result of highly magnetized volcanic rocks that could be found in the area. It covers the northwestern and central part of the study area.

From this the newly relocated route, will be preferably constructed in the north side of the profile-Profile-2 and 4 where there are few weak zones and relatively shallow depth to the bedrock. In addition to the information obtained from the total magnetic anomaly profiles explained above, the total field magnetic map of the area clearly shows a NNW and SSE trending fissures in the NW part of the Lake.

In conclusion, most of the magnetic high responses coincide the 2D inversion models and with the geological structures map of the area. However, high magnetic signatures, which are not observed on the structural map, are manifested on the magnetic map and 2D inversion models. The high signature is possibly the continuation of geological structures and formations of volcanic materials.

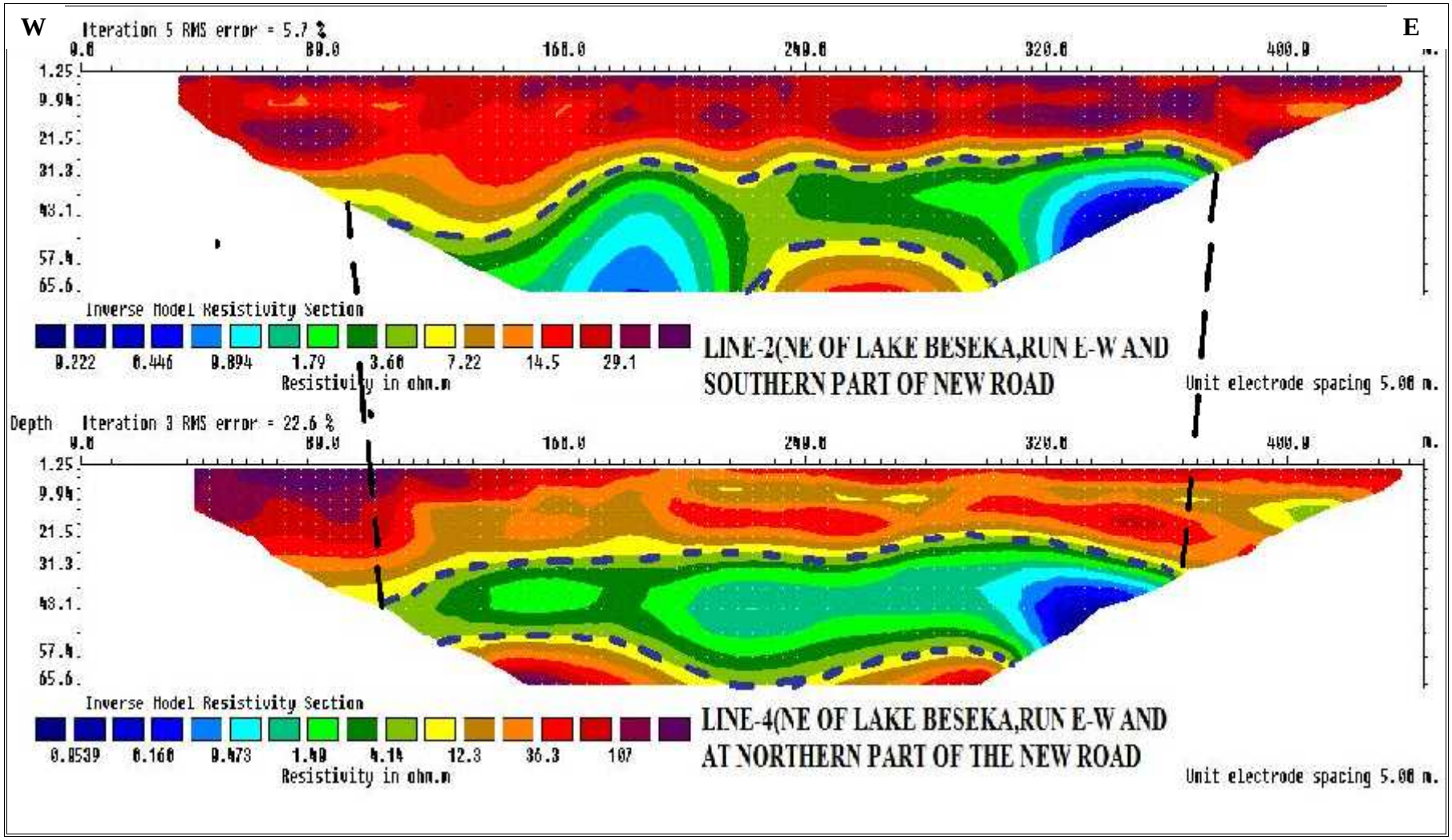

Figure.5.7. Combination of 2D inversion model for profile 2 & 4.

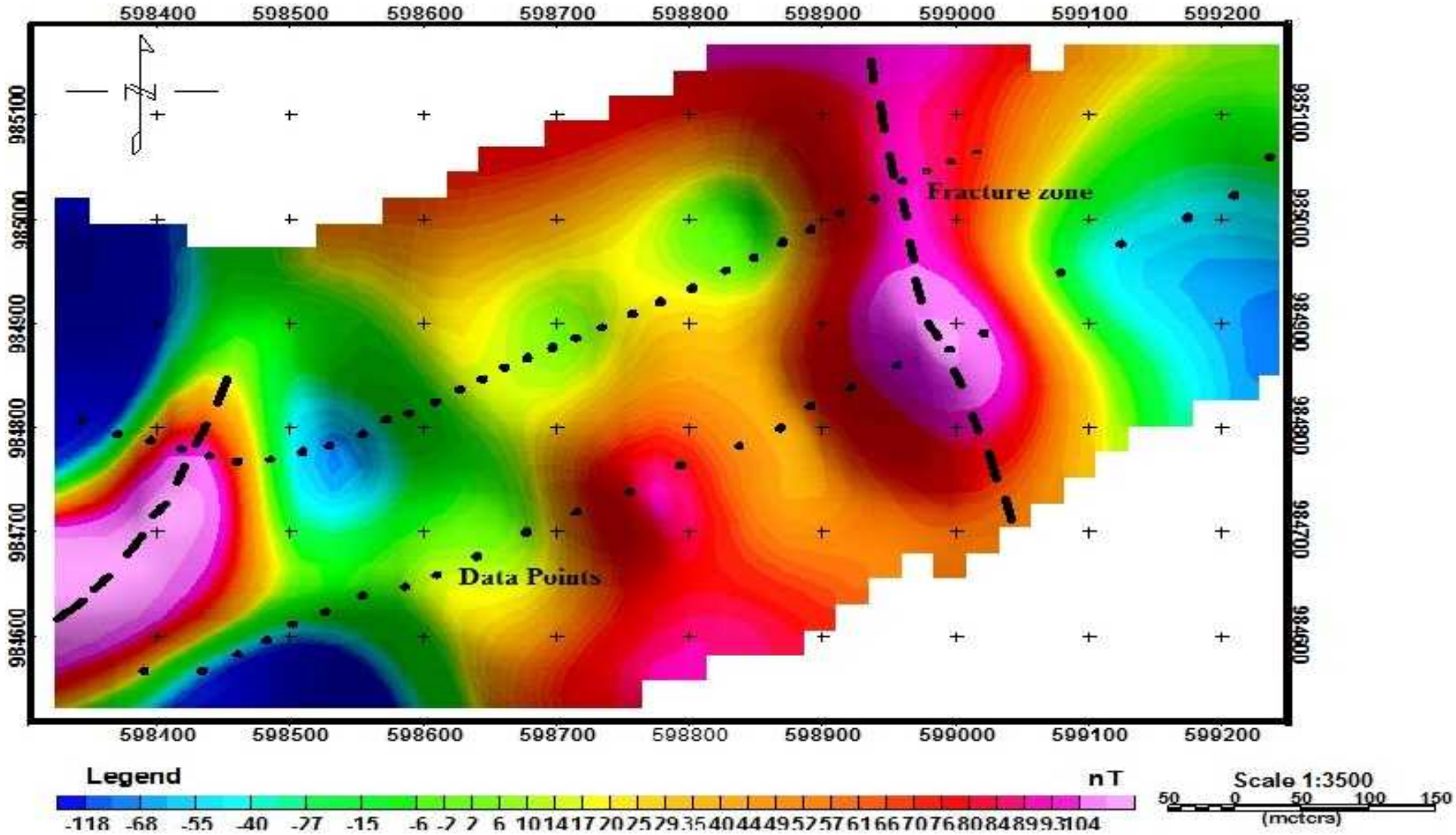

Figure.5.8 Combination of total magnetic field anomaly map of Line 2 and 4

5.2.2. 2D Inversion of Profile 3 and total magnetic anomaly combination of line 1 and 3

Figure 5.9 represents the correlation of total magnetic field anomaly map of the line -1 and 3 and 2D inverse model profile-3. The magnetic anomaly map shows relatively high magnetic response almost along line 1 and 3 at a few distances from the northwestern tip and the south eastern sections.

This magnetic high response is probably due to the result of highly magnetized volcanic formations that could be found in the area and some weak zones. Whereas, the low magnetic responses particularly NW of lake Beseka, could be the result of heat source around the Lake and the consequence of residual effect. Therefore, the magnetic profiles as observed form the map is marked by various magnetic picks that are associated with surface scoracious basalt or the formation of volcanic materials at shallow depth where it is covered by soil.

From 2D inversion model, the extremely low resistivity values may be caused due to the intrusion of the lake water through the fractures or weak sections. This portion can be characterized as probably saturated silty sand materials and highly weathered formation. The high resistivity may describe as slightly weathered volcanic scoracious basalt.

Furthermore ,both figures show the existence of a geological weak zone, probably a fissure or cracks that cuts all the profiles at nearly area, around 160-240m from the western and central portion of the survey line. This is the place where the newly relocated route passes through. This way of representation is important to understand the continuity of the weak zones within the survey area.

As a result, very high magnetic responses values were detected around the western and eastern part, possibly the fractured, weathered volcanic formations. Since these materials have high susceptibility, the response for the magnetic measurement is positive. These anomalies have trending in NNE-SSW directions, which is similar to the general trend of MER axis of the area.

Moreover, the result shows contacts or possibly the structures, broad at the south end form the lake side and becomes gradually narrow to the north, suggesting the propagation direction. So opening of the fissure are deep seated at the south than to the north. Consequently, the western section discontinuities/fractures that propagate from south to the north are also with some small vertical movement as well as E- W extension direction.

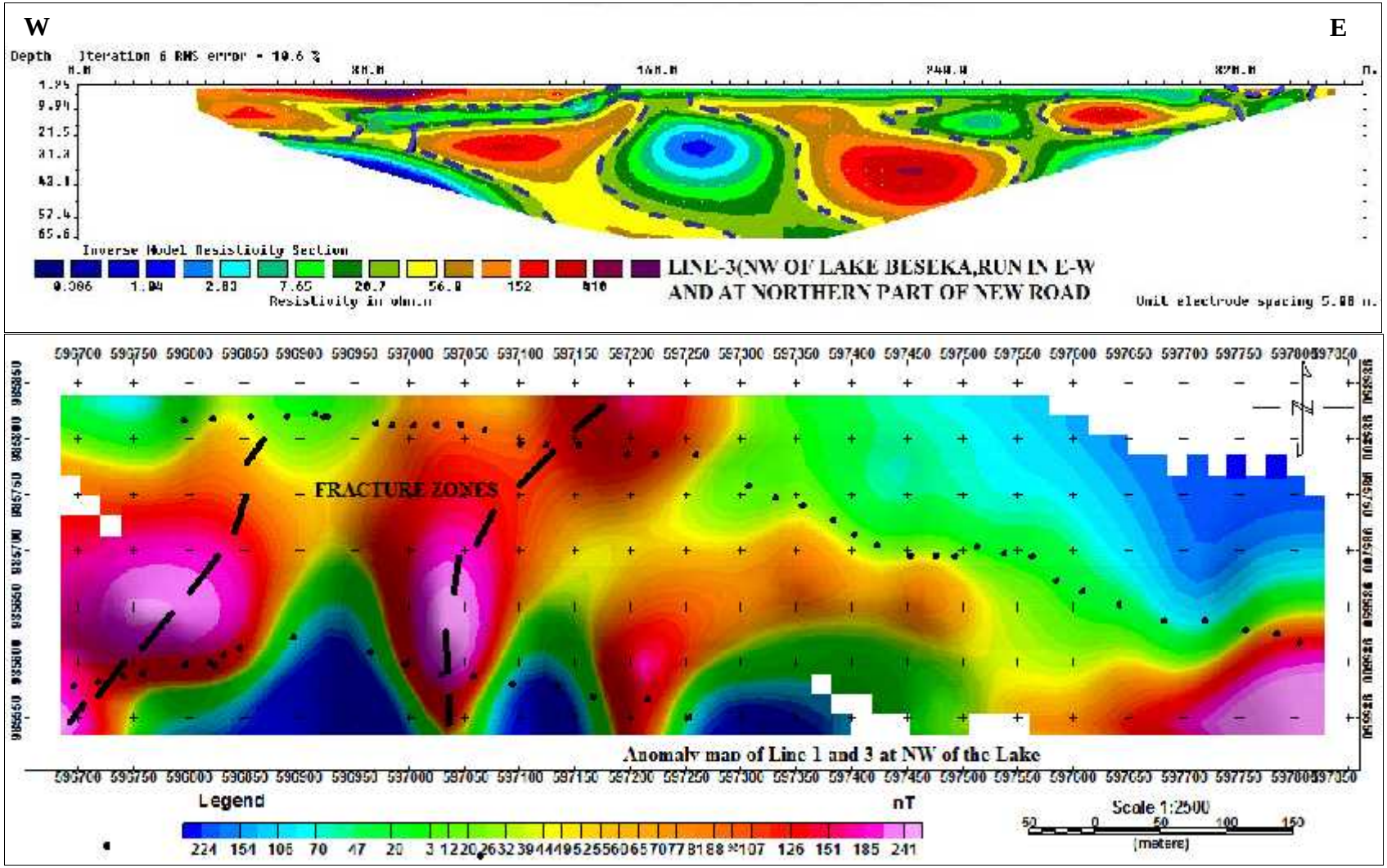

Figure.5.9 Combination of 2D inversion model and total magnetic anomaly map

5.3. Geotechnical Evaluation of the study area

Sub-grade soils with nearly similar soil type are grouped together and their extent has been determined. These extensions were then used to avoid narrow soil stretches from being overlooked. The residual formations are mostly stiff gray sandy silty clay soil and light gray sandy clay loam soil mixed with scoracious gravel (subgrade soil summarized in Table 5.4 below.)

Site characterization consists of the compilation of information on the site subsurface soil conditions. The evaluation of the ground shaking hazard and site geologic hazards like fault, fissures, or ground cracks related to expansions of Lake Beseka were not discussed in the detailed Engineering design document preparations for realignment program.

.

According to the local Consultant (Core Consulting Engineers) for detailed Engineering Design for realignment, tender document preparation and Construction Supervision, the detailed site investigation works were conducted to assess the overall condition of the area. The consultant also collected all relevant information required for the design purposes. The field work conducted were include describing and logging of the natural Sub- grade materials from the test pits excavated every 1km, soil extension survey, in-situ density test on the existing embankment layer where the new alignment passes Soils and Rock samples were collected for laboratory tests.

5.3.1. Visual Subgrade Soil Extension Survey

The soil extension survey along the project route corridor was carried out by thorough visual observation such as color, texture and appearance on the wall of test pits per 0.500 - 1 km intervals. Based on this, different soil and rocks formations were identified, described and determined for the proceeding investigations. Accordingly, the materials observed along the route was categorized into light grey sandy clay, dark grayish clayey and sandy silt mixed with gravels of ignimbrites and scoracous basalt from km; 0+000 ~ 0+ 720. Secondly, slightly weathered, dark grey, volcanic tuff and vesicular with scoracous basaltic flow from km; 1+720 ~ 2+330, 3+500 ~ 4+500 and 6+000 ~ 7+000. Occasionally, volcanic tuff and scattered blister caves are set up.

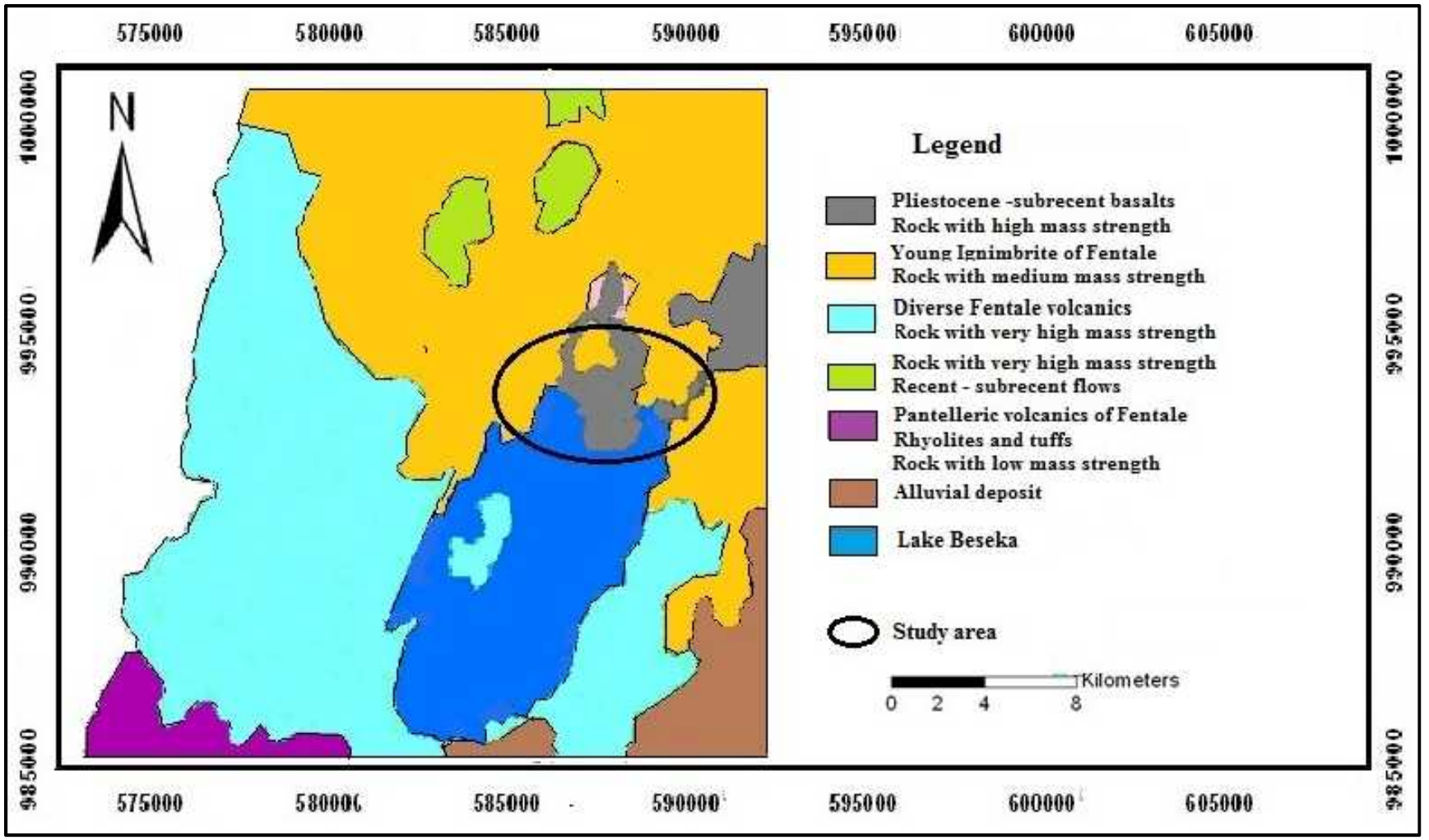

Sources: (Extract and Modified from Engineering Geological map of Nazareth sheet NC 37-15)

Figure.5.10 Engineering Geological map of Study area and its surrounding

Table 5.2 Occurrence of soil and rock formation along the project route corridor

Material Description	Length(km)	% of Coverage	Remarks
Light Gray to gray clayey and sand silt mixed with friable gravels	**3**	**41**	Good road bed materials, owing to the test result and visual inspection
Slightly weathered volcanic tuff and vesicular basaltic materials	**4.28**	**59**	Below 1-2m the rock are difficult to excavate (rock sections and require improved subgrade)

No	Station (from ~ to) with coordinate		Length(m)	Material Description	Remark
1	0+000	0+500	500	Light Gray clayey silt mixed with friable gravels	at a place exposed welded tuff and easily dozable
	594604	595035			
	985599	985388			
2	0+500	1+710	1210	Slightly weathered tuff overlain by thin layer of light gray clayey silt mixed with friable gravels	Easily dozable(excavated)
	595035	596148			
	985388	985858			
3	1+710	2+335	545	Moderately to slightly weathered, vesicular basalt lava flow(AA Lava flow) and distigrated into cobbles and gravels	Easily dozable(excavated)
	596148	596768			
	985858	985941			
4	2+335	2+617	1282	Light Gray clayey silt mixed with friable gravels	
	596768	597049			
	985963	985963			
5	2+617	3+500	883	Slightly weathered tuff with friable gravels	Easily dozable (excavated)
	597049	597814			
	985963	985512			
6	3+500	4+550	1050	Moderately to slightly weathered, vesicular basalt lava flow(AA Lava flow) and distigrated into cobbles and gravels	Only 1-1.5m depth are dozable (excavated) and as depth increase it is difficult to excavate
	597814	598432			
	985512	984672			
7	4+550	5+720	1270	Slightly weathered tuff overlain by thin layer of light gray clayey silt mixed with friable gravels	Easily dozable (excavated)
8	5+720	6+000	280	Light Gray clayey silt mixed with friable gravels	
9	6+000	7+000	1000	Moderately to slightly weathered, Scoarious basalt lava flow(AA Lava flow) and distigrated into cobbles and gravels	Easily dozable(excavated)
	599658	600132			
	985173	984351			
10	7+000	7+286	286	Slightly weathered tuff overlain by thin layer of light gray clayey silt mixed with friable gravels	Easily dozable(excavated)
	600132	600150			
	984351	984066			

Table 5.3 Summary of visual identification soil formation and sample taken spot

The summary of the laboratory test results for various soil properties is tabulated as Annexure-3 together with individual test results. Graphic logs and description of the material in each test pit are shown through Annexure - 2

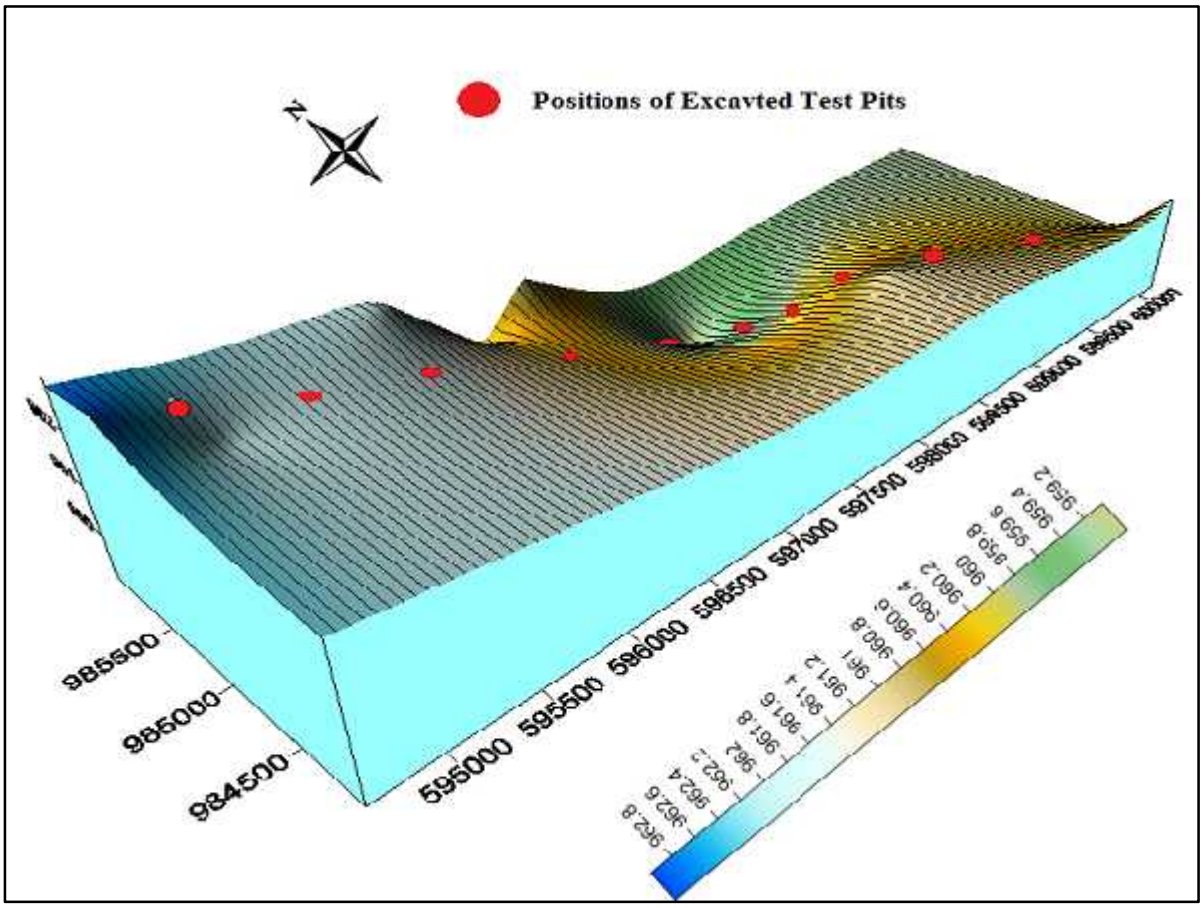

Figure.5.12 the position of excavated test pit on 3D elevation map

5.3.2 Laboratory Test Result

The following subtopics briefly sketch the test result associated with subgrade soils and relevant remedial measures to be considered. The subgrade soils can often be the overriding factor in pavement performance. Problematic soils are considered to bring undesirable property during the life service of the road, if any along the route. The main problematic soil type that attracts the attention of the engineering geologist includes; Soils with much lower strength, posses a CBR value less than 5% and loose top soils which exhibit a considerable amount of volume change up on change in moisture content and that of non-plastic materials. (Abinet Gebremedhin, 2006)

Six samples were submitted and tested for Atterberg limits, classification, modified proctor, three points – CBR and swelling testes to determine the engineering properties of natural subgrade ,and later were correlated with the in-situ test results so as to asses and determine the performance of the natural subgrade materials..

Table 5.4 Type and test Method of AASHTO

Type of Test	Test Methods	Subgrade/fill
Moisture – Density relation	**AASHTO T-199 & 180**	**YES**
Three point CBR	**AASHTO T-193**	**YES**
Atterberg Limits	**AASHTO T-89 & T-90**	**YES**
Soil Classification(Based on gradation test and Atterberg limits test)	**AASHTO M-145**	**YES**
Gradation Test	**AASHTO T-27 & T-11**	**YES**

5.4 Subgrade Soil Test Results

5.4.1. In-situ Density determination and the test result

The in-situ density test was conducted on the embankment layer constructed on the new alignment where the alignment crosses and /or passes over the embankment. The embankment is constructed with rock fill materials except for the top 20cm, which is constructed with scoarecous materials with silty clay volcanic ash with one to one ratio.

The method employed for in-situ density test was sand replacement method that involves excavating a hole in the ground, filling with sand using sand cone apparatus, and then determining the volume of the hole based on the amount of sand required to fill the hole. Given the wet mass of the soil/gravel removed from the hole divided by the volume of the hole, the wet density of the materials can be calculated. Then representative's samples of the sub grade materials were collected from 500m intervals and the required depth of the test pits. The types of tests carried out in the laboratory include; Soil Classification tests such as; Grain size distribution and Atterberg Limits, Strength tests, Moisture/Density Relationship (compaction), CBR (California Bearing Ratio), and Swell tests.

The level of compaction of the top of the layer of the relocated detour embankment was determined by comparing the results of the field density with the maximum dry density (MDD) determined in the laboratory. Accordingly the level of compaction of the top layer of the embankment was found to be below the minimum requirement of the specification i.e., below 95% of the maximum dry density achieved by the heavy compaction test.

Thus , based on the in-situ density test result, it is recommended that the existing top part of the embankment materials needs to be scarified, reshaped and re-compacted so that it serves as road bed for the additional embankment layer and the new pavement structure.

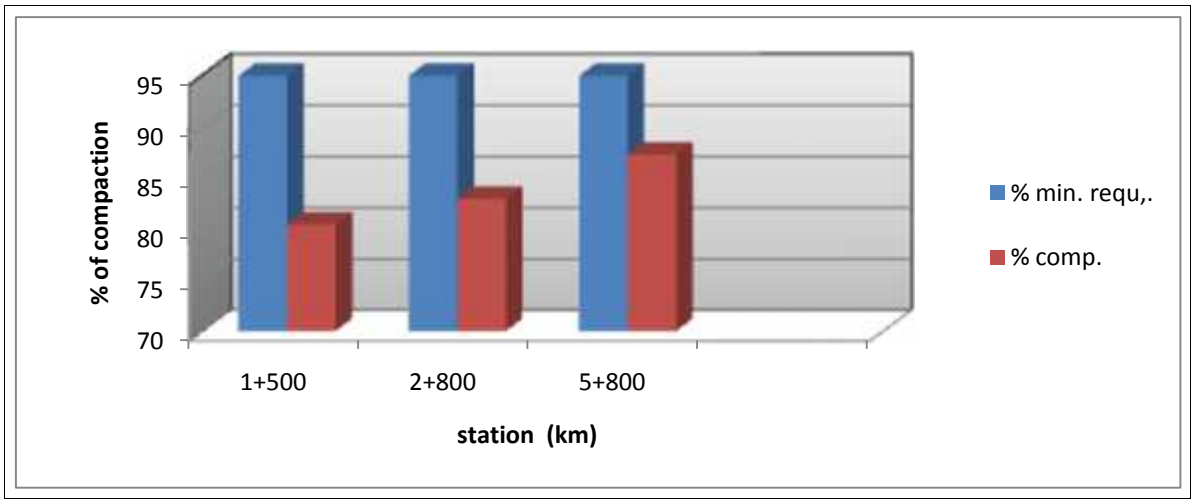

Figure.5.13 graph of compaction level of subgrade and minimum requirement

The subgarde compaction level shall be at least 95 % of the maximum dry density of the modified AASHTO compaction. As displayed in figure 5.13 above, the compaction level of the existing subgrade soil is much lower than the required compaction level for subgrade.

From the in-situ density test results, the subgrade soil shall be reworked and compacted to achieve the specified compaction level before the application of improved subgrade.

The details of the laboratory test results of the subgrade are presented in Annex.

It is noted that the natural moisture content of the subgrade soil is also lower than the optimum moisture content indicating the soil not wet. From the in-situ density test results, the subgrade soil shall be reworked and compacted to achieve the specified compaction level before the application of the pavement layer.

Table 5.5: In-situ Field Density determination test conducted by Core consulting Engineers, Representative of ERA.

Project:	**Metehara - Awash Road Relocation for Lake Beseka Crossing**		**Date Tasted**	*28/03/2011*	
Client:	*Ethiopian Roads Authority*		**Reported by**	*Core Consulting Engineers*	
Date reported	*15/04/2011*		**Lab.no**	*570-11*	
FIELD DENSITY OF SOILS IN - PLACE BY THE SAND CONE METHOD ASTM Test Method D - 1556 - 96 (1996)/AASHTO DESIGNATION: T 191					
Repr. Section: Km 1+500, 2+500 and 5+800			*Layer :*	*Sub grade*	
Density of sand (Unit Wt. of Sand)	*Ds (g/cm3)*	*1.400*	*Lab refe.*	*CORE/GE/RF/061/B*	
Mass of Sand in Cone	*Wsc (g)*	*1507*	*Material Source :*	*(Borrow)*	
Test Reference					
Density Jar (Apparatus) No.			*1*	*2*	*3*
Stretch/Station			*km; 1+500*	*km: 2 + 800*	*km: 5 + 800*
Test Point (Station)			*km 1+500 CL*	*km 2+800 RHS*	*km 5+800 RHS*
Depth (Thickness)		*cm*	15	15	15
Max. Dry Density	*Dmax*	*g/cm³*	1.71	1.71	1.71
Opt. Moisture Content	*Mopt*	*%*	12.1	12.1	12.1
Bulk Density determination					
Mass of Wet Soil from hole	*Wws*	*g*	*2740*	*2735*	*3110*
Mass of sand + jar Before pouring	*Wsb1*	*g*	*7660*	*7440*	*7235*
Mass of sand + jar After pouring	*Wsb2*	*g*	*3450*	*3340*	*2890*
Mass of sand in Hole & cone	*Wsbc = Wsb1 - Wsb2*	*g*	*4210*	*4100*	*4345*
Mass of sand in Hole	*Wsh = Wsbc - Wsc*	*g*	*2703*	*2593*	*2838*
Volume of Test Hole	*Vsh = Wsh/Ds*	*cm³*	*1931*	*1852*	*2027*
Bulk Density of Wet soil	*WD = Wws/Vsh*	*g/cm³*	*1.42*	*1.48*	*1.53*
Moisture Content Determination					
Container No.			*A*	*B*	*C*
Wt. of Wet soil + Container	*A*	*g*	*673*	*593.6*	*584.9*
Wt. of Dry soil + Container	*B*	*g*	*654.7*	*572.9*	*570.7*
Wt. of Container	*C*	*g*	*64.6*	*54.3*	*65.3*
Wt. of Water	*A - B*	*g*	*18.3*	*20.7*	*14.2*
Wt. of Dry soil	*B - C*	*g*	*590.1*	*518.6*	*505.4*
Moisture Content	*Mc = (A-B)/(B-C)*	*%*	*3.1*	*4.0*	*2.8*
Dry Density of soil	DD = (WDX100)/(Mc+100)	*g/cm³*	*1.38*	*1.42*	*1.49*
% Compaction	DDX100/Dmax	*%*	*80.5*	*83.0*	*87.3*

5.4.2 Proctor Compaction Test (Moisture – Density Relationship)

For the present study the compaction test was conducted on six soil samples from the natural subgrade and test results are presented at the appendixes but one sample wasn't conducted for full test. Compaction increase soil unit weight, thereby producing important effects such as an increase in shear strength, a decrease in future settlement, and a decrease in permeability. The maximum dry unit weight was used by designers in specifying design shear strength, resistance to future settlement, and permeability characteristics. A common compaction test is known as the modified proctor test, uses a 44.5-N hammer that was dropped 457mm. This produces greater compaction and, hence, greater soil unit weight (since the hammer is heavier, drops farther, and therefore exerts greater compaction effort on soil sample). Therefore, the modified proctor test was used since greater soil unit weight was required. The results obtained from proctor test, OMC, MDD are utilized for CBR soaking and field density or present compaction evaluation.

Moisture density relationship of soil Test method: *(AASHTO T-180 method D)*

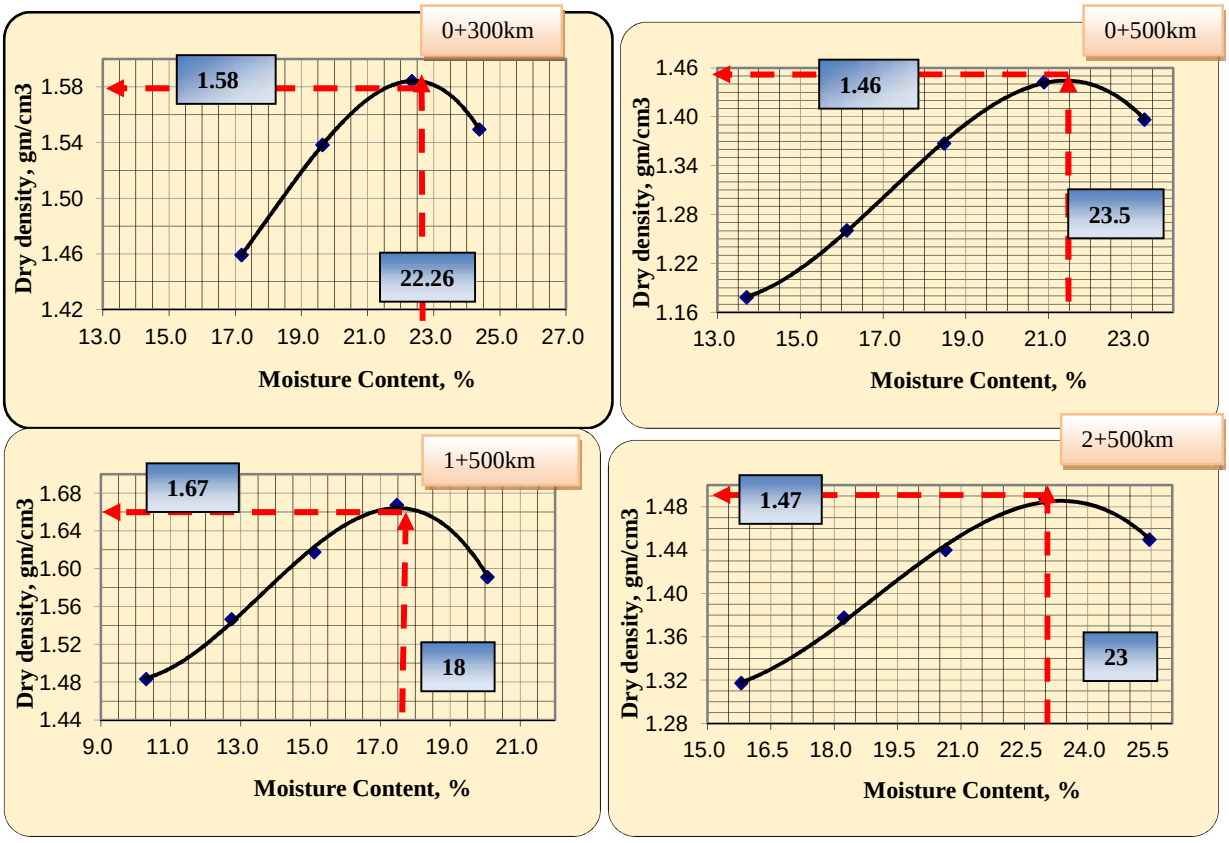

.

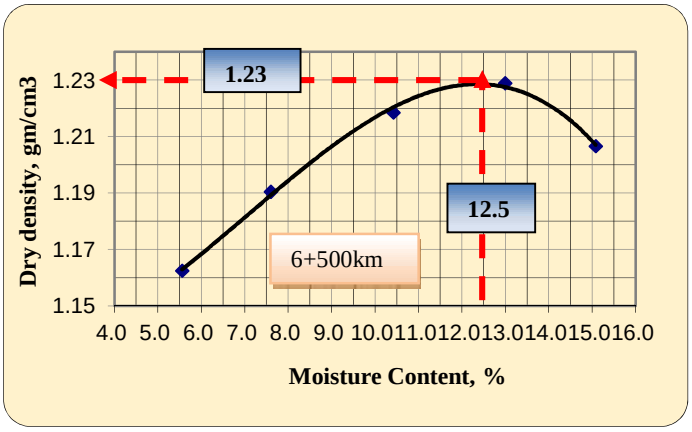

Figure 5.14 Graph of moisture - density relationship

5.4.3. Atterberg Limits

The limits represent the water holding capacity at different states of consistency and understand the correlation between the limits and engineering properties like compressibility, shear strength and permeability. This test determines the nature and response of sub-grade soils upon change to moisture content. High clay content soils exhibit higher shrinkage and swelling upon Change in moisture content.

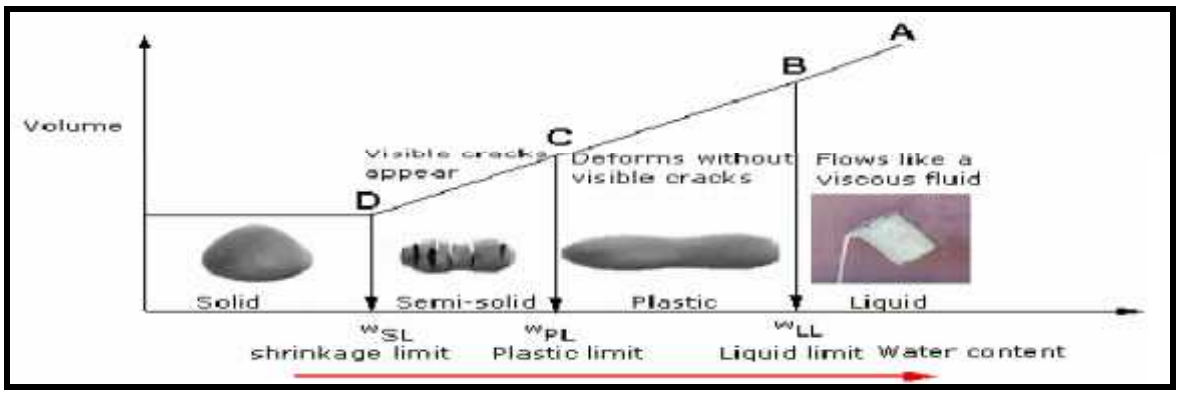

Figure 5.15 Consistency limit and the plastic index with the moisture content factor

In present study area, for this route, consistency limits and the plasticity index were used in the identification and classification of soils. Both the liquid limit and plastic limit depend on the type and amount of clay in the soils. In soils having same values of liquid limit, but with different values of plasticity index; it is generally found that rate of volume change and dry strength increases and permeability decreases with increase in plasticity index. On the other hand, in soils having same values of plasticity index but different values of liquid limit, it is seen that compressibility and permeability increase, and dry strength decreases with increase in liquid limit. Soils that cannot be rolled to a thread at any water content are termed as Non-Plastic (NP).

Soil consistency test result (*test method*： AASHTO T89, T90)

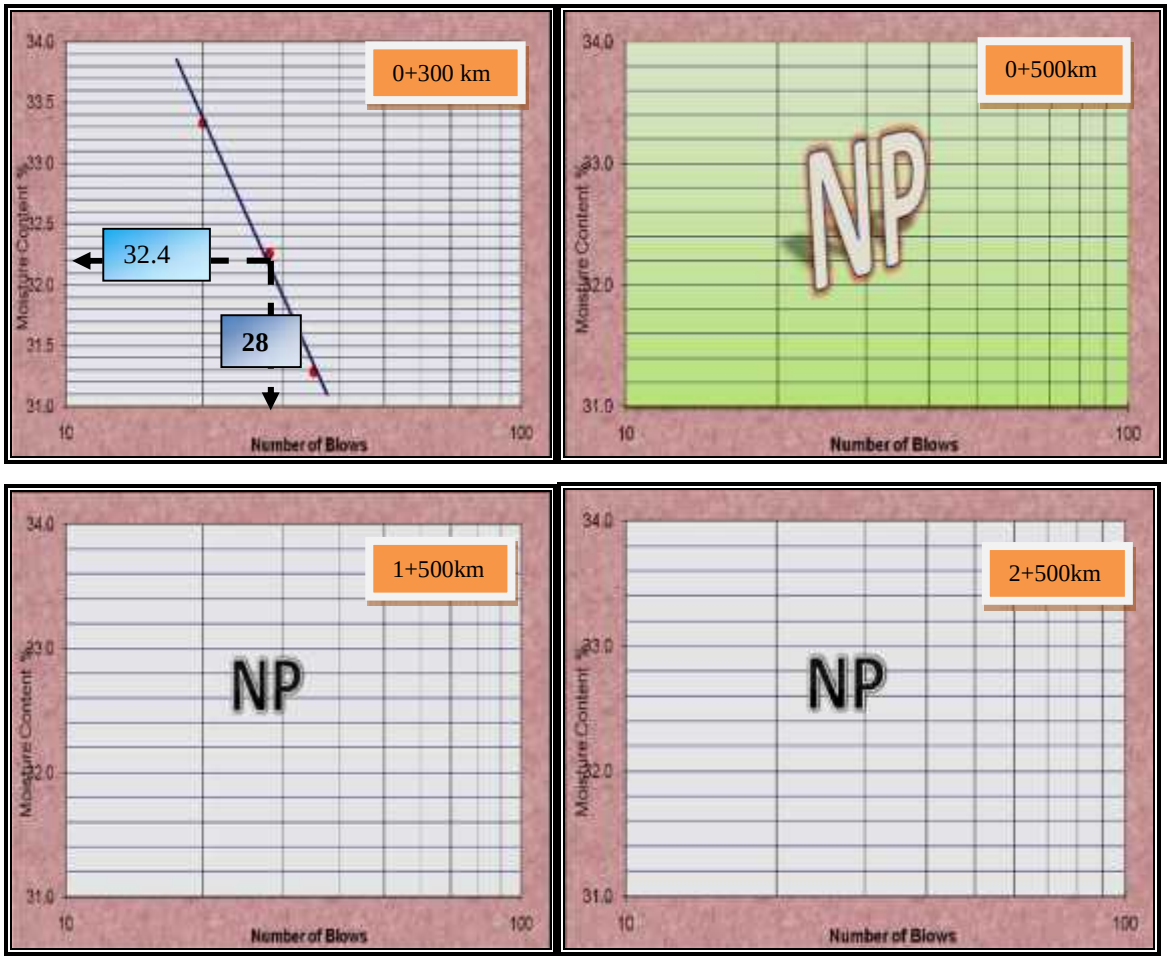

Figure 5.16 graph of Atterberg limit test

The Atterberg Limit depends on the type of predominant material in the soil. In general, soils that exhibit plastic behavior over wide ranges of moisture content and that have high liquid limits have greater potential for swelling and shrinking. For this reason, the present research has focused on the sub-grade soils that resulted with higher plasticity index. Further shrinkage limit was carried out to determine the weighted problematic nature of the sub-grade soils.

All of the materials exhibit non-plastic natures. Therefore based on this result the A-4 materials group cover more than 4.3km of the project length, and composed of light grayish to grey clayey and sandy silt mixed with gravels of scoraceous basalt. They are good subgrade materials.

5.4.4. Grain Size Distribution

Wet sieve analysis was employed to determine the grain size distribution of sub-grade soils in accordance with AASHTO T-88 Test Method for Particle-Size Analysis of Soils. It is one of the most important soil characterizations as the particle size distribution affects many properties of the soil such as density, strength, void ratio, and permeability.

The results obtained from the sieve analysis are plotted with the percentage of particle size on the y-axis on the arithmetic scale paper and the grain size on the x–axis on the logarithm scale. The shapes of the curves indicate the nature of the soil tested. On the basis of the shapes we can classify soils as: uniformly graded or poorly graded, well graded and gap graded soils.

Table 5403/1 Grading Requirements for Gravel Wearing Course and Gravel Shoulder

Test Sieve Size(mm)	Percent (%) by mass of total aggregate passing test sieve					
	Type 1	Type 2	Type 3	Type 4	Type 5	Type 6
50	-	-	-	100	-	-
37.5	100	-	100	80-100	-	-
28	-	100	95 - 100	-	-	-
20	80 - 100	95 - 100	85-100	60-80	100	-
14	-	80-100	65 - 100	-	-	-
10	55 - 100	65 - 100	55 - 100	45-65	80 - 100	100
5	40 - 60	45 - 85	35-90	30-50	60 -85	80-100
2.36	30 - 50	-	-	20-40	45-70	50-80
2	-	30 - 65	22-75	-	-	-
1	-	25-55	18-60	-	-	-
0.425	15 - 30	18 - 45	15-50	10-25	25-45	25-45
0.075	5 - 15	12-32	10-40	5-15	10-25	10-25

Figure.5.17 Figure of standard grain size distribution.

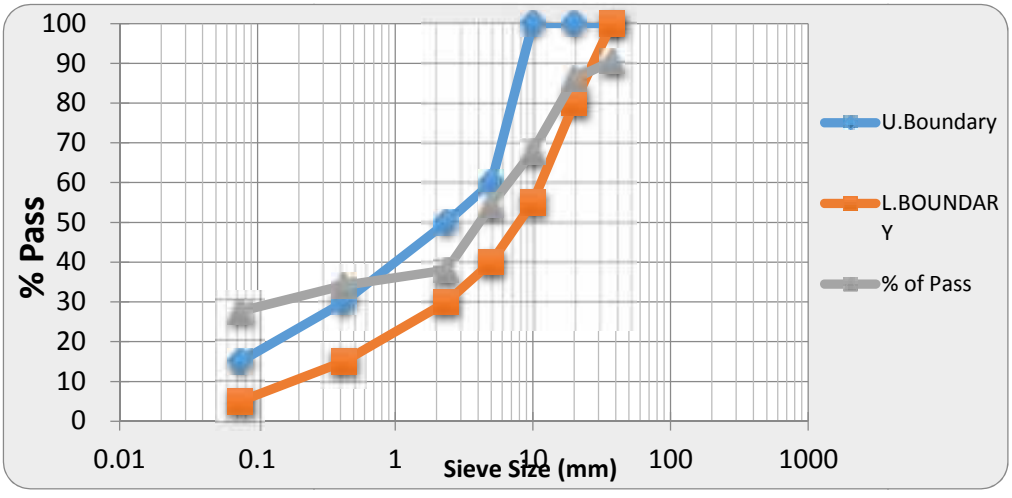

Figure 5.18 Graph of gradation test of Natural gravels used for embankment construction

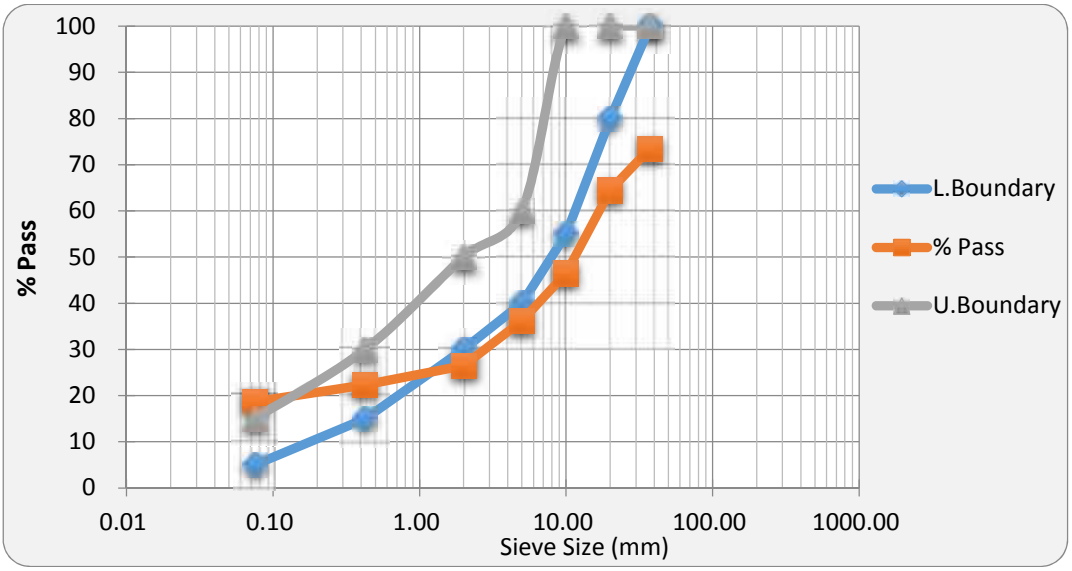

5.4.5. Soil Classification

The AASHTO soil classification method for the sub grade soils was adopted for the present research study.

These tests are indicators of the physical properties of the sub-grade soils and verify their suitability as roadbed material and incorporate in the pavement design process. These tests were carried out usually over short intervals and all sub-grade samples collected during the site investigation period were taken to material laboratory for further investigation.

All of the tasted samples displayed grouped under the A-4 AASHTO materials class. The CBR Values (at 95% of MDD) are ranging from 22% - 87% and the swell indices area well below 2% for all materials. The maximum dry density and optimum moisture content of these materials fall in the range of 1.23g/cc-1.67g/cc and 14%-24% respectively.

The classification of a given soil is based on its particle size distribution, LL, and PI. Soils are evaluated within each group by using an empirical formula to determine the *group index (GI)* of the soils, given as;

GI = (F - 35)[0.2 + 0.005(LL - 40)] + 0.01(F - 15)(PI - 10)

Where, **GI** = group index

F = % of soil particles passing 0.075 mm (No. 200) sieve in whole number based on material passing 75 mm (3 in.) sieve,

LL = liquid limit expressed in whole number, and **PI** = plasticity index expressed in whole number. Table 5-5 AASHTO soil classification system

The result of classification tests conducted on sub grade soil from km 0 to km7 of the project route shows dominantly A-4 AASHTO soil group. The A-4 type of soil covers almost 90 % of the road section .A-4 soils are non-plastic or moderately plastic soils. Similarly the A-6 soil

group constitutes 10 % of the alignment soil. The performance rating of the sub-grade soil of AASHTO M-145/91 is reported in Figure 3.4 above.

In general, according to the AASHTO system of classification, the suitability of a soil deposit for use in highway construction can be summarized as follows.

- Materials classified as A-2-6, A-2-7, A-4, A-5, A-6, A-7-5, and A-7-6 will require a Layer of sub base material if used as subgrade. If these are to be used as embankment Materials, special attention must be given to the design of the embankment.

Generally, as the GI of a soil increases its value as subgrade material decreases. For example, a soil with a GI of 0 (an indication of a good subgrade material) will be better as a subgrade material than one with GI of 20 (an indication of a poor subgrade material).

Table 5.6 Soil cover and their test result for classification

Material Description.	Soil group	CBR (At 95%)	% swell	MDD	OMC	PI	Percentage Road Length km
Clayey and sandy silt with gravels of scoraceous basalt	A- 4	22-87	< 2	1.23-1.67	14-24	NP	4.3

5.4.6. California Bearing Ratio (CBR)

The California Bearing Ratio (CBR) tests were conducted on the samples the subgrade soil at about an interval of 0.500 - 1km (0+500,1+500,2+500,6+500 and 7+200km). The 3-point CBR tests are conducted at modified compaction, and test results are presented for CBR values at 95 mod AASHTO compaction.

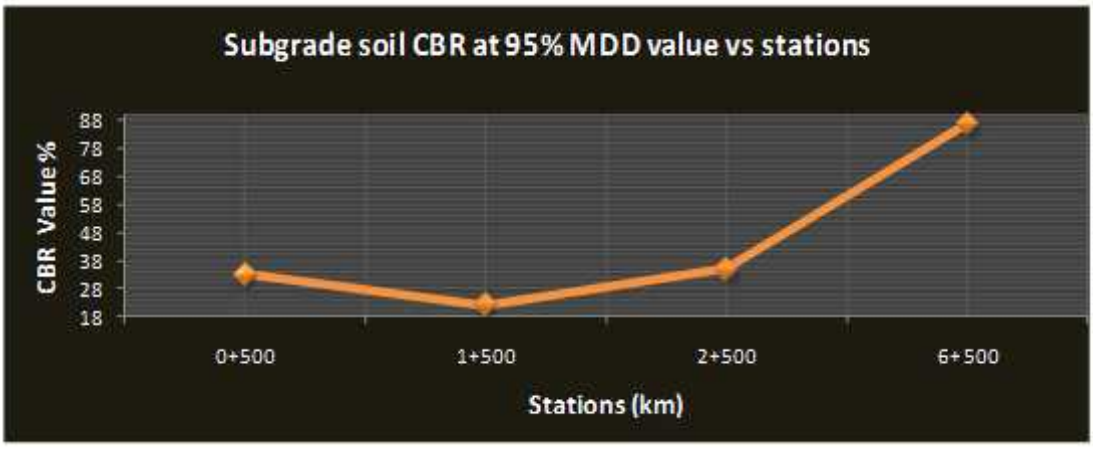

Figure 5.19 CBR value of subgrade soil with respect to stations

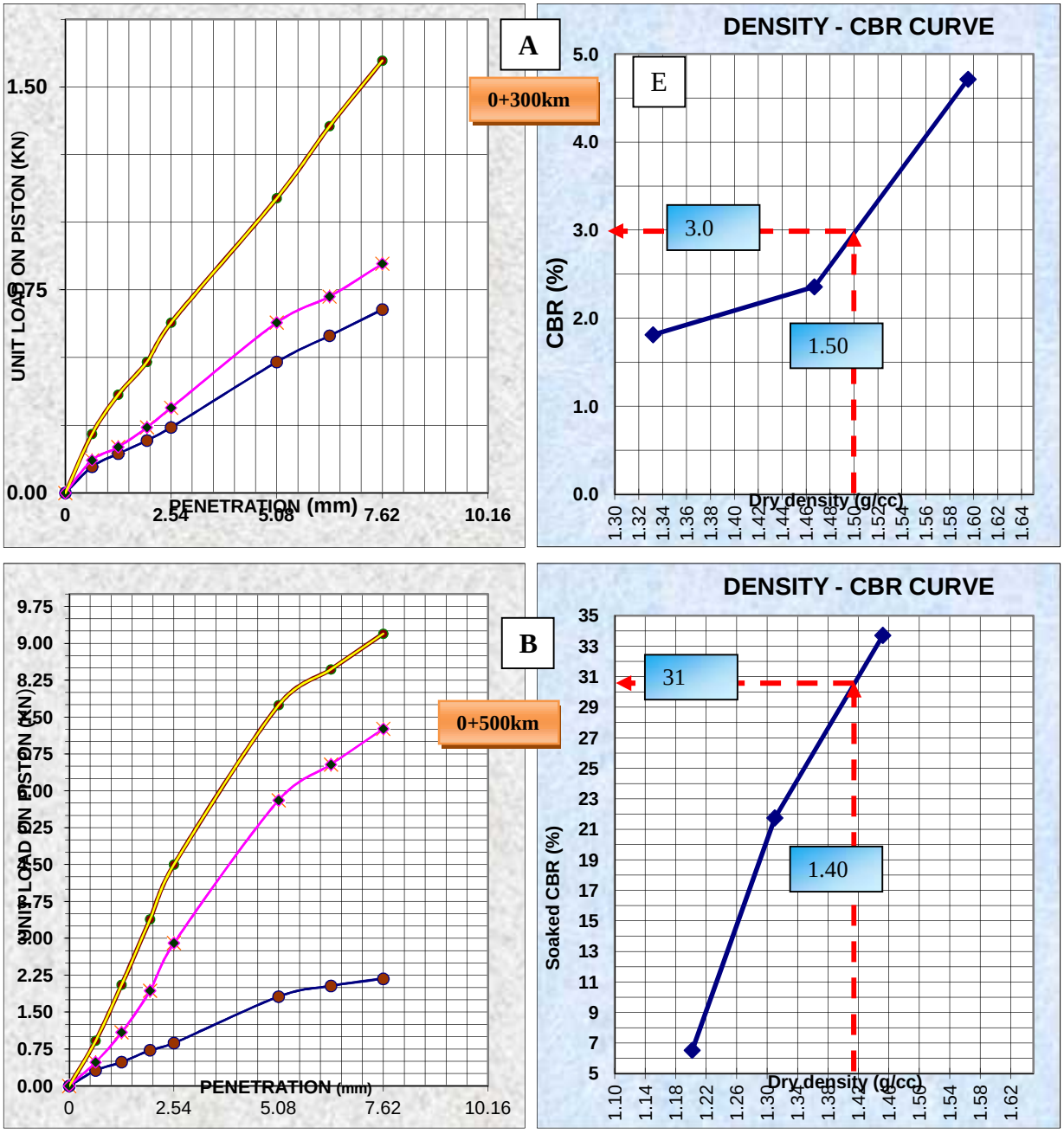

The Majority of the subgrade soil shows CBR values between 30 and 90 %, and make up 95 % of the route alignment. The sections with soil A-2-4 and A-4 group having CBR >25, constitutes 90% of the route alignment. Low strength soils whose CBR values less 3 % were not encountered all through the project route corridor. The variation of CBR values along the project are presented and discussed in section below. The swell percentage of the alignment subgrade soils are below 2.0%.

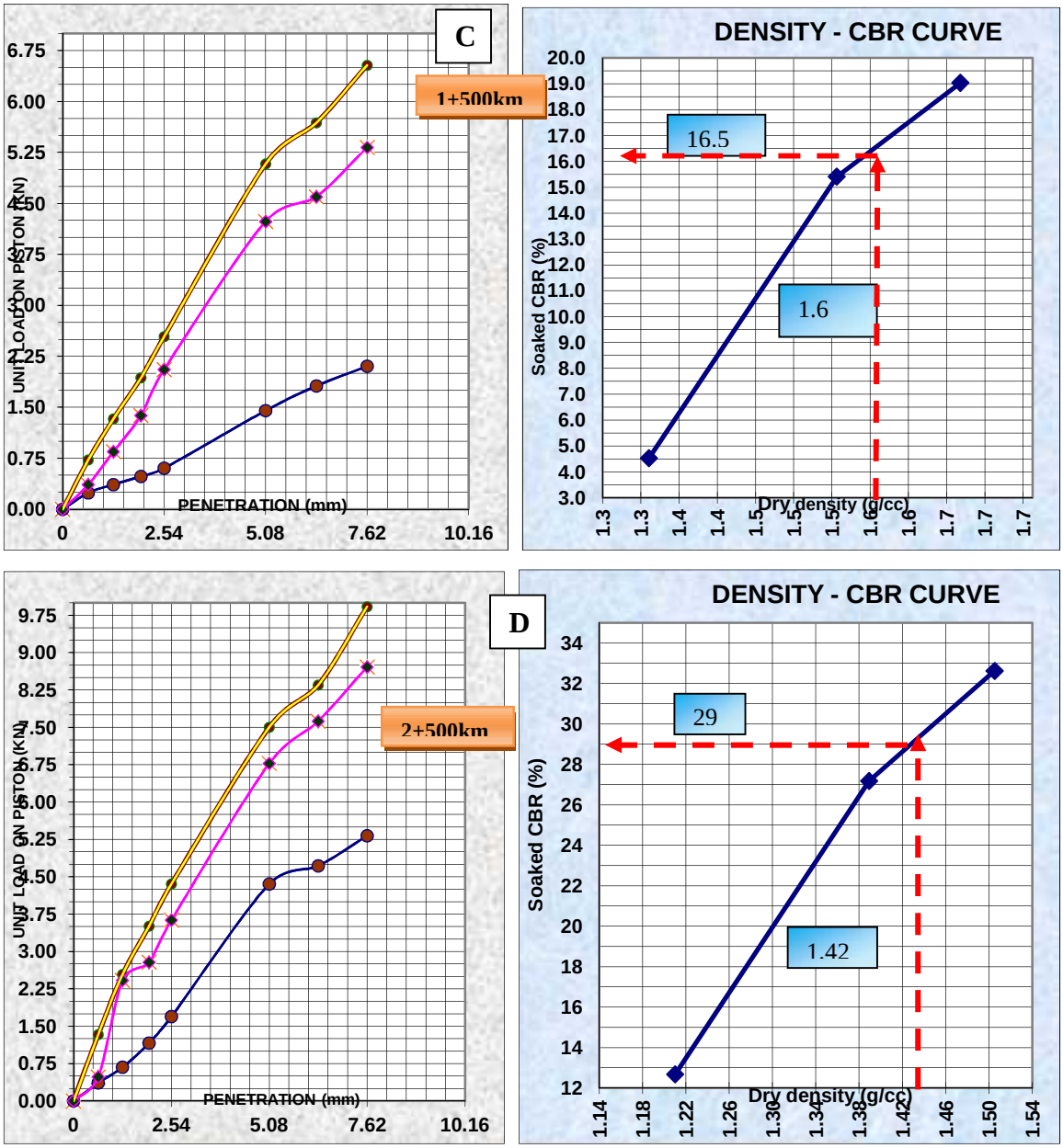

5.4.6.1 Design CBR and design subgrade strength class

Table 5.7 shows a detailed dry density/moisture content/CBR relationship (adapted from ERA Manuals) for a sandy-clay soil that was obtained by compacting samples at several moisture contents to three levels of compaction. By interpolation, a design subgrade CBR of about15 per cent is obtained if a relative density of 100 per cent of the maximum dry density obtained in the ASTM Test Method D 698 Test is specified and the subgrade moisture content is estimated to be 20 percent.

.

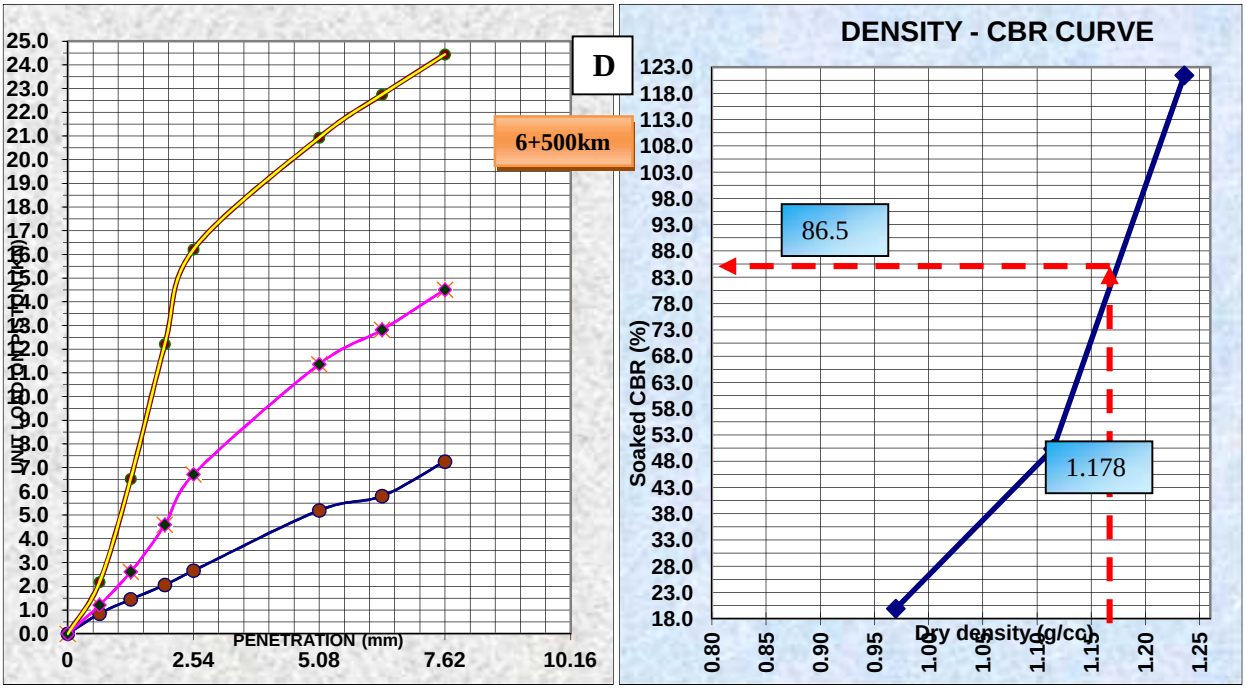

Figure 5.20 **A, B, D**, and **E** are graph of CBR value of subgrade soil with respect to dry density.

Table 5.7 Subgrade strength classes

Class	Range (CBR %)
S1	2
S2	3 – 4
S3	5 – 7
S4	8 – 14
S5	15 – 29
S6	30+

Table 5.8 Subgrade soil test result Summary for determination of design classes

Station	Depth (cm)	Material Description	% pass this sieve(mm) AASHTO T27			Atterberg Limit AASHTO T89 ^90			AASHTO Soil Class	AASHTO T 180		3-Point CBR% AASHTO T-193			Swell, %	CBR at 95% MDD
			2	0.425	0.075	LL, %	PL, %	PI, %		MDD T-180, g/cm^3	OMC, %	No of Blows	Dry density	CBR, %		
0+500	45-115	Light gray ,loose clayey soil mixed with friable gravels	92	75	62	NP			A-4(5)	1.44	21	10	1.20	9.00	0.19	33
												30	1.31	29.00	0.12	
												65	1.45	39.00	0.05	
1+500	0 - 50	Light gray ,loose clayey soil mixed with friable gravels	77	61	44	NP			A-4(2)	1.67	18	10	1.35	7.00	0.28	22
												30	1.55	21.00	0.19	
												65	1.67	25.00	0.09	
2+500	0 - 90	gray ,silty soil mixed with friable gravels	86	68	53	NP			A-4(4)	1.49	24	10	1.21	22	0.22	35
												30	1.39	34	0.12	
												65	1.51	37	0.07	
6+500	15 - 100	Light gray ,loose clayey silt soil mixed with friable gravels	73	60	48	NP			A-4(3)			10	0.97	26	0.22	87
												30	1.11	57	0.16	
												65	1.24	125	0.07	
7+200	15 - 40	Grayish sandy silt soil mixed with friable gravels	83	65	47	NP			A-4(2)							

5.5. Integration of geophysical and geotechnical results

Integration of geotechnical results with the resistivity section shows that subsurface terminated in low resistivity materials interpreted as saturated sandy silt clay. All the tomography images highlight a sub-surface heterogeneity in which pockets of saturated sandy silt clay and blocks of ignimbrites are sandwiched within fractured or weak zones. The presence of saturated and fractured horizons is viewed as being inimical to subgrade and or foundation health due to its low bearing capacity. In addition, some weak zone varieties gradually reopen and expand when they saline water invade through it. These fractures/cracks types expand through wet and dry periods due to weathering. This is because saline water from the lake becomes generate a wave to the weak zones and becomes move by the capillary action and finally manifest on the surface, and as such, structures sitting on top of such soils rise and fall with the soils. The result is differential foundation and subgrade movement which causes cracking and distress in the subgrade and finishes. This might probably responsible for road failures in some of the structures erected in the study area

The high compressibility characteristics of sandy silt clay with volcanic ash coupled with high shrinkage on drying, high porosity, poorly graded and low shear strength owing to fractures slightly weathered scoracious basalt make it unsuitable for most construction work particularly when medium to massive traffic load are being considered. The soils with some gravels, even when they are not under a long-term process of compression and stiffening, are more susceptible to subsidence. However, citing ridged asphalt concrete across such low bearing capacity material will results to road failure or differential settlement or embankment sinking of the soils. Therefore, in addition to tectonic activity of the area, the presence of low penetrative resistance, low resistivity saturated sandy clay and weathered ignimbrites in the study area is identified as the cause of cracking and sinking of road in this area. On the basis of this, shallow subgrade foundation may not be possible in the study area unless adequate soil treatment is done; otherwise shifting to a competent soil and rock section area to depth of pronounced thickness of subgrade materials with less frequency of geological structures is recommended to northern part from the current route line near the periphery of the lake. This would transfer loads of such highway to a stratum of high bearing capacity even if the cost of excavation to the geometric design level is too high.

CHAPTER 6: CONCLUSION AND RECOMMENDATION

6.1 Conclusions

Geophysical approaches

The result of geophysical methods, 2-D electrical resistivity image and magnetic methods of traverse 2 and 4 conducted in the NE of Lake Beseka have shown that a homogenous materials at top sections with high resistivity is present. This high resistivity area, are due to the outcropped Fentale ignimbrites layers, dry sandy silt and volcanic ash. The low resistivity zone highlighted at the bottom middle section of the formation. This sequence of highly saturated portion is welded tuff and minor fragments of fractured scoracious basalt of varying thickness. There is an evident of geological feature such as intensive fracture/fault within the subsurface which can aid subsidence in the area and the main conduit for the advancement of the lake water as well as contribute for the flood to the neighboring area. Again, the total magnetic field intensity map and profile plot indicate the presence of geologic structures (fractures and cracks) along all the lines. From the northeastern of lake, it is clearly seen that the fractures or fissures propagate from the southerly part of the survey area near from the lake.

The inverted model resistivity conducted at NW (Line 1 and 3) of the Lake shows more heterogeneity in its electrical resistivity response. Relatively conductive zone or low resistive located at depth of about 55 m. This suggests that the subsurface is densely fractured. The extremely low resistivity values may be caused due to the intrusion of the lake water through the fractures or weak sections. This portion can be characterized as probably saturated silty sand materials and highly weathered formation of volcanic rocks. The high resistivity portion may describe as fragments of slightly weathered volcanic rock (scoracious basalt). The magnetic survey conducted at this area, NW, of the Lake Beseka has outlined probable weak zone/fissure or ground cracks. From the total field magnetic intensity map, in the NW tip of the survey line, a NW and SE trending of local weak zones or fractures is identified. It may follow or intersect the NNE and SSW trending of regional structures. This is through which the lake water and thermal spring may come to the surface.

Therefore, a total of four traverse lines are depicted on the maps with different orientation. All map clearly outlined the areas with densely fractured and presence of other weak zones. The general orientations of the structures are dominantly N-S and NE-SW.

Geotechnical result

This section is intended to define, conclude and recommend the various options to define slightly affected route line for homogeneous pavement sections for the pavement design. Existing highway line was experiencing sinkage and cracking that affected their stability at Lake Beseka area, Metehara town. The spate of highway failures throughout the study area has assumed an alarming aspect, with Metehara being the worst hit.

From the laboratory test result, the sandy silty clay material categorized to A-4 AASHTO soil group constitute 90 % of the project section, which is rated as fair to poor as subgrade soil. The remaining 10 % gravely sandy silty clay soil sections are covered with A-2-7 AASHTO soil groups which are also rated as fair to poor in accordance with AASHTO soil classification. It can be seen from the PI distribution graph presented under this section that PI is non-plastic (NP) for the whole stretch of the alignment.

According to ERA Pavement Design Manual soil class, the dominant native soil types are fall in upper S4 and S6 classes. The alignment subgrade soils are almost similar; and have CBR values rang of 18 to 87 % and exhibit low to non swelling potential.

Grain size analysis results revealed that soils of the study area are mainly dominated by silt and clay size particles with sand grains and some volcanic gravel. The grain size analysis curves show that a missing of particle size of soils which implies that the soils of the project site is not well graded. Therefore, soils of the area are not suitable for road construction unless it is properly treated and mixed with different ratio.

Moreover, the test result and observations suggests that the sub-soils at these locations have poor geotechnical properties which can cause differential sinking of foundation soils with consequent damage to the highways. This behavior was corroborated by the values obtained from interpreted geophysical data showing low resistivity values which clearly shows dry to saturated Sandy silt clay materials.

Therefore, the existing and new roads were located over anomalous subsurface zones which were inappropriate for bearing the load of a engineering structure owing to poor geotechnical properties and inferred geological structures. Consequently, recent damages to the infrastructure and the nearby structures, call for attention and further investigation using non destructive geophysical methods to guide geotechnical investigations.

6.2 Recommendations

Any remedial measures should consider for the lake advancement through the fractures and fissures and the effect on the infrastructures of the study area. Therefore, an integrated geophysical and geotechnical investigations offer very useful approach for characterizing near surface earth and thus can help in preparation before engineering structures are found on same. The road alignment should again require additional geophysical investigation to determine the propagation and extension of such fractures in form of fissures/local faults.

Based on the findings and results of the study, some important recommendations can be drawn as follows

- It will be better to move/shift the site of highway route line slightly (by about 250 m) to the north side of the current position, which is an indicative of fewer densities and frequencies of geological structures.
- Careful consideration should be given to the weak zones (fractures, local faults or fissures) mapped from the survey at some stage in construction phase. Localized zones within the survey site where the structures and prominent zones of weakness are identified. These areas need special design considerations.
- Removal of undesirable soils (to depths of 3-4 m) from the foundation area and backfilling it with non compressible and well graded soils (well compacted granular soils). It is therefore recommended that foundation (subgrade) should not be constructed on soils comprised of highly saturated soils horizons and highly fractured zones.
- Practically it is difficult to backfilled 65m depth open weak zone therefore, as an option, the design should include shifting the route to less affected by geological structures to prevent differential settlement and minimize cycles of maintenance.
- The current study covered only partial part of the road corridor. So, additional investigation will be required for the future expansion of the lake following the geological structures possibly of the fissure and fractures.
- In general, the nature of cracks/fractures, densities and times of formations, and the engineering behavior of scoracious basalt, action of saline water from the lake to neighboring areas: piping and hydro- compaction are the best possible option that can compromise realities and theories, observations and uncertainties, if the client is discarded to shifting the existing new line to the north.

REFERENCE

Abebe, Bekele., 1992. Studio geologico-strutturale del Rift Etiopico a sud di Asela. Ph. D dissertation, University of Firenze, Firenze, Italy, 153 pp.

Abebe, Bekele., Acocella, V., Korme,Tesfate., Ayalew, D., (2007). Quaternary Faulting and Volcanism in the Main Ethiopian Rift. Journal of African Earth Sciences 48, pp 115-124.

Abinet Gebremedhin, 2006, *Engineering geological problems and countermeasures for flexible pavement on expansive soils* – a case study on Addis Ababa- Jima road section

Acocella, V., Gudmundsson, A. & R.Funiciello, (2000): Interaction and linkage of extension fractures and normal faults: examples from the rift zone of Iceland. *Journal of Structural Geology*, vol. 22, pp. 1233- 1246

Acocella, V. & Korme, T. (2002): Holocene extension direction along the Main Ethiopian Rift, East Africa, *Terra Nova*, vol. 14, pp. 191- 197

American Association of State Highway and Transportation Officials (AASHTO). (2000) AASHTO Guide for Design of Pavement Structures. American Association of State Highway and Transportation Officials. Washington, D.C.

Asfaw, Laike Mariam., 1990. Implication of shear deformation and earthquake distribution in the East African Rift between 4 N and 6 N. Journals of African Earth Sciences 10, 745–751.

Asfaw, Laike Mariam., 1992. Constraining the African pole of rotation. Tectonophysics 209, 55–63.

Asfaw, Laike Mariam., 1998. Environmental hazard from fissures in the Main Ethiopian Rift. Journal of African Earth Sciences 27, 481–490.

Ayalew Luelseged., Yamagishi, H., Reik,. G. (2004). Ground cracks in Ethiopian Rift Valley: facts and uncertainties Engineering Geology 75: 309-324.

Bahat, D., 1979. On the African Rift System, theoretical and experimental study. Earth planetary Sci. Jour. Vol. 45, No.2

Berhe, Seyoum .M., Kazmin, V., Aguma, A., Medhanie, A., Desta, B., Megersa, B., Michael, B., Hailu, T., Kebede, G., Balcha, T., Wondm-Agegnehu, B. (1978): Nazret [Geological Map]. Scale 1:250,000, Ministry of Mines, Energy and Water Ressources, Addis Abeba.

Berihun Abadi. 2001. Geophysical investigation for lake level rise studies, northern part of Lake Beseka. M.Sc Thesis, Department of Geology and Geo- physics, Addis Ababa University.

Bilham, R., Bendick, R., Larson, K., Braun, J., Tesfaye, S., Mohr, P. & Asfaw, L. (1999): Secular and tidal strain across the Ethiopian rift. Geophysical Research Letters, vol. 37, pp. 2789- 2984.

Boccaletti, M., Bonini, M., Mazzuoli, R., Abebe, B., Piccardi, L., Tortorici, L., 1998. Quaternary oblique extensional tectonics in the Ethiopian Rift (Horn of Africa). Tectonophysics 287, 97–116.

Boccaletti, M., Mazzuoli, R., Bonini, L., Trua, T. & Abebe, B. (1999): Plio-Quarternary volcanotectonic activity in the northern sector of the Main Ethiopian Rift: Relationships with oblique rifting. *Journal of African Earth Science*, vol. 29, pp. 679- 689.

Buchwitz, M. (2006): Sturctural Geology and Quaternary Devolopment of Lake Beseka Basin, Ethiopia.

Burke, K., Wilson, J., 1976. Hot spots on the earth's surface. Scientific American 235, 46–57.

Carpenter, M.C., 1993. Earth fissure movements associated with fluctuation in groundwater levels near the picachoMountains, South-central Arizona, 1980-84. US Geological Survey Profetional Paper 497-H, Wasington. 40 pp.

Casey, M., Ebinger, C.J., Keir, D., Gloaguen, R., Mohamad, F., 2006. Strain accommodation in transitional rifts: extension by magma intrusion and faulting in Ethiopian rift magmatic segments. In: Yirgu, G., Ebinger, C.J., Maguire, P.K.H. (Eds.), The Afar Volcanic Province within the East African Rift System: Geological Society Special Publication, vol. 259, pp. 143–163.

Chernet Tadesse., Hart, W., Aronson, J.L. and Walter, R.C., 1998. New age constraints on the timing of volcanism and tectonism in the northern Main Ethiopian Rift.-southern Afar transition zone (Ethiopia). J. Volcanol. Geotherm. Res., 80. 267-280.

Chorowicz, J., Collet, B., Bonavia, F.F. and Korme, T.1992. Northwest to north-northwest extension direction in the Ethiopian Rift deduced from the orientation of extension structures and fault-slip analysis. Bull. Geol.Soc.Am., 105, 1560-1570.

Chu, D. and Gordon, R.G., 1999. Evidence for motion between Nubia and Somalia along the Southwest India Ridge. Nature, 398, 64-67.

Degefu Wolde. 1987; 'Some aspects of meteorological drought in Ethiopia', Drought and hunger in Africa. MH Glantz Cambridge, Cambridge University press: p. 23-36.

Di Paola, G.M., 1972. The Ethiopian Rift Valley Between $7^{o}00`$and $8^{o}40`$ LatNorth: Volcanol., v.36, p. 517-560.

Ebinger, C.J., 1989a. Geometric and kinematic development of border faults and accommodation zones, Kivu-Rusizi Rift, Africa. Tectonics, 8, 117-133.

Ebinger, C.J., 1989b. Tectonic development of the western branch of the East African Rift System. Bull. Geol.Soc.Am., 101.885-903.

Ebinger, C.J., Bechtel, T.D., Forsyth, D.W. and Bowin, C.O., 1989. E ffective elastic plate thickness bebeath the East African and Afar plateau and dynamic compensation of the uplifts. J.Geophys. Res., 94, 2883-2901.

Ebinger, C.J. and Hayward, N.J., 1996. Soft plates and hot spots: views from Afar. J.Geophys. Res., 101, 21, 859-21,876.

Ebinger, C.J., Casey, M., 2001. Continental breakup in magmatic provinces: an Ethiopian example. Geology 29, 527–530.

Ethiopian Building Code Standard (1995). Code of Standards for Seismic Loads. Ministry of Works and Urban Development, Addis Ababa, Ethiopia.

ERA 2003, Road Sector Development Program II (2002-2007), Ethiopian Roads Authority, March 2003.

Foster, A.N., Jackson, J.A., 1998. Source parameters of large African earthquakes: implications for crustal rheology and regional kinematics. Geophysical Journal International 134, 422–448.

Getech (2007). Advanced Processing and Interpretation of Gravity and Magnetic Data (Available at http: //www.getech.com.).

Gibson, L., 1969. The structure and volcanic geology of an axial portion of the Main Ethiopian Rift. Tectonophysics, 8, 561-565.

Gibson, I.L., Tazieff, H., 1970. The structure of the Afar and the northern part of the Ethiopian Rift. Philosophical Transactions. Royal Society of London 267, 331–338.

Görner A.& Jolie, E. (2005). Water level rise of Lake Beseka (Main Ethiopian Rift): A multi-method approach. Mapping and Project Report [unpublished], 39 pp., TU Bergakademie Freiberg.

Griffiths, M.J., Kingham, T.J, Waddams, A.E., Birchall, C.R., and Teferra, T. 1975.' Development prospects in the southern Rift Valley. Ethiopia', Tolworth, Land Resources Div., U.K. Min. Overseas Devel,:270.

Halcrow & Partners, 1979. Master plan for the development of the surface water resources in the Awash basin, vol. 6. Ministry of Water Resources, Addis Ababa, Ethiopia.

Hayward, N.J., Ebinger, C.J., 1996. Variation in the long-axis segmentation of the Afar Rift System. Tectonics 15, 244-257.

Holtz, R.D and Kovacs, W.D. (1981). An introduction to geotechnical engineering prentice-Hall, Inc., Englewood Cliffs, New Jersey, 719 pp.

Kazmin, V., Seifemichael, B., 1978. Geology and Development of the Nazret Area. E.I.G.S. Note no. 100, p26 Addis Ababa, Ethiopia.

Kazmin, V., Seifemichael, B., and Walsh, J., 1980b. Report on the Geological Map of the Ethioipian Rift Valley, E.I.G.S, Addis Ababa, Ethiopia.

Keir, D., C. Ebinger, G. Stuart, E. Daly, Ayele, A. 2005. Strain accommodation by magmatism and faulting as rifting proceeds to breakup: Seismicity of the northern Ethiopian rift. Submitted to J.Geophys. Res.

Keranen, K., Klemperer, S.L., Gloaguen, R., Eagle working group, 2004. Three-dimensional seismic imaging of a protoridge axis in the Main Ethiopian rift. Geology 32, 949–952.

Korme Tesfaye, Acocella, V., Abebe, B., 2004. The role of pre-existing structures in the origin, propagation and architecture of faults in the Main Ethiopian Rift. Gondwana Research 7, 467–479.

Kurz, T., Gloaguen R., Ebinger, C., Casey, M. & Abebe, B. (2005): Deformation distribution and type in the Main Ethiopian Rift (MER); a remote sensing study, *J. Afr. Earth Sc.* (Accepted.)

Le Pichon, X. and Francheteau, J., 1978. A plate tectonic analysis of the Red Sea –Gulf of Aden area. Tectonophysics, 46, 369-406.

Loke, M.H. (1999). Electrical imaging surveys for environmental and engineering studies. A practical guide to 2-D and 3-D surveys, Penang, Malaysia, 57 pp.

Mamo Tilahun., Getaneh, E., (2003). The geology and surface hydrothermal alteration mapping of Fantale geotheramal prospect, intern report of the Geological Survey of Ethiopia, Hydrogeology, Engineering Geology and Geothermal Department, 29 p.

McKenzie, D.P., Davies, D. and Molnar, P., 1970. Plate tectonics of the Red Sea and East Africa. Nature, 226, 243-248.

Mengesha Tefera., Chernet, Tadesse. and Worknesh, Hailu.,(1996). Exploration of the Geological Map of Ethiopia. E.I.G.S. 2 nd edition.

Merla, G., Abbate, E., Canuti, P., Sagri, M., Tacconi, P., 1979. Geological map of Ethiopia and Somalia and comment with a map of major landforms (scale 1:2,000, 000). Consiglio Nazionale delle Ricerche, Rome. 95.

Mohr., P.A., 1962a. The Ethiopian Rift System. Bull. Geophys.Observ.Addis Ababa 5, 33-62.

Mohr, P., 1967. The Ethiopian Rift System. Bulletin of the Geophysical Observatory of

Addis Ababa 11, 1–65.

Mohr, P., 1983. Volcano tectonic aspects of the Ethiopian Rift evolution. Bulletin Centre Recherches Elf Aquitaine Exploration Production 7, 175–189.

Mohr, P., 1968. Transcurrunt faulting in the Ethiopian Rift. System. Nature, 218,938-941.

Mohr., P.A., 1987. Patterns of faulting in the Ethiopian Rift Valley. Tectonophysics 143, 169-179.

Mohr, P., Mittchell, J.G., Raynolds, R.G.H., 1980. Quaternary volcanism and faulting at O'a caldera, central Ethiopian Rift. Bulletin of Volcanology 43, 173–189.

Morley,C.K., 1992. Extension, detachments and sedimentation in continental rifts (with particular reference to East Africa). Tectonics, 8, 1175-1192

MWR (1999): Study of Lake Beseka (Main Report, Vol. 1). Ministry of Water Resources, Addis Ababa, Ethiopia, 2013.

Nigatu Fekadu (2006). Engineering Geological Studies for Suitability of Construction Material and Foundation Condition Evaluation – With Special Emphasis on Seepage Studies, Tendaho Dam, Afar Region, Ethiopia. Unpublished MSc Thesis, Addis Ababa University, Addis Ababa, Ethiopia, 111 pp.

Raghuvanshi, T.K. (2010). Lecture Notes: Geotechnical Investigation, Addis Ababa University, Ethiopia.

Rooney, T., Furman, T., Yirgu, Gezahegn., Ayelew, D., 2005. Structure of the Ethiopian lithosphere: evidence from mantle Xenoliths. Geochemica et Cosmochimica Acta 69, 3889–3910

Reynolds, J.M. (1997). An Introduction to Applied and Environmental Geophysics. John Wiley and Sons limited, England, UK. pp. 116-209, 415-522.

Tanzania 1999, Tanzanian Pavement and Materials Design Manual, The United Republic of Tanzania Ministry of Works.

Tamiru Alemayehu. (2006). Groundwater occurrence in Ethiopia. Addis Ababa , Ethiopia

Tesema Zelalem. (1998). Hydrochemical and water balance approach in the study of high water level rise of Lake Beseka. MSc. Thesis, University of Birmingham, UK, 90.

Tigistu Haile (2010). Applications of electrical resistivity tomography (at www.mawari.net.).

Tilahun Mammo (2005). Site-specific ground motion simulation and seismic response analysis at the proposed bridge sites within the city of Addis Ababa, Ethiopia. Engineering Geology, 79: 127–150.

Thomas, M.B. (2003). Introduction to geophysical exploration: magnetic notes on main magnetic field (available at galitzin.mines.edu/…/notes).

Williams, F.M., Williams, M.A.J., Aumento, F., (2004).Tensional fissure and crustal extension rates in the northern part of the Main Ethiopian Rift.Jornal of African Earth Sciences 38, pp.183-197.

Woldegabriel, G., Aronson, J.L., 1987. Chow Bahir: a 'failed' rift, in Southern Ethiopia. Geology 15, 430-433.

Woldegabriel, G., James L., Aronson and Robert, C., Walter, 1990. Geochronology and rift basin development in the central sector of the Main Ethiopian Rift. Geol.Soc. Of American Bull., Vol.102, pp.439-458, April 1990.

Wolfenden, E., Ebinger, C., GezahegnYirgu, Deino, A. & Dereje Ayalew (2004): Evolution of the northern Red Sea rift: Birth of a triple junction. Earth and Planetary Science Letters, vol. 224, pp. 213- 228.

WWDSE (Water Works Design and Supervision Enterprise) (1999). Awash river diversion for Irrigation Project, Canal Design, Unpublished Report, Addis Ababa, Ethiopia.

Yirgu Gezahegn., Ebinger, C.J., Maguire, P.K.H. (Eds.), 2006. The Afar Volcanic Province within the East African Rift System: Geological Society Special Publication, vol. 259.

ANNEXTURES